

**Republic of Iraq  
Ministry of Higher Education and  
Scientific Research University of  
Babylon Faculty of Materials  
Engineering Department of  
Metallurgical Engineering**



# **A Preparation and Investigation of Composite Coating on Commercial Purity Titanium Substrate by Micro-Arc Oxidation**

**A Dissertation Submitted to the Council of the Faculty  
of Materials Engineering/University of Babylon in  
Partial Fulfillment of the Requirements for the Master  
Degree in Materials Engineering/Metallurgical  
by**

**Suja Adil Hamzah Jasem**

**Supervised by**

**Asst. Prof. Nabaas Sattar Radhi (PhD.)**

**2021 A.D**

**1443 A.H**

بِسْمِ اللَّهِ  
الرَّحْمَنِ  
الرَّحِيمِ  
" نَرْفَعُ  
دَرَجَاتٍ مِنْ  
نَشَاءٍ وَفَوْقَ

كل ذي علم  
عليه

صدق الله

العظيم

الآية ( ٧٦ )

من سورة يوسف

## **Supervisors Certification**

We certify that this thesis entitled (**A preparation and investigation of composite coating on commercial purity titanium substrate by Micro-arc oxidation**). Was prepared by (**Suja Adil Hamzah Jasem**) under our supervision at Babylon University / College of Materials Engineering/Department of Metallurgical , in Partial Fulfillment of the Requirements for the Award Master Degree of Science in Materials Engineering Metallurgical.

Signature:

Name: **Asst. Prof. Dr. Nabaasattar Radhi**

Date: / / 2021

## **Examining Committee Approval Sheet**

We certify that we have read this dissertation entitled (**A preparation and investigation of composite coating on commercial purity titanium substrate by Micro-arc oxidation**) and as an examining committee, we have examined the student (**Suja Adil Hamzah Jasem**) in contents and that is related to it, and that in our opinion it meets the standard of thesis for the Master Degree in Material's Engineering /Metallurgical Engineering.

Signature

**Prof. Dr. Haydar H.J. Jamal AlDeen**

Committee Chair

Date: / / 2021

Signature

**Asst. Prof. Dr. Zaineb Fadhil Kadhim**

Committee member

Date: / / 2021

Signature

**Asst. Prof. Dr. Heider Yasser Thamir**

Committee member

Date: / / 2021

Signature

**Asst. Prof. Dr. Nabaa sattar Radhi**

Supervisor

Date: / / 2021

**Approval of the Department  
of Metallurgical Engineering**

Head of Metallurgical Engineering Departme

**Approval of the Faculty  
of Material's Engineering**

Dean of the Faculty of Material's Engineering

Signature

**Prof. Dr. Saad Al-Shafaie**

Date: / / 2021

Signature

**Prof. Dr. Imad Ali Disher**

Date: / / 2021

## **Dedication**

Man cannot bear the burdens of life alone, for cooperation helps man to do good deeds, and a cooperative person is one of his qualities, loves goodness for all.

I dedicate this modest effort to:

Dear father, my dear mother, my brothers and sisters, my friends. To everyone who taught me a letter, encouraged me and provided advice.

With all my affection... for my life partner "Who walked with me step by step towards my dream...". We planted it together... and we'll keep it together. God bless you, if he will (my husband)

**SAJA ADIL AL. ZUBAIDI**

## **Acknowledgments**

First and foremost, praises and thanks to God, the Almighty of blessings throughout my research work to complete the research successfully.

I would like to express my deep and sincere gratitude to my research supervisor, Dr. Nabaa Sattar Radhi, for giving me the opportunity to do research and providing invaluable guidance throughout this research.

I am extremely grateful to my parents for their love, prayers, caring and sacrifices for educating and preparing me for my future. I am very much thankful to my husband and my daughters for their love, understanding, prayers and continuing support to complete this research work. Also I express my thanks to my sister, for her support and prayers.

My Special thanks goes to my aunt Suhaila and her daughters for the keen interest shown to complete this thesis successfully. I am extending my thanks to the students and staff of the Faculty of Materials Engineering / University of Babylon for their kindness.

Finally, my thanks go to all the people who have supported me directly or indirectly in completing the current study.

**SAJA ADIL AL. ZUBAIDI**

## Abstract

Coating techniques are simple and intuitive approaches to obtain a modified surface. Micro arc oxidation (MAO) is one of the most applicable methods to deposit a porous bioceramic layer on commercial pure titanium (CP-Ti) and its alloys. The present study investigates the effect of micro arc oxidation variables (time, electrolyte components) on the properties of deposited layer to determine the best values of micro arc oxidation variables. The coated layers are HA or HA incorporated with nano silver Ag added (0.5, 1, 1.5, 2) g/L to coated solution.

The results of coating thickness increased in the thickness of the coating with the increase in the coating time. Field emission scanning electron microscopy of specimens showed that increase in time led to increased deposition of nano silver. Atomic force microscopy of specimens showed the surface roughness increases with decrease deposition time. The effect composite coating (HA & HA/Ag) on CP-Ti substrate was clearly effective against bacteria where this type of coating killed bacteria compared to the base specimen. The specimens (HA45Ag1) is preferable where it has the lowest corrosion rate, the angle of contact differed with the increase in the percentage of nano silver in the hydroxyapatite (HA) electrolyte and the best wettability achieved when using HA/Ag1.5 electrolyte and surgical procedure and implantation in vivo test if the percentage of silver is more than 1 g/L, the solution becomes toxic and does not apply in the human body.

## List of contents

<b>Item</b>	<b>Item Subject</b>	<b>Page No</b>
	Supervisors Certification	I
	Examining Committee Approval Sheet	II
	Dedication	III
	Acknowledgments	IV
	Abstract	V
	List of Contents	VI-IX
	List of Abbreviations	X-XI
	List of Symbols	XII
	List of Figures	XIII-XV
	List of Tables	XVI
<b>Chapter One</b>		
<b>Introduction</b>		
1.1	General View	1
1.1.1	Properties of Biomaterials	3
1.1.2	Characteristics of Biomaterials	4
1.2	Main Issues	6
1.3	Aim of Work	8
<b>Chapter Two</b>		
<b>Theoretical Part and Literature Survey</b>		
2.1	Introduction	9
2.2	Historical Background	9
2.3	Titanium (Ti)	13
2.3.1	Structural Properties of Titanium	14
2.3.2	The Properties of Ti	15

2.3.3	Biocompatibility of Titanium	16
2.4	Corrosion Resistance	18
2.5	Mechanical Properties of Natural Bone	19
2.6	Failure of Implants	20
2.6.1	Mechanism of Implant Failure	21
2.7	Surface Modification with Coating Layer	22
2.8	Composite Coatings	23
2.9	Bioactive Coatings	24
2.10	Properties of Bioactive Coatings	26
2.11	Coating Materials	27
2.11.1	Ceramics	27
2.11.1.1	Hydroxyapatite	28
2.11.1.1.1	Crystal Structure of HA	31
2.11.1.1.2	The Biochemical Properties of HA	32
2.11.1.1.3	Biological Properties of HA	33
2.11.1.1.4	Medical Applications of HA	33
2.11.2	Composite	34
2.12	Micro-Arc-Oxidation	34
2.12.1	Process of Micro-Arc-Oxidation	35
2.13	Nano Coating	38
2.13.1	Nano-Hydroxyapatite Coating	38
2.14	Silver (Ag)	39
2.14.1	Biocompatibility of Ag	39
2.14.2	Medical Application of Ag	40
2.14.3	Ag Coating	41
2.15	Literature Survey	42
2.15.1	Nano Ag/HA Deposition	42
2.15.2	Micro Arc Oxidation	45

<b>Chapter Three</b>		
<b>Experimental Part</b>		
3.1	Introduction	48
3.2	Flowchart of Experiment Work	49
3.3	Preparation of Commercial Pure Titanium (CP-Ti) Substrate	50
3.4	Materials	51
3.5	Equipments and Apparatus	51
3.5.1	Preparation Before Coating	51
3.5.2	Characterizations of Deposited Specimens	51
3.6	Micro Arc Oxidation (MAO)	52
3.6.1	Micro Arc Oxidation Requirements	53
3.6.2	Experimental Procedure	53
3.7	Testing and Characterization	54
3.7.1	Coating Thickness Measurements	55
3.7.2	Light Optical Microscope (LOM) Analysis	55
3.7.3	Field Emission Scanning Electron Microscopy (FESEM) Analysis	56
3.7.4	Atomic Force Microscopy (AFM) Analysis	57
3.7.5	Antibacterial Test	58
3.7.6	Corrosion Rate Measurements	58
3.7.7	Contact Angle Test	59
3.7.8	Surgical Procedure and Implantation Test	60
3.7.8.1	Methodology	60
3.7.8.2	Histological Testing	63
<b>Chapter Four</b>		
<b>Results and Discussion</b>		
4.1	Introduction	65

4.2	Coating Thickness Results	65
4.3	Light Optical Microscope (LOM)	66
4.4	Field Emission Scanning Electron Microscopy (FESEM)	71
4.5	Atomic Force Microscopy (AFM)	102
4.6	Antibacterial	108
4.7	Corrosion Rate (CR)	109
4.8	Contact Angle	112
4.9	Histological results	115
<b>Chapter Five</b>		
<b>Conclusions and Recommendations</b>		
5.1	Conclusions	121
5.2	Recommendations	122
<b>References</b>		

## List of Abbreviations

Symbol	Definition
ACP	Amorphous calcium phosphate
Ag	Silver
$\text{AgC}_2\text{H}_3\text{O}_2$	silver acetate
Ag-FHA	fluoride, silver and hydroxyapatite
Ag-Nano-ZSM-5	nanocrystalline zeolite
Ag-ZSM-5	silver ion-exchanged conventional zeolite
BCC	Body center cubic structure
CHAp	carbonate apatite
COS	Chitooligosaccharide
Cp - Ti	Commercially pure titanium
CR	Corrosion Rate
CS/nHAp/nAg	chitosan/nano-hydroxyapatite/nano-silver particles
DC	Direct Current
DCPD	dicalcium phosphate dehydrate
EDX	Energy Dispersive X-ray
FESEM	Field emission Scanning electron microscopy
FSP	friction stir processing
HA	Hydroxyapatite
hcp	hexagonal close-packed
iNOS	inducible nitric oxide synthase
LOM	Light Optical Microscope
MAO	Micro arc oxidation
nHA	nano hydroxyapatite
NPs	Nanoparticles

OCP	Octacalcium phosphate
PCL	Polycaprolactone
SBF	simulated body fluid
TCP	Tricalcium phosphate
Ti	Titanium

## List of Symbols

Symbol	Definition
$\alpha$	Alpha phase
$\beta$	Beta phase
$TiO_2$	titanium dioxide
$Ca_{10}(PO_4)_6(OH)_2$	Hydroxyapatite
$ZrO_2$	Zirconium dioxide
$SiO_2$	Silica
$ZnO$	Zinc oxide
OH	Hydroxyl
$PO_4$	Phosphate
Ca	Calcium
$Ca_3(PO_4).5H_2O$	Tricalcium phosphate
$Ca_8H_2(PO_4).5H_2O$	Octacalcium phosphate
$CaHPO_4.2H_2O$	Dicalcium phosphate dehydrate
E. coli	Escherichia coli
S. aureus	Staphylococcus aureus

## List of Figures

Figure No	Title	Page No
1.1	Some applications of biomaterial in different biological	2-3
1.2	scheme of biomaterials properties	4
2.1	Alpha, beta and crystal structures of titanium	14
2.2	Factors and their effects on biocompatibility	18
2.3	The structure of hydroxyapatite	31
2.4	Schematic of the MAO coating system	35
2.5	Schematic illustration of the plasma discharge during different stages of the MAO process	37
2.6	Various modes of action of silver nanoparticles (Ag) on bacteria	40
3.1	Flow chart of experiment work	49
3.2	The spark during coating process	52
3.3	Schematic of MAO coating system	53
3.4	Thickness measuring device	55
3.5	Light optical microscope device	56
3.6	Field emission Scanning electron microscopy (FESEM) system	57
3.7	Atomic force microscopy system	57
3.8	Water bath device	59
3.9	Contact angle inspection device	60
3.10	Surgical clips and towels around the surgical site, reflection of skin and reflection fascia and muscles	61
3.11	Preparation of holes	61

3.12	The hole	62
3.13	Insert the implants	62
4.1	Microstructures of HA & HA/Ag coating	66-71
4.2	SEM of Nano Silver 20 nm	71
4.3	FESEM micrographs of CP-Ti specimen	72
4.4	FESEM micrographs of HA30 specimen	73-74
4.5	FESEM micrographs of HA45 specimen	75-76
4.6	FESEM micrographs of HA60 specimen	77-78
4.7	FESEM micrographs of HA30Ag0.5 specimen	79-80
4.8	FESEM micrographs of HA45Ag0.5 specimen	81-82
4.9	FESEM micrographs of HA60Ag0.5 specimen	83-84
4.10	FESEM micrographs of HA30Ag1 specimen	85-86
4.11	FESEM micrographs of HA45Ag1 specimen	87-88
4.12	FESEM micrographs of HA60Ag1 specimen	89-90
4.13	FESEM micrographs of HA30Ag1.5 specimen	91-92
4.14	FESEM micrographs of HA45Ag1.5 specimen	93-94
4.15	FESEM micrographs of HA60Ag1.5 specimen	95-96
4.16	FESEM micrographs of HA30Ag2 specimen	97-98
4.17	FESEM micrographs of HA60Ag2 specimen	99-100
4.18	EDX Analysis for Ti	101
ε, 19	EDX Analysis for composite coating (HA) on CP-Ti.	102
ε, 20	EDX Analysis for composite coating (HA/Ag) on CP-Ti.	102
4.21	AFM of HA specimens	103
4.22	AFM of HA/Ag0.5 specimens	104

4.23	AFM of HA/Ag1 specimens	105
4.24	AFM of HA/Ag1.5 specimens	106
4.25	AFM of HA/Ag2 specimens	107
4.26	Results of the antibacterial test	108-109
4.27	The relationship between corrosion rate and time	111
4.28	Contact angle between CT-Ti specimen and HA electrolyte	113
4.29	Contact angle between CT-Ti specimen and HA/Ag0.5 electrolyte	113
4.30	Contact angle between CT-Ti specimen and HA/Ag1 electrolyte	114
4.31	Contact angle between CT-Ti specimen and HA/Ag1.5 electrolyte	114
4.32	Contact angle between CT-Ti specimen and HA/Ag2 electrolyte	115
ε, 33	A section in the bone treated with CP-Ti group at 40 day	116
ε, 34	A section in the bone treated with coating (HA60) on CP-Ti group at 40 day	116-117
ε, 35	A section in the bone treated with composite coating (HA60Ag0.5) on CP-Ti group at 40 day	118
ε, 36	A section in the bone treated with composite coating (HA60Ag1) on CP-Ti group at day	118
ε, 37	A section in the bone treated with composite coating (HA60Ag1.5) on CP-Ti group at 3 day	119
ε, 38	A section in the bone treated with composite coating (HA60Ag2) on CP-Ti group at 3 day	120

## List of Tables

<b>Table No</b>	<b>Title</b>	<b>Page No</b>
1.1	Different Classes of Materials	2
1.2	Characteristics of biomaterials	4
2.1	Comparison of metallic biomaterials used in the human body	10
2.2	Mechanical properties of metallic implant materials and cortical bone	12
2.3	The properties of titanium	15
2.4	Mechanical properties of bone vs HA	29
2.5	Solid phases of biological calcium-phosphate	32
3.1	Chemical analysis of (CP-Ti) substrate	50
3.2	Parameters of MAO process	54
3.3	Composition of Ringer's solution	59
ε, λ	Result of coating thickness	65-66
4.2	Chemical Composition of nAg	72
4.3	Roughness of specimens	102-103
4.4	Antibacterial results	108
4.5	Corrosion rate measurements	109-111
4.6	Contact angle between (CP-Ti) specimen and electrolytes	112

## *Chapter One*

### *Introduction*

#### **1.1 General View**

Biomaterials are defined as any synthetic or modified natural materials which come into contact with body tissues or fluids. Biomaterials research is aimed toward providing the biomedical community with the best possible materials needed to aid in the restoration of bodily function and / or appearance [1]. For decades, biomaterials have been successfully used in medical applications to improve both the quality and the length of life of many people. Their wide ranges of functions vary from drug delivery systems to replacing, augmenting, or repairing tissues, organs, or functions of the body. But these functions were only achieved after many different attempts, research works, and historical developments made over the centuries [2].

Biomaterials are an artificial content that is implanted into living organisms to substitute body organs for fulfilling typical functionalities of the whole body for an extended span of time or even for the entire life [3]. As such, these must be nontoxic, non-cancerous, synthetically dormant, stable, and mechanically sufficiently solid to withstand the rehashed strengths for the lifetime [4]. It is rare to find the material that satisfies all the requirements suitable for human body environment. Hence, researchers attempt to combine the properties of various materials to cope with these challenges [3].

The materials that are used to build biomedical devices (orthopedic, dental, bone cements, etc.) can be classified into metallic materials, ceramics, polymers, and composites [5] they are listed in table (1.1). Most of the biomaterials available today are developed either singly or in

combination of the materials of these classes. These classes of materials have different atomic arrangement which present the diversified structural, physical, chemical, and mechanical properties and hence offer various alternative applications in the body [6] shown in figure (1.1) [3].

Table 1.1 Different Classes of Materials are Used for Designing Biomaterials and Their Advantages and Disadvantages in Application Filed [6].

Class of the Material	Advantages	Disadvantages
Polymers (Nylon, silicones, PTFE)	Resilient, Easy to fabricate	Not strong, Deform with time, May degrade
Metals (Titanium, stainless steels, Co Cr alloys, gold)	Strong, Tough, Ductile	May corrode , high density and difficult to make
Composites (Various combinations)	Strong, Tailor-made	Difficult to make
Ceramics (Aluminum oxide, carbon, hydroxyapatite )	Highly biocompatible, Inert, high modulus, Compressive strength, Good esthetic properties	Brittle, Difficult to make, , Poor fatigue resistance

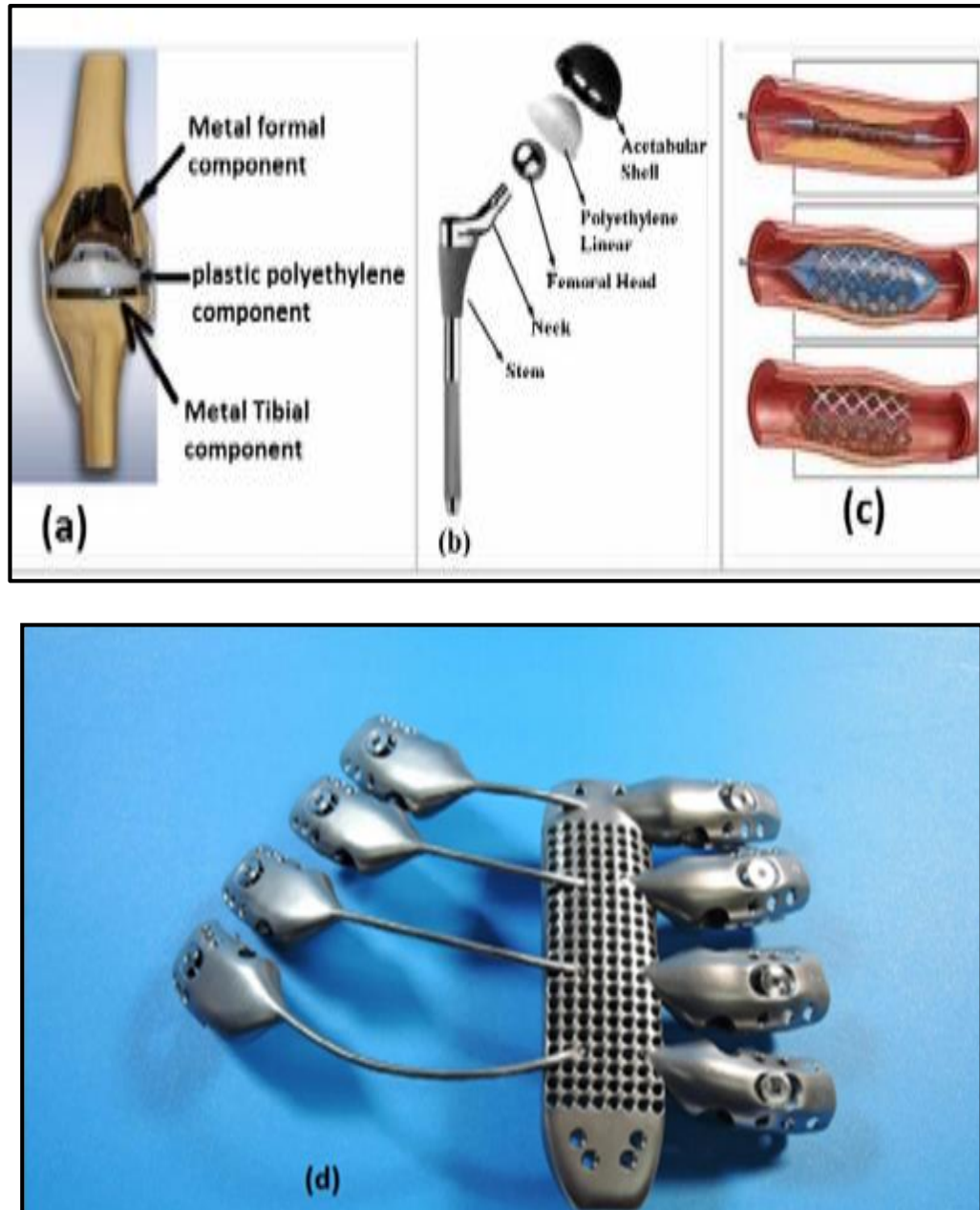


Figure 1.1 Some applications of biomaterial in different biological systems (a) Artificial Knee joint (b) Hip joint (c) Mesh type (d) 3D printed sternum and rib cage [3].

### 1.1.1 Properties of Biomaterials

The different properties of biomaterials have been shown to have an important influence in their dynamic interactions with the biological surroundings when used as medical implants and organ or tissue replacements. The performance and success of each one of these implants

depend upon the properties and biocompatibility of the biomaterial used to construct it. Thus, when designing any medical device or implant, it is critical to evaluate the material properties within the context of its future biomedical application. In general, the most important properties associated with biomaterials are classified into chemical, physical, mechanical, and biological in relation to the bulk and surface of the material. These are summarized in Figure 1.1.

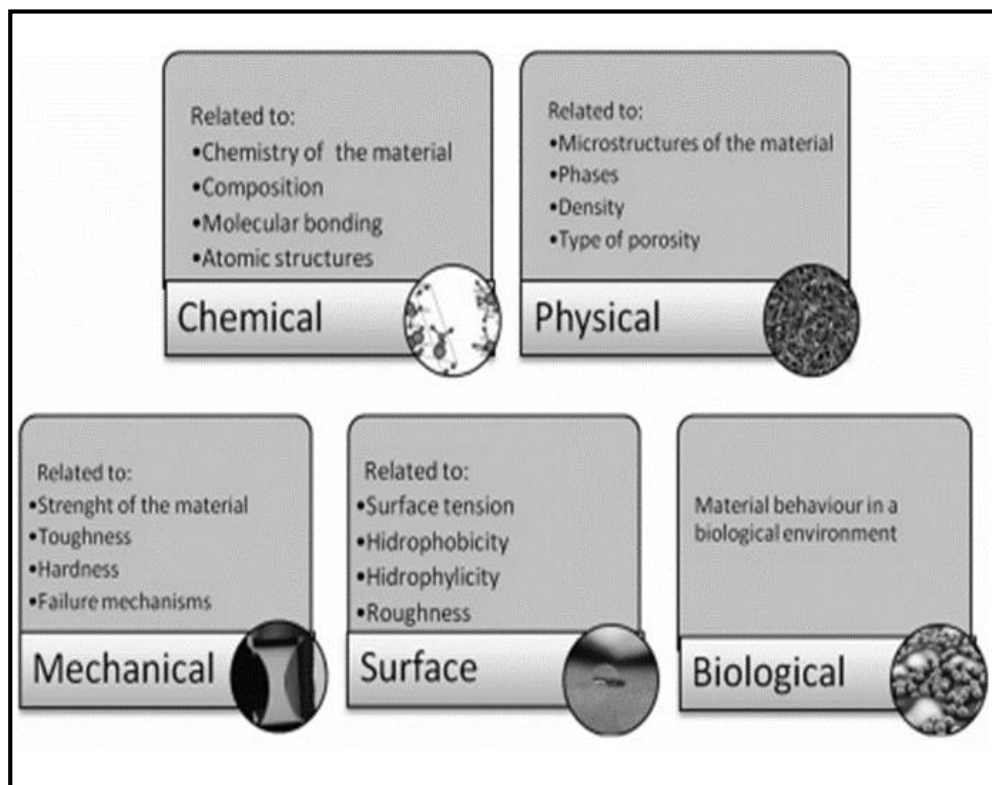


Figure 1.2 scheme of biomaterials properties [2].

### 1.1.2 Characteristics of Biomaterials

The fundamental characteristics that a biomaterial should possess in order to run successfully as an implant in the living system are mentioned below table (1.2) [5].

Table (1.2) Characteristics of biomaterials

Properties of Biomaterials	Explanation
Biocompatibility	Non-toxic and does not cause allergic reaction when implanted into the body. Ideal implants or their wear particles do not cause complication.
High Wear Resistance	Upon usage in artificial joints, only a few wear particles are produced, thus solving the primary issue of bio implants and prolonging the lifespan of artificial joints. It reduces volume loss to minimise the risk of wearing via polyethylene cup that increases the stability of prostheses.
High corrosion resistance	High corrosion resistance mitigates damage caused by corrosive wear, hence reducing wear rate. Metal alloys are popular for fabricating femoral heads, and the quantity of metallic ions released into synovial fluids is related to bio implant corrosion resistance. Prostheses, made of material with higher corrosion resistance, generate very few metal ions, thus reducing the possibility of allergic reaction [7].
Good mechanical properties	Hip or knee prostheses must bear 3—5 times the load of our body weight in vivo. The mechanical properties of biomaterials can withstand in vivo condition. Elastic modulus is crucial, but large modulus may cause bone atrophy, while high fatigue strength decreases the risk of catastrophic failure due to cyclic loading.

	Considering other mechanical properties (stiffness, hardness, and tensile & shear strength) is vital when selecting implant biomaterials [8].
Osseo-integration	<ul style="list-style-type: none"> <li>• Development of integration between an implant and bone without intercede the delicate tissue.</li> <li>• For great Osseo-integration, the aspects such as surface science, surface unpleasantness and surface geography are the significant factor [9].</li> </ul>

## 1.2 Main Issues

Commercially pure (CP)-Ti and Ti-6Al-4V are the most commonly used implants in biomedical applications [10] but when they are used in implants present several main problems:

Although the inert behaviour of Ti is a good property, its bone attachment is difficult because it do not react with the human tissues [11]. When implants do not undergo surface modification to enhance the osteoconductivity, it takes a relatively long time to fix the metallic implant to bone such that it is stable. There are many approaches for improving the osteoconductivity of Ti and its alloys [12]. One approach to improving implant lifetime is to coat the metal surface with a bioactive material that can promote the formation and adhesion of hydroxyapatite (HA) ( $Ca_{10}(PO_4)_6(OH)_2$ ), the inorganic component of natural bone [11]. The porous and rough morphology produced by the micro arc oxidation (MAO) process increased the cell attachment and mechanical interlocking of the tissue and implant. Moreover, the Ca and P sources, incorporated from the electrolyte into the coating

layer, improved the osteoblast cell responses and further osseointegration [13].

Although success rates of these kinds of implants are dependent on bone-implant osteointegration, the success and long-term survival of the implants are also dependent on the prevention of bacterial infection after implant placement [14]. One way to prevent such infections is to modify the implant surface with antibacterial coatings when maintaining good biocompatibility [15]. The battle against bacteria profits from the rapid development of nanotechnology allowing the use of antimicrobial materials in a more efficient way. In this spirit, antibacterial effects of silver nanomaterials are strongly exploited in consumer products [16]. We therefore need more research for a better understanding of potential implications for human health. The development of biomaterials that are both bactericidal and biocompatible has many applications in medicine and are currently under scrutiny. To improve osteointegration, a way of obtaining both bioperformance and biocompatibility could be by means of bioactive coating. For instance, HA and silver together are suitable because HA is a component of bone biomimetic hydroxiapatite, while silver nanoparticles have the antibacterial effect [17]

Coating techniques are simple and intuitive approaches to obtain a modified surface [18]. Typical coating methodologies like, plasma spraying, alkaline treatment, acid etching, laser surface treatment, anodic oxidation and MAO are extensively studied at laboratory scale. Compared with other surface modification techniques, MAO is one of the most applicable methods to deposit a porous bioceramic layer on Ti and its alloys [19].

### **1.3 Aim of Work**

The micro arc oxidation coated surface can contain calcium and phosphorus ions according to the selected electrolyte. These precipitations containing Ca–P ions in the titanium oxide layer can further crystallized into HA through a hydrothermal treatment. The HA facilitates the adhesion of cells and growth of new bones. So MAO should be a good surface modification process to improve the biological properties of titanium.

In this work used CP-Ti modify with composite coating (HA or HA/nAg) by micro arc oxidation technique to study the in vitro and in vivo properties of the sample before and after coating process. The in vitro test included FESEM, EDX, AFM, antibacterial, corrosion test in Ringer's solution, while in vivo test included surgical process and embed the implants in the rabbit for 40 day.

***Chapter Two******Theoretical Part and Literature Survey*****2.1 Introduction**

This chapter explains commercial pure titanium and its biocompatibility and modify its surface with composite coating (hydroxyapatite / nano silver) by micro arc oxidation technique. Literature survey for studies about the current work will be highlighted.

**2.2 Historical Background**

Metallic materials are used as structural materials for medical devices in the fields of orthopedic surgery, blood circulatory system dentistry. Approximately 70% of the structural materials employed in implants are found to be metallic materials [21]. The use of metallic materials for medical implants can be traced back to the 19th century, leading up to the era when the metal industry began to expand during the industrial revolution [22]. The first metal alloy developed specifically for human use was the “vanadium steel” which was used to manufacture bone fracture plates (Sherman plates) and screws. Most metals such as iron (Fe), chromium (Cr), cobalt (Co), nickel (Ni), titanium (Ti), tantalum (Ta), niobium (Nb), molybdenum (Mo), and tungsten (W) that were used to make alloys for manufacturing implants can only be tolerated by the body in minute amounts. Sometimes those metallic elements, in naturally occurring forms, are essential in red blood cell functions (Fe) or synthesis of a vitamin B12 (Co), but cannot be tolerated in large amounts in the body. The biocompatibility of the metallic implant is of considerable concern because these implants can corrode in an in vivo environment. The consequences of corrosion are the disintegration of the implant material per se, which will weaken the implant, and the harmful effect of corrosion products on the surrounding tissues and organs [23].

Researchers were successfully able to develop different biomaterials and technologies related to joint replacement in human body such as metallic materials (stainless steel, Co-Cr Alloys and Ti and its Alloys). These materials are selected mostly based on their bulk mechanical properties nearly matching with human bone properties and inertness towards the body tissues or fluid [24].

Table 2.1 Comparison of metallic biomaterials used in the human body [25].

Metals and alloys	Selected examples	Advantages	Disadvantages	Principal applications
Titanium based Alloys	CP-Ti, Ti-Al-V, Ti-Al-Nb, Ti-13Nb-13Zr, Ti-Mo-Zr-Fe	High biocompatibility, low Young's modulus excellent corrosion resistance, low density	Poor tribological properties, toxic effect of Al and V on long term	Bone and joint replacement, fracture fixation, dental implants, pacemaker encapsulation
Cobalt and Cr alloys	Co-Cr-Mo, Cr-Ni-Cr-Mo	High wear resistance	Allergy consideration with Ni, Cr and Co much higher modulus than bone	Bone and joint replacement, dental implants, dental restorations, heart valves
Stainless	316L	High wear	Allergy	Fracture

steels	stainless steel	resistance	consideration with Ni, Cr and Co much higher modulus than bone	fixation, stents, surgical instruments
Other	Ni-Ti	Low Young's modulus	Ni cause allergy	Bone plates, stents, orthodontic wires
	Platinum and Pt-Ir	High corrosion resistant under extreme voltage potential and charge transfer conditions	Hard	Electrodes
	Hg-Ag-Sn amalgam	Easy in situ formability to a desired shape susceptible to corrosion in the oral environment	Concerns related to Hg toxicity	Dental restorations

Metals are used as biomaterial due to their excellent electrical and thermal conductivity and mechanical properties. Since some electrons are independent in metals, they can quickly transfer an electric charge and thermal energy. The mobile free electrons as the binding force to hold the positive metal ions together. This attraction is strong, as evidenced by the

closely-packed atomic arrangement resulting in high specific gravity and high melting points of most metals. Since the metallic bond is essentially non-directional, the position of the metal ions can be altered without destroying the crystal structure, resulting in a plastically deformable solid [23].

Table 2.2 mechanical properties of metallic implant materials and cortical bone [26].

Materials	Young's modulus/Gpa	Ultimate tensile strength/MPa	Fracture toughness (MPa.m <sup>1/2</sup> )
CoCrMo alloys	240	900-1540	100
316L stainless steel	200	540-1000	100
Ti alloys	105-125	900	80
Mg alloys	40-45	100-250	15-40
NiTi alloy	30-50	1355	30-60
Cortical bone	10-30	130-150	

The high strength and resistance to fracture that this class of material can provide, assuming proper processing, gives reliable long-term implant performance in major load-bearing situations. Coupled with a relative ease of fabrication of both simple and complex shapes using well-established and widely available fabrication techniques (e.g., casting, forging, machining) [27].

Metallic implants are used for two primary purposes:

- (i) implant devices used as prostheses serve to replace a portion of the body and include devices such as total joint replacements and skull plates and
- (ii) as fixation devices that are used to stabilize broken bones and other tissues while normal healing [28].

### **2.3 Titanium (Ti)**

The name “Titanium” comes from the mythological first sons of the Earth, the Titans in Greek mythology. Chemically, titanium is one of the transition elements in the group IV and period 4 of periodic table [29]. Being a transition element, titanium has an incompletely filled shell in its electronic structure, which enables titanium to form solid solutions with most substitutional elements [30]. Commercially pure titanium (CP-Ti) and titanium alloy are preferred for dental and orthopedic implants or prosthesis because of their corrosion resistance, biocompatibility, durability, and strength. However, being bioinert, the integration of such implants in bone is not in good condition [31].

The first report on CP Ti for medicine was appeared in 1940, and excellent bone compatibility was found based on an animal test. Thereafter, the compatibility to bone and soft tissue of rabbits, noncytotoxicity due to excellent corrosion resistance in biological environments, and excellent biocompatibility in dogs were reported. The largescale industrial manufacturing process for Ti achieved in the last half 1940s made it possible to conduct many studies for medical applications, revealing excellent biocompatibility in long-term animal testing. Thereafter, the usefulness of CP Ti was widely recognized by the last half 1960s [32].

### 2.3.1 Structural Properties of Titanium

Titanium is widely used in various applications because of the possibility of modifying its properties by varying the alloying element composition. Titanium undergoes an allotropic transformation i.e. it changes from one crystallographic form to another. At room temperature, it exists in hexagonal close-packed (HCP) structure and this is called alpha ( $\alpha$ ) phase. At 883 °C it changes to body centered cubic structure (BCC) called the  $\beta$  phase. The temperature at which  $\alpha$  or  $\alpha + \beta$  changes to all  $\beta$  is called  $\beta$  transus temperature [10]. The two forms of unalloyed titanium are shown in Figure 2.1 a ,b. The  $\alpha$  to  $\beta$  transformation temperature varies when alloying elements are added to Ti, depending on the nature of these elements and their concentration. Alloying elements such as Al, O, N, and C tend to stabilise the  $\alpha$ -phase and are known as  $\alpha$  stabilisers. The addition of these elements increases the beta transus temperature. The elements, such as V, Mo, Nb, Ta, Fe, and Cr, stabilise the  $\beta$ -phase and are known as  $\beta$  stabilisers [33]. The addition of these elements decreases the  $\beta$  transus temperature, Figure 2.1 c

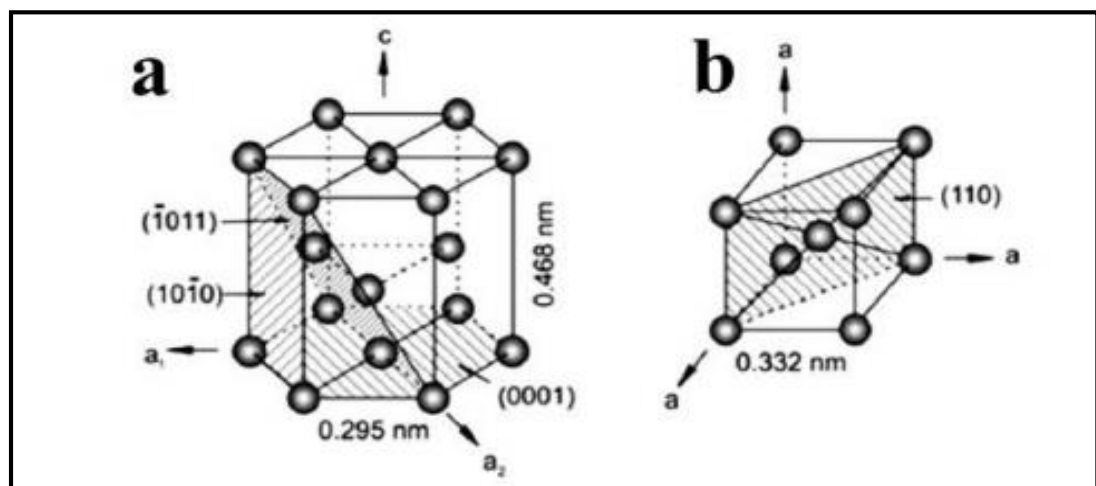


Figure 2.1 Alpha (a) and beta (b) crystal structures of titanium and the different categories of titanium phase diagrams depending on the alloying elements [33].

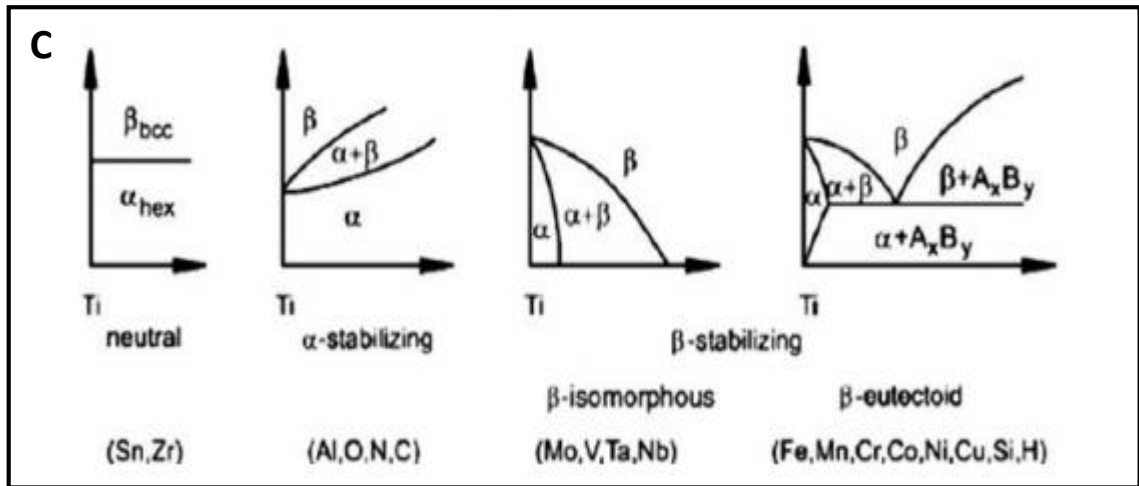


Figure (2.1): Alpha (a) and beta (b) crystal structures of titanium and the different categories of titanium phase diagrams depending on the alloying elements (Contd)

### 2.3.2 The Properties of Ti

The properties of unalloyed titanium are summarised in Table (2.3).

Table (2.3): The properties of titanium [29].

Property	Value
Atomic number	22
Atomic weight (g/mol)	47.90
Crystal structure	
Alpha, hexagonal, closely packed	
c (Å)	4.6832 ± 0.0004
a (Å)	2.9504 ± 0.0004
Beta, cubic, body centered	
a (Å)	3.28 ± 0.003
Density (g cm <sup>-3</sup> )	4.54
Coefficient of thermal expansion at 20 °C (K <sup>-1</sup> )	8.4 * 10 <sup>-6</sup>
Thermal conductivity (W/(m K))	19.2

Melting temperature (°C)	1668
Boiling temperature (estimated) (°C)	3260
Transformation temperature (°C) from $\alpha$ to $\beta$	882.5
Electrical resistivity	
High purity ( $\Omega\mu\text{cm}$ )	42
Commercial purity ( $\Omega\mu\text{cm}$ )	55
Modulus of elasticity (GPa)	105
Yield strength (MPa)	692
Ultimate strength (MPa)	785

### **2.3.3 Biocompatibility of Titanium**

Biocompatibility is defined as “the ability of a material to perform with an appropriate host response in a specific application”. The biocompatibility of a material is governed by initial and continuous reactions between the material and host body: adsorption of molecules, protein adsorption, cell adhesion, bacterial adhesion, activation of macrophage, formation of tissues, inflammation, etc. In addition, the reaction occurs with a temporal and spatial hierarchy. CP Ti shows a unique property, “osseointegration,” among metals. It is the “formation of a direct interface between an implant and bone, without intervening soft tissue. No scar tissue, cartilage or ligament fibers are present between the bone and implant surface. The direct contact of bone and implant surface can be verified microscopically”. Osseointegration shows the excellent hard-tissue property of Ti [32].

The biocompatibility of these materials is a direct consequence of the chemical stability and structural integrity of a titanium oxide film [34]. To

improve the bone bonding ability of titanium implants, many attempts have been made to modify the structure, composition, and chemistry of the titanium surfaces including deposition of bioactive coatings. Among the various techniques, hydroxyapatite (HA) coatings by micro arc oxidation [35].

Biocompatibility is the primary requirement for biomaterials. Biocompatibility of implant devices relies on several issues, as illustrated in (Figure 2.2), which ultimately affects the performance of implant device. Inappropriate design of the implant devices, unwanted device degradation/corrosion and/or development of adverse host tissue reaction can lead to device failure. A foreign material when placed in or entered the human body as a result of corrosion process, tissue reacts with it in a variety of ways. These reactions are usually highly undesirable and have the potential to lead to reactions such as chronic inflammation and or hypersensitivity. Hypersensitivity, is either immediate or delayed response due to the contact with metals, corrosion products or metallic salts and is fairly common, affecting more than 15% of the population. Metal ions may also be associated with problems such as cytotoxicity, genotoxicity, carcinogenicity, etc [7].

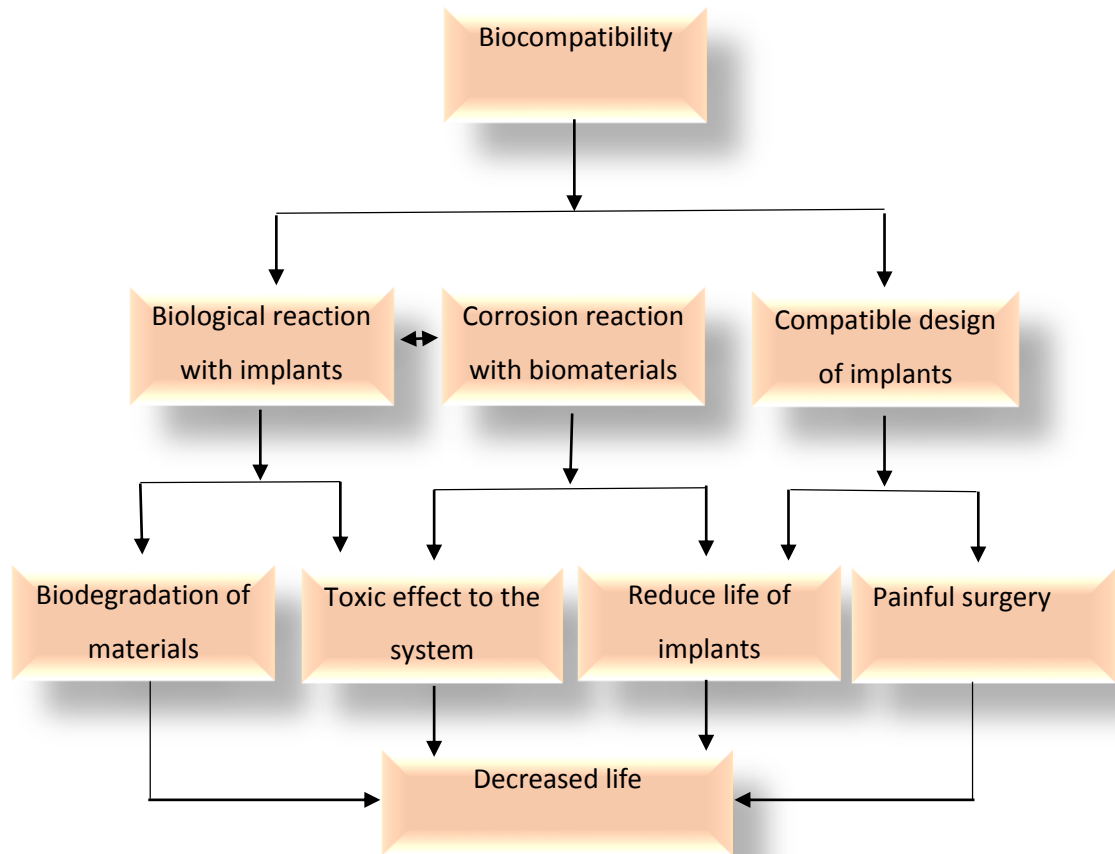


Figure (2.2) Factors and their effects on biocompatibility [7].

## 2.4 Corrosion Resistance

Ti shows excellent corrosion resistance compared with other metals, inducing low toxicity [34]. One of the reasons for the excellent biocompatibility of Ti is caused by the excellent corrosion resistance, while the corrosion resistance is not sufficient condition for the biocompatibility. Even the best corrosion resistant metal, Au, is inferior in tissue compatibility. In addition, electric plating of Pt to Ti increases the corrosion resistance but depletes bone formation, because a property of Ti is shielded, and the bone formation ability is prevented. These results reveal that hard-tissue compatibility is not induced only by the corrosion resistance. In other words, the corrosion resistance is a necessary condition but not a sufficient condition for biocompatibility [32].

**2.5 Mechanical Properties of Natural Bone**

Human bone is a connective tissue made up of fibres and cells. Bone provides internal support, protects vital organs and presents an anchorage site for muscles. Also, the bone has to maintain calcium homeostasis and hematopoiesis. In order to serve these functions, bone has to be stiff to avoid bending. On the other hand, it should be able to absorb energy hence needs to be flexible. Human skeleton can be divided into two kinds of bone tissue, namely cortical and trabecular. Cortical bone shows high compressive strength because of its high mass per unit volume and low porosity (10%). It provides the strength and rigidity to the bone. Trabecular bone, on the other hand, displays high porosity. Out of the total trabecular bone volume around 50-90% is made up of pores [10]. Hence, it has a lower value of Young's modulus and ultimate compressive strength. It allows red bone marrow and bone vessels to come in contact with bone by providing increased surface area.

To use titanium as an implant one needs to ensure that the mechanical properties are similar to those of the human bone i.e. there is no mechanical mismatch between the bone and the implant. The elastic modulus of human cortical and trabecular bone are 4-30 GPa and 0.2-2 GPa, respectively. Compressive strength values of cortical and trabecular bone are 20 -193 MPa and 2-80 MPa whereas yield strength of femoral bone and tibial bone are 104–121 MPa and 120–140 MPa [37].

Mismatch of Young's modulus between the bone and implant has been identified as one of the major issues associated with the current implant materials. This phenomenon is called stress shielding. Under normal circumstances, bone carries the load by itself. When an implant is introduced in the bone, the load is shared between the bone and the implant. So, the bone will experience reduced stress and hence will experience stress

shielding. According to Wolff's law, the bone tries to oppose the applied load and accordingly develop the most suitable structure. As a result, the areas of the bone that are under high load will have increased bone mass. The areas with lesser load would experience a decrease in bone mass. This decrease in bone mass is called bone resorption and can cause failure of the implant [10].

### **2.6 Failure of Implants**

Surgical implants are usually submitted to aggressive working conditions in terms of corrosion, wear and mechanical loading (static and dynamic). The premature failure of metallic implants are influenced by several factors, which include: mechanical design; material selection; manufacturing practice; medical installation procedure; postoperative complications; and patient's misuse [38].

After implantation, the performance of an implant falling below a specific acceptable level is a major issue that affects its intended therapeutic time and can even lead to surgical revisions. The biocompatibility, functionality, and retention of the implant material should be positively encouraged and focused on the interaction between the material and the host system [39]. Various factors, such as particulate matter and debris from ions (caused by corrosion/wear), fibrous encapsulation (caused by insufficient bone integration), inflammation, low fracture toughness, low fatigue strength, variations in the modulus of elasticity of the implant material and the surrounding bone (stress shielding) and infection can lead to failure of an implant. This unstable fixation of implants can be overcome by stable, rapid bone formation in the deficient bone site that makes for firm fixation of an implant to the adjacent bone. To accomplish the requisite surface properties of the implant material, an appropriate surface modification procedure is necessary to enhance its biomedical applications. Hence, the material

comprising an implant should be well tolerated by the biological system. The implant causes the development of a fibrous collagen sheath of low cellularity, which encapsulates and separates the implant from normal tissue. If the thickness of the sheath around the implant is very thin, the tolerability by the host system is easy and fewer corrosion products are formed [40,41].

### **2.6.1 Mechanism of Implant Failure**

Uncoated metal implants have a chance of causing implant loosening or rejection coupled with bacterial colonization. Even when coated with a bioactive material, the rate of dissolution of a coating may decrease the lifetime of an implant. Rapidly dissolving HAP coatings are resorbed by osteoclasts. The resorbed coatings are integrated into the normal bone remodeling process and replaced with new bone by the osteoblasts. The dissolution rate of HAP coatings is significant because a rapidly dissolving coating can lead to bone growth. However, rapid dissolution of the coating may also lead to loss of fixation, implant loosening and the production of particle debris. The second mechanism of implant failure with surface coatings is attributed to third-body wear, which results in osteolysis. Osteolysis is degradation of the bone caused by osteoclasts, or bone-resorbing cells. Mechanical stress placed on a hip implant by the patient is believed to be the source of third-body wear [41].

The literature searches show that the application of ceramic coatings to metal alloys can impart corrosion resistance, wear resistance and bioreactivity that are beneficial for medical devices. Particularly, HA ceramic coatings on metallic substrates attract special attention from the research communities because of their excellent biocompatibility and bioactivity properties [42]

**2.7 Surface Modification with Coating Layer**

Biological responses to implants largely depend on the surface properties of biomaterials, such as surface chemistry and physical structure. As implants are inserted in human body, a variety of acute or chronic responses occur at the biomaterial surface [43].

Materials implanted in vivo initially contact with extracellular body fluids such as blood and interstitial fluid. The chloride ion concentration in plasma is 113 mEq l<sup>-1</sup> and in interstitial fluid is 117 mEq l<sup>-1</sup>, which may corrode metallic materials. Body fluids contain amino acids and proteins that tend to accelerate corrosion. Body fluids also act as a buffer solution and accordingly, their pH changes little. The pH of normal blood and interstitial fluid is 7.35–7.45. However, the pH decreases to about 5.2 in the hard tissue due to implantation, and recovers to 7.4 within 2 weeks. Thus, corrosion due to an abrupt change in body fluid pH appears negligible. Whatever the cause, toxicity and allergy occur in vivo if metallic materials are corroded by body fluid, if metallic ions are released into the fluid for a long time, and if ions combine with biomolecules such as proteins and enzymes. Finally, we provide improved materials processed by surface modification [44].

Coating techniques are simple and intuitive approaches to obtain a modified surface. A variety of conventional physical and chemical coating methods (e.g. solvent evaporation, plasma spraying, and physical/chemical vapor deposition (CVD)) have been industrialized, while novel approaches involving recently developed and developing techniques are continuously coming forth. What will be introduced in this section are state-of-the-art physical and chemical methods for creating functional coatings on different biomaterial surfaces [43].

Bioimplants surface alteration methods include chemical vapor deposition (CVD), physical vapor deposition (PVD), sol-gel, plasma spraying, laser surface melting, electrochemical deposition, spray pyrolysis, electrophoretic deposition, dip coating [43], sandblasting, plasma spraying, alkaline treatment, acid etching, laser surface treatment, anodic oxidation and micro arc oxidation [18] and so on which have some limitations such as being unable to produce defect-free, porous surfaces and demanding extra processing cost because they are not able to shape and deposit at the same time while they have some advantages as well [45].

### **2.8 Composite Coatings**

Biomaterials can be made as composites for advanced applications if a single material is incapable of fulfilling the various requirements of the given application. Composite coatings are an emerging area of surface modification of metallic biomaterials in which a functional surface layer with the required physical, mechanical, or biological properties covers a bulk biomaterial. For instance, titanium/porous titanium composites have advantageous mechanical properties, Ti/ceramic composite show special biological properties with improved osseointegration features, and the special physical properties of Ti/ceramic composites make them suitable for heart pacemaker leads [46]. In the course of developing metallic biomaterials, various combinations such as ceramic/ceramic and ceramic/polymer have been proposed recently.

The incorporation/immobilization of biomolecules into calcium phosphate has received a considerable interest in the coating of metallic biomaterials. The presence of appropriate biomolecules at the surface may provide signals to selected types of cells and promote their adhesion or function [47]. Besides biocompatibility and osseointegration, the composite coatings may also enhance the corrosion resistance. To increase the Ti

ability to bond with bone, a mixture of titanium dioxide ( $\text{TiO}_2$ ) and CaP was fabricated and deposited as a coating [48]. Therefore, CaP/ $\text{TiO}_2$  coatings can be expected to combine the advantages of  $\text{TiO}_2$  with those of CaP. Inspired from the structure of natural bone, biopolymers such as collagen, gelatin, silk fibroin, chitosan, and poly(lactide-co-glycolide) have been used to make composite with bioactive inorganic materials such as calcium phosphate [49].

The resultant composites are mechanically superior to individual component due to the ductile properties of the biopolymer, which increase the fracture toughness of the inorganic component [50]. In an attempt to rectify the disadvantages of a single CaP or polymer coating, a composite coating composed of dicalcium phosphate dehydrate (DCPD) and polycaprolactone (PCL) was prepared on the MgZn alloy. Compared to the DCPD-coated alloy, the DCPDePCLcoated alloy showed higher corrosion resistance, as manifested by the elevated corrosion potential, reduced corrosion current, and less hydrogen released [48].

## **2.9 Bioactive Coatings**

Bioactive refers to a material, which upon being placed within the human body interacts with the surrounding bone and in some cases, even soft tissues. This occurs through a time– dependent kinetic modification of the surface, triggered by their implantation within the living bone. An ion-exchange reaction between the bioactive implant and the surrounding body fluids-results in the formation of a biologically active carbonate apatite (CHAp) layer on the implant that is chemically and crystallographically equivalent to the mineral phase in bone. Prime examples of these materials are synthetic hydroxyapatite [ $\text{Ca}_{10}(\text{PO}_4)_6(\text{OH})_2$ ], glass ceramic and bioglass [51]. Bioactive ceramics have been employed in many clinical applications

during the last decades, for non-load-bearing applications, such as periodontology [52].

The use of bioactive ceramics in structural components is strictly limited by their intrinsic brittleness, which can lead to sudden and unpredictable fractures. Furthermore, these materials generally have low strength. Although some bioactive materials have been designed to have good mechanical properties, such as the AW glass-ceramic, their use is limited to components under compressive loads. In order to overcome such limitations, bioceramics can be successfully used as coatings on a strong bioinert metal implant to improve its adhesion to bone tissue. For example, this approach is commonly applied in total joint hip replacement. A hip implant must primarily meet mechanical requirements, since it is severely stressed. The elements composing a total joint hip replacement are the acetabular cup, and the femur part, which is composed by the stem and the head of the femur. Since the acetabular cup and the femoral head are mainly stressed in compression, and they are subjected to intense wear, these parts can be made of ceramic such as alumina and zirconia (the cup also in UHMWPE). The stem, instead, is subjected to compression and flexion. Accordingly, this component must be realized with a tough material as stainless steel, titanium and its alloys or Cr-Co alloy.

Nowadays it is an established practice to increase the adhesion of the stem through the use of bioactive coatings. The increased adhesion has been demonstrated to be positive in terms of life expectancy of the prosthesis and rehabilitation of the articulation [53]. Bioactive ceramic coatings have been successfully used on dental screws as well. In this case, a screw usually made of titanium or its alloys, is fixed into the jaw to lock a dental prosthesis. The introduction of a bioceramic coating greatly improves the screw stability and hence its life expectancy [54]. This kind of coatings has

been used on metallic implants in dentistry and orthopaedics since the middle of the '1980s.

### **2.10 Properties of Bioactive Coatings**

The microstructure of coatings strongly depends on the production technique and on the feedstock materials. Generally speaking, a good coating should have a compact structure, small grain size with high cohesion, and no defects such as cracks or large pores [53]. A defectfree microstructure usually results in good mechanical properties and resistance. If functional coatings are considered, such as bioactive ones, these parameters may not be the most important ones. In fact, although a good adhesion and cohesion are essential properties for all kinds of coatings [55], other properties can play an important role. As far as the bioactivity is concerned, porosity is a crucial parameter, since it influences the interactions at the implant host tissue interface, especially the reaction rate. In fact, the open porosity controls the specific area in contact with body fluids [56, 53]. Moreover, a porous coating allows a deeper penetration of cells inside the biomaterial, and thus higher levels of cell attachment can be reached [57]. Porosity can also be a way to tune the stiffness of a material, as it happens for natural bones. In this way, it is possible to reduce the stiffness of biomedical materials, to match that of natural bone tissue, thus limiting the so-called “stress shielding” effect. On the other hand, an excessive porosity can lead to poor cohesion and low bonding strength, which may cause some parts of the coating to peel off during the dissolution process. It is worth noting that debris and fragments from bioactive materials are usually innocuous from a chemical point of view. In commercial HA coatings, the porosity may vary from 1% up to 50% [53].

Also the surface roughness of a bioactive coating affects the dissolution rate and bone growth. In fact, the surface exposed to the

physiological medium increases with increasing roughness. Moreover, the beneficial effect of morphological and biological fixation becomes relevant. A marked roughness is also positive for the biological activity, since the surface asperities promote both the absorption of organic metabolites and the cell attachment [58]. Another key parameter is the coating thickness. The thickness, indeed, affects both the resorption and the mechanical properties of bioactive coatings. Most of the commercial coatings for orthopedic use are produced in the thickness range 50-75  $\mu\text{m}$  [53].

## **2.11 Coating Materials**

### **2.11.1 Ceramics**

Bioceramics used as implants can take several forms, such as dense implant, porous network micro- and nano- particale and sphere, coating and composite with polymeric materials. Owing to the limited mechanical properties and superior bioactivity of bioceramics, bioinertness and excellent mechanical strength of the metallic biomaterials, bioceramic coating on the metal implants is a very promising approach for orthopedic implants with both strength and bioactive. Bioceramic coatings can provide stable fixation with tissue and shield the metal implants from corrosion environment. The thickness of the bioceramic coating varies from several microns to several hundreds microns [59].

The inherent properties of ceramics, including their high compressive strength, compared to metallic materials due to the formation of atomic bonding at elevated atmospheres, and their combination of ionic and covalent bonds, make them suitable for replacing various parts of the body, particularly bone and dental crowns in dentistry. These implantable ceramic materials, termed bio-ceramics are used for the repair and reconstruction of diseased and damaged body parts. They are categorized as bio-inert, bio-

reactive and bio-resorbable in reference to their interaction with the biological environment. Bio-ceramics are generally free from debris and can be designed with properties close to those of bone natural materials. Bio-ceramics of these types are used to produce femoral head components of the ball and socket, an acetabular component of the hip implant. Materials such as silicates, metallic oxides, carbides, and selenides are used in enhanced applications due to their improved physio-chemical properties. Bioinert ceramic materials have been found to have more mechanical properties than other ceramics. Some ceramics such as glass and calcium phosphates are classified as bioactive ceramics depending on their formation of bonds in physiological solutions. These bioactive ceramics are used mainly as coating materials in orthopedic and dental implants due to their characteristic ability to form bond between the bone and surrounding tissues. Bio-ceramics with low tensile strength and low fracture toughness are limited to use in heavy load applications. These drawbacks can be overcome by using them as coatings on metallic material and for such heavy load applications as joint replacements [33] Such as Hydroxyapatite (HAP), Titanium dioxide ( $\text{TiO}_2$ ), Zirconium dioxide ( $\text{ZrO}_2$ ), Silica ( $\text{SiO}_2$ , Bioglass), Zinc oxide ( $\text{ZnO}$ ) [41].

#### **2.11.1.1 Hydroxyapatite**

Hydroxyapatite is biocompatible and osteoconductive, allowing the growth of bone cells on its surface. As a result of its favourable biological properties, it has been used successfully for many applications in restorative dentistry and orthopaedics. One such application is a coating applied to hip implants, where it provides implant fixation [60]. Coating of implants with biomaterials is gaining more and more popularity for many reasons. The coating reacts with the body fluids producing a new bone surface. Instead of having a mechanical fixing only, this way a strong biochemical bond is formed between the implant surface and the bones [61]. Synthetic

hydroxyapatite (HA), with the complex chemical formula  $\text{Ca}_{10}(\text{PO}_4)_6(\text{OH})_2$ , is the most well-known CaP material.

When an HA-based ceramic is implanted, a fibrous tissue-free layer containing carbonated apatite forms on its surfaces and contributes to the implant bonding to the bone. This results in earlier implant stabilization and superior fixation of the implant to the surrounding tissues [62]. In addition, early biological responses to HA coatings are influenced by the surface roughness of the coating which affects osteoblast cell attachment and thus bone growth on the coating once is implanted into the body. Whereas fibroblasts and epithelial cells prefer smoother surfaces, osteoblasts attach and proliferate better on rough surfaces. Thus, it is clear that in order to improve implant life, the tailoring of the properties of HA coatings is of utmost importance [61].

Despite its excellent bone regeneration properties, HA has also some important disadvantages: HA-based ceramics are very brittle in bulk [60] and are characterized by poor mechanical properties, especially in liquid media. Therefore, HA-based materials cannot be used in bulk for orthopedic devices, which must withstand the application of high loads during their lifetime [64]. To overcome these drawbacks, HA can be applied as a coating onto the surface of metallic or polymeric implants, which aim to significantly improve implants' overall performances, by successfully combining the excellent bioactivity of the ceramic with the mechanical advantages of the substrate implants [62].

Table 2.4 Mechanical properties of bone vs HA [65]

Mechanical properties	Cortical bone	Cancellous bone	Dentine	Dental enamel	Dense HA	Porous HA
Compressive	100-230	2-12	295	384	120-900	2-100

strength/ Mpa						
Flexural/tensile strength /Mpa	50-150	10-20	51.7	10.3	38-300	3
Fracture toughness / MPa.m <sup>1/2</sup>	2-12	NA			1	
Young's/Elastic modulus/GPa*	18-22		18-21	74-82	35-120	
Vickers Hardness/GPa					3-7	

Natural hydroxyapatite is usually extracted from biological sources or wastes such as mammalian bone (e.g. bovine, camel, and horse), marine or aquatic sources (e.g. fish bone and fish scale), shell sources (e.g. cockle, clam, eggshell, and seashell), and plants and algae and also from mineral sources (e.g. limestone) [66]. HA can be synthesised chemically or extracted from natural sources. Prior research has reported on the various methods for synthesising synthetic and natural HA. Synthetic HA can be fabricated through various methods including dry methods (solid-state and mechanochemical), wet methods (chemical precipitation, hydrolysis, sol-gel, hydrothermal, emulsion, and sonochemical), and high temperature processes (combustion and pyrolysis) [67, 68]. Compared to synthetic HA, natural HA is non-stoichiometric since it contains trace elements such as Na, Zn<sup>2+</sup>, Mg<sup>2+</sup>, K<sup>+</sup>, Si<sup>2+</sup>, Ba<sup>2+</sup>, F, and CO<sub>3</sub> which make it similar to the chemical composition of human bone [68].

### 2.11.1.1.1 Crystal Structure of HA

HA structure is hexagonal with space group P63/m, with approximate lattice parameters  $a=b=9.37 \text{ \AA}$ ,  $c=6.88 \text{ \AA}$  [67]. The crystal structure of calcium hydroxyapatite powder (Figure 2.3) synthesized by precipitation method the presence of simulated body fluid (SBF) at  $37 \text{ }^\circ\text{C}$  [70].

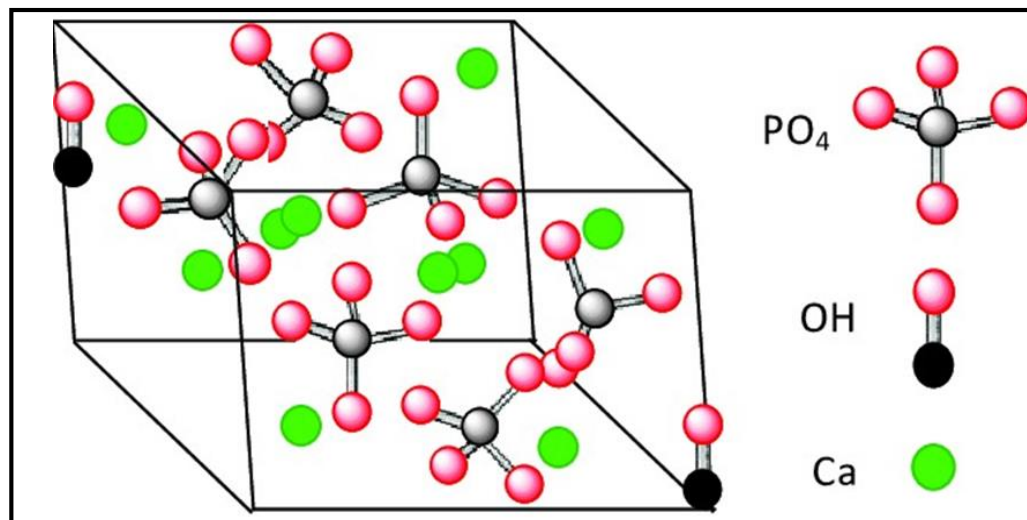


Figure (2.3) The structure of hydroxyapatite crystals [70].

Phosphates (PO<sub>4</sub>) in the general formula of HAp can be CO<sub>3</sub>, SO<sub>4</sub>, VO<sub>4</sub>, AsO<sub>4</sub>, or SiO<sub>4</sub>. A variety of metals can take the place of Ca in the formula. In case of natural apatites, the main cation is Ca and the secondary one is Mg. The last group (OH)<sub>2</sub> can be F<sub>2</sub>, Cl<sub>2</sub>, Br<sub>2</sub>, or CO<sub>3</sub> [71]. Chemical analysis has shown that in hard biological tissues, i.e., bone, enamel, and dentine, the biological apatites are not pure HAp, but contain a mixture of minor elements, including CO<sub>3</sub>, HPO<sub>4</sub>, F, Cl, Mg, and Na ions [72]. Based on the knowledge derived from biological mineralization systems, researchers, especially material scientists and chemists, are now seeking biomimetic apatite-related biomaterials [71].

Table 2.5 Solid phases of biological calcium-phosphate

Name	Formula	Abbreviation	Molar ratio
Hydroxyapatite	$\text{Ca}_{10}(\text{PO}_4)_6(\text{OH})_2$	Hap	1.67
Tricalcium phosphate	$\text{Ca}_3(\text{PO}_4)_2$	TCP	1.50
Octacalcium phosphate	$\text{Ca}_8\text{H}_2(\text{PO}_4)_5 \cdot 5\text{H}_2\text{O}$	OCP	1.33
Dicalcium phosphate dehydrate	$\text{CaHPO}_4 \cdot 2\text{H}_2\text{O}$	DCPD	1.00
Amorphous calcium phosphate		ACP	1.30-1.50

### **2.11.1.1.2 The Biochemical Properties of HA**

The interaction between HA and “living” bone has a partly chemical and partly biological character. Among the phenomena occurring when bioactive ceramics enter in contact with a biological environment, as listed below, the first step have a purely chemical character and the last four steps have a purely biological character:

- dissolution of ceramics
- precipitation from solution on the ceramics
- ion exchange ( $\text{H}^+$ ,  $\text{Ca}^{2+}$ ,  $\text{HPO}_4^{2-}$  and so on) and structural rearrangement at the ceramic–tissue interface
- interdiffusion from the surface boundary layer into ceramics
- solution-mediated effects on cellular activity

- deposition of the following phases without integration into the ceramic surface: – mineral phase – organic phase
- deposition of the above phases with integration into the ceramics
- chemotaxis to the ceramic surface
- cell attachment and proliferation
- cell differentiation
- extracellular matrix formation [73].

#### **2.11.1.1.3 Biological Properties of HA**

Calcium phosphate biomaterials are attracting attention in the field of bone regeneration, particularly due to their excellent biological properties. The highly complex environment of the body requires that calcium phosphate biomaterial must be able to degrade at a suitable rate to achieve a balance with the regeneration of new bone tissue, and simultaneously provide an ideal place for cell growth [74].

#### **2.11.1.1.4 Medical Applications of HA**

HA is used to modify or replace the natural elements of the skeletal system. Examples include:

- joint replacements (hips, knees), together with titanium, Ti6Al4V alloy, stainless steel and polyethylene
- bony defect repairs
- dental implants for tooth fixation, together with titanium, Ti6Al4V alloy, stainless steel, polyethylene, and alumina [73].

**2.11.2 Composite**

A composite is a combination of two or more material with distinct constituents that offers synergistically improved applications with different physical and mechanical properties. Composites, properties such as particle size, surface area, and mechanical properties differ from those of their original constituent materials in ways that make them suitable candidates for various biomedical applications. The mechanical properties of the natural hard tissue are comparatively higher than those of individual ceramic biomaterials. Their mechanical properties are generally weaker, which limits their property and limits their usage in high load-bearing applications. Development of various composite coatings such as ceramic-ceramic or polymer-ceramic coatings for metallic implants is producing better mechanical properties with improved biomedical applications [41].

**2.12 Micro Arc Oxidation**

Micro arc oxidation (MAO) or Plasma electrolytic oxidation (PEO) is a perspective technological process, demanded in many sectors of industry: automobile, aircraft and aerospace manufacturing, electronics, medicine, photonics and nanotechnology. Its essence lies in the surface treatment of parts made of valve metals and alloys, in particular aluminum, to impart them unique properties: high micro-hardness, wear resistance and corrosion resistance (increase the reliability and durability of machine parts); high thermal conductivity (allows us to produce smaller radiators with the same power dissipation) [75]; excellent bonding strength with substrate and relatively low cost [76]; good biocompatibility (used in prosthetics); ordered pores structure of the top layer of the MAO coating (allows to grow arrays of nanowires in a matrix of aluminum oxide, for example, to obtain metamaterials) [75]. Micro-arc oxidation is an advanced electrochemical oxidation method to produce porous ceramic coatings over transition metals

(Ti, Al, Mg, Zr etc.,) and their alloys by rapid micro-arc discharges. The micro-arc discharge takes place when an applied voltage exceeds the dielectric break down voltage of ceramic/oxide coatings [76].

### 2.12.1 Process of Micro-Arc-Oxidation

The MAO can be described as a combination of electrochemical oxidation, plasma chemical reaction and thermal diffusion in an electrolyte [20]. During the MAO process, the component is immersed in an aqueous electrolyte bath which contains modified species in form of dissolved salts (e.g. silicates, phosphate and calcium salts) [77]. The valve metals (e.g. Al, Ti and Mg) serve as anodes and stainless steel plates are used as cathodes in the electrolytic bath. A water-cooled stainless steel vessel serves as the container. The MAO treatment is typically carried out for 5–180 min at a current density ranging from 500 to 2000  $A \cdot m^{-2}$  and voltage of up to 1000 V [18]. Figure (2.4) illustrates the schematic representation of MAO setup [78].

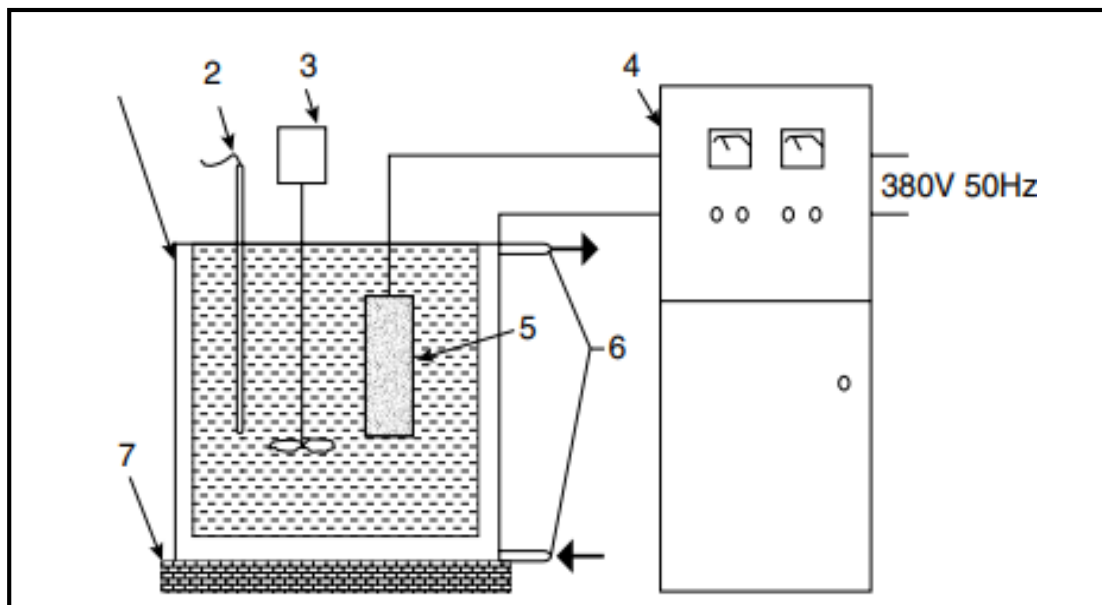


Figure (2.4) Schematic of the MAO coating system: 1 stainless steel tank (cathode); 2 thermocouple; 3 mixer; 4 AC power supply unit; 5 specimen (anode); 6 cooling system; 7 insulating plate [78].

The discharge appearance changes and the plasma emission intensities vary with the plasma coating process. The detailed mechanism of MAO process has not yet been revealed; however, most investigators agree that during each alternating current (AC) period several principal stages occur

Stage I: The voltage exhibits a rapid and linear increase with time to the breakdown voltage. Some tiny oxygen bubbles and an oxide layer can be observed on the sample surface, corresponding to the traditional anodizing stage (Figure (2.5)(a)).

Stage II: When the applied voltage exceeds a certain critical value, dielectric breakdown takes place, resulting in the formation of spark discharges. In this stage, the current flow concentrates only at regions of breakdown, leading to localized thickening of the oxide coating. The new formed coating can restore the resistance to current flow while other regions where the resistance is smaller are prone to breakdown. In this stage, simultaneous with a shrill sound, numbers of small white sparks are randomly distributed and quickly moving over the entire anode surface (Figure (2.5)(b)).

Stage III: The continuous formation and breakdown of the oxide film causes the cell potential to fluctuate. Gasification of both the valve metals and the electrolyte enables direct formation of ceramic oxide coating. Breakdown of the coating occurs at a vulnerable spot of the growing oxide film. With the increase of processing time, the discharge sparks grow bigger and their color varies from white to orange or red. In this region, the micro-arcs transform into powerful arcs (Figure (2.5)(c)).

Stage IV: The intense sparking and gas release trigger the formation of large size pores and thermal cracking of the film. Along with the disappearance of sparks and gas bubbles, the voltage decreases rapidly, implying the end of the MAO process (Figure(2.5)(d)). The architecture of the MAO coating is a

twolayered morphology: a barrier inner layer and a porous outer layer with numerous fine and coarse cavities. The thickness of the coating varies from 1 to 100  $\mu\text{m}$  [20].

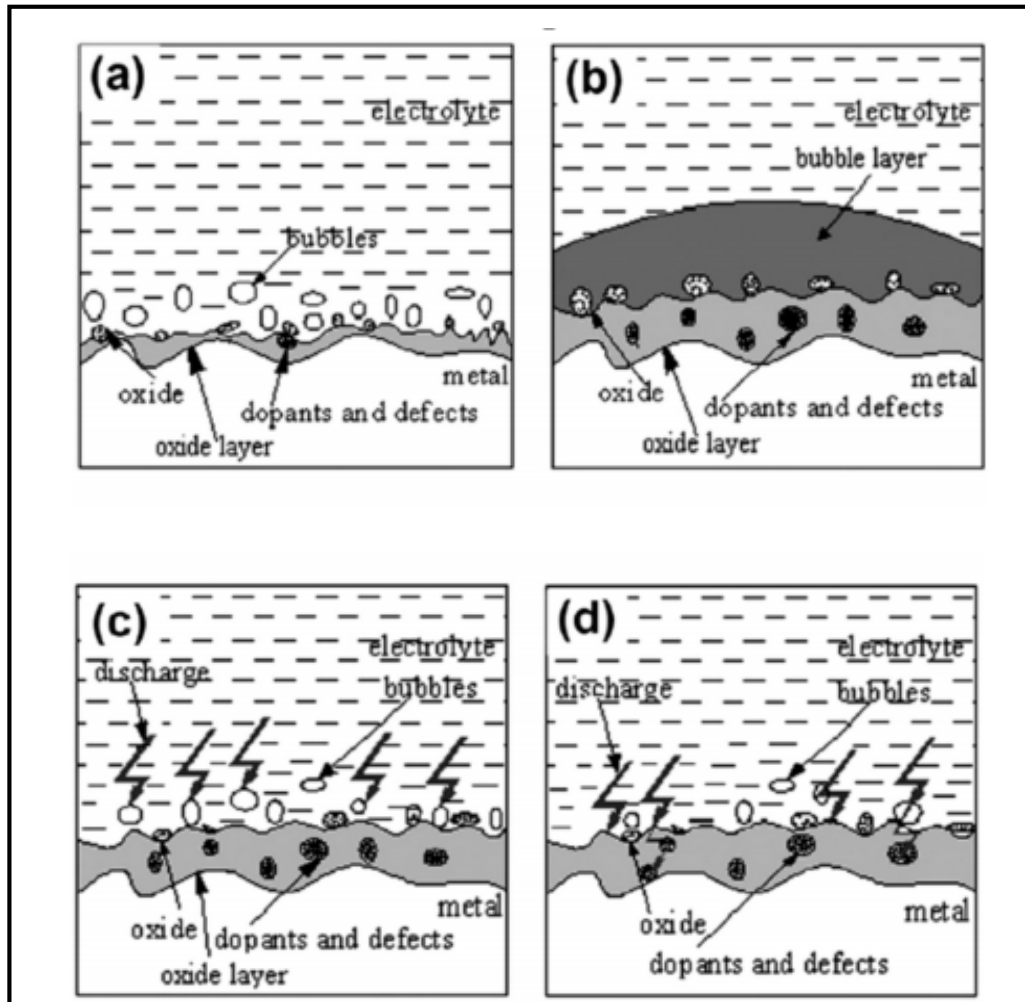


Figure (2.5) Schematic illustration of the plasma discharge during different stages of the MAO process. (a) Stage I, (b) stage II, (c) stage III, and (d) stage IV [79].

### 2.13 Nano Coating

Nanotechnology is a great technology that deals with structures measuring less than 100 nanometres. A nanometre is one-billionth of a metre. Nanotechnology is used in robotics, sensing technology, process

technology, biotechnology and medicine, among other areas. In the recent years some investigations which exploit the biomorphic ceramics as new scaffold for bone implants were studied. Implantation of bone autograft or allograft is a known strategy for the treatment of large bone defects. Tissue engineering is trying to solve this problem by development of bone substitutes using cells and bioscaffolds. Whereas, most of them have relatively poor mechanical strength and cannot meet the requirements for many applications. Hence, there is a need to fabricate new scaffolds with improved mechanical properties and biocompatibility [80].

### **2.13.1 Nano-Hydroxyapatite Coating**

Hydroxyapatite is manufactured in many forms and can be prepared as a dense ceramic , powder, ceramic coating or porous ceramic [81] as required for the particular applications. However, in recent years, nano-sized hydroxyapatite (nHA) with appropriate stoichiometry, morphology and purity have stimulated great interest in scientific research. It is believed that nHA with grain size  $< 100$  nm in at least one direction has a high surface activity and ultrafine structure similar to the mineral found in hard tissues [82].

With the advent in technology and developing interest, various methods for preparing hydroxyapatite can be widely classified into-dry methods, wet methods, high temperature processes, synthesis from biogenic sources and combination of above stated procedures. Among all the methods, chemical precipitation, combination methods and hydrothermal processes are the most popular methods for fabricating nHA. The mechanical properties of hydroxyapatite are greatly determined by the morphology and crystallography of the particles, which in turn depends on the mode of fabricating Hydroxyapatite [81].

### **2.14 Silver (Ag)**

Silver (Ag) ions or salts are known to have a wide antimicrobial effect and they have been used for years, in different fields in medicine, including wound dressings, catheters, and prostheses. Besides being a potent antimicrobial, Ag has many advantages, such as low toxicity and good biocompatibility with human cells, long-term antibacterial activity, due to sustained ion release, and low bacterial resistance [83].

#### **2.14.1 Biocompatibility of Ag**

Silver has no known biological roles, and its possible health effects of are a disputed subject [84]. Although silver itself is non-toxic, most silver salts are, and some may be, carcinogenic [85]. Silver ions can bind to sulphur groups in inter-molecular bonds in some biomolecules.

Silver ions and silver compounds show a toxic effect on some bacteria, viruses, algae and fungi, but without causing the high toxicity to humans. Its germicidal effects can kill many microbial organisms. Because of this, silver salts and the metal itself have played an important part in the development of medicine. Interest in the use of silver is being rediscovered in a wide variety of biomedical applications, where it can prevent the growth of microorganisms responsible for disease. The antimicrobial properties of silver are used in the form of silver salts and nano-scale complexes that break down to release silver ions ( $\text{Ag}^+$ ) [84] as shown in figure (2.6) that distinctive mechanisms are described during the interaction of AgNPs with bacterial cells.

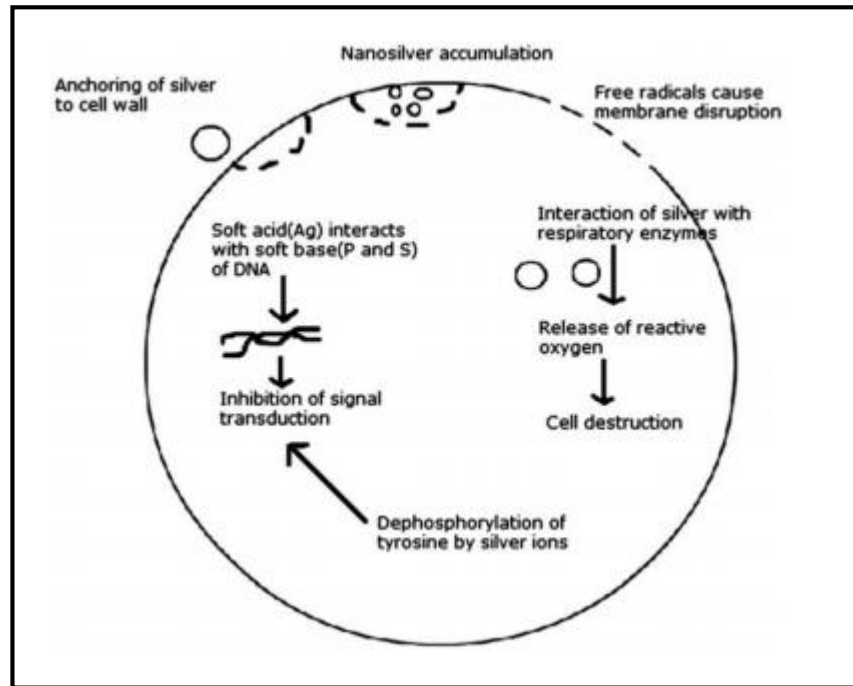


Figure (2.6) Various modes of action of silver nanoparticles (AgNPs) on bacteria [86].

### **2.14.2 Medical Application of Ag**

There are many applications for AgNPs in medical field [87].

1. Dental Material.
2. Wound Dressings.
3. Contact Lens.
4. Medical Catheters.
5. Bone Cement.
6. Surgical Meshes.

Metallic silver is also used in a number of surgical applications, both for structural devices (e.g. cranial support plates, suture wire, aneurysm clips, and tracheostomy tubes) and for prostheses [84].

### 2.14.3 Ag Coating

Orthopedic and dental implants are dependent on bone implant osseointegration. The success and long-term survival of these implants are also dependent on the presence of bacteria surrounding the implants. Bacterial infection after implant placement is a significant rising complication. In order to reduce the incidence of implant-associated infections, several biomaterial surface treatments have been proposed as coating of implant surfaces with quaternary ammonium compounds, iodine, or silver (Ag) ions [88]. Silver has proven to possess excellent antimicrobial activity against a broad spectrum of pathogens, including gram positive and gram-negative bacteria [89]. The main antibacterial effect of silver is mediated by the release of biocidal Ag<sup>+</sup> ions, which interact with the bacterial cell wall and disturb its permeability, inactivate essential proteins and cause DNA condensation [90].

Silver-coated substrates prevent adhesion of *S. aureus* and *Staphylococcus epidermidis* in vitro [91]. Silver coatings on megaprosthesis and fracture fixation pins reduce the rate of adhesion and infection by *S. aureus* in vivo. High Ag levels associated with burst release is toxic to osteogenic cells. Various carriers of Ag have been developed. Ag can be loaded onto calcium phosphate coatings to impart anti-microbial properties to metallic substrates.

HA nanocrystals loaded with Ag show anti-microbial activity against *S. aureus* and *E. coli* in vitro [92]. Nanotechnology is an essential technology of 21 century with groups of atom at nanoscale of 1-100nm. Nanoparticles (NPs) can be obtained from natural sources or chemically synthesized or one of the by-products. Due to its higher surface to volume ratio and antibacterial properties they have found applications in the field of medicine. Among the various existing nanomaterials, AgNPs has gained

attention owing to their distinctive physical and bio-chemical properties in contrast with their macro and micro complements. Silver is a safe antimicrobial agent which has a potential to kill 650 different types of diseases causing organisms [93].

### **2.15 Literature Survey**

Researchers were and still are trying to make the titanium more compatible by modifying its surface with various techniques and methods to make it safe and long-term use in the human. This is done by coating pure titanium with a coating composite (HA, HA/nAg) by micro arc oxidation (MAO) technique.

#### **2.15.1 Nano Ag/HA Deposition**

**In 2011 Saravanan et al.** studied a bio-composite scaffold containing chitosan/nano-hydroxyapatite/nano-silver. Particles (CS/nHAp/nAg) was developed by freeze drying technique, followed by introduction of silver ions in controlled amount through reduction phenomenon by functional groups of chitosan. The scaffolds were characterized using SEM, FTIR, XRD, swelling, and biodegradation studies. The testing of the prepared scaffolds with Gram-positive and Gram-negative bacterial strains showed antibacterial activity. The scaffold materials were also found to be non-toxic to rat osteoprogenitor cells and human osteosarcoma cell line. Thus, these results suggested that CS/nHAp/nAg bio-composite scaffolds have the potential in controlling implant associated bacterial infection during reconstructive surgery of bone [94].

**In 2016, Kondepudi et al.** studied silver ion-exchanged nanocrystalline zeolite (Ag-Nano-ZSM-5) and silver ion-exchanged conventional zeolite (Ag-ZSM-5) were synthesized. Zeolites were incubated in simulated body fluid at 310K for different time periods to grow

hydroxyapatite in their matrixes. Significant large amount of hydroxyapatite was grown in Ag-Nano-ZSM-5 matrix after incubation in simulated body fluid when compared to Ag-ZSM-5. The resultant material was characterized using X-ray diffraction, N<sub>2</sub>-adsorption, scanning/transmission electron microscopy, energy dispersive X-ray, and inductively coupled plasma analysis. Mechanical properties such as compressive modulus, compressive strength, and strain at failure of the parent materials were evaluated. Biocompatibility assays suggested that Ag-Nano-ZSM-5 and hydroxyapatite grown in Ag-Nano-ZSM-5 were compatible and did not impose any toxicity to RAW 264.7 cells macrophase and Caco2 cells suggesting considerable potential for biomedical applications such as bone implants [95].

**In 2018, Yang et al.** studied numerous antibacterial biomaterials have been developed, but a majority of them suffer from needy biocompatibility. With the purpose of reducing biomaterial-related infection and cytotoxicity, friction stir processing (FSP) was employed to embed silver nanoparticles [Ag NPs] in a Ti-6Al-4V substrate. Electrochemical impedance spectroscopy (EIS) shows that both FSP and the addition of silver have positive effects on corrosion resistance. The modified samples effectively inhibit both (*S. aureus* and *E. coli* strains) and slightly reduce their adhesion, while not displaying any cytotoxicity to bone mesenchymal stem cells [BMSCS] in vitro. The antibacterial effect is free of silver ion release and is likely due to the number of embedded silver nano particles on the surface, which directly contact and subsequently destroy the cell membrane. This study shows that the TC4/Ag metal matrix nano composite is a potential infection-related biomaterial and that embedding (Ag NPs) tightly on a biomaterial surface is an effective strategy for striking a balance between the antibacterial effect and bio compatibility, providing an innovative approach

for carefully controlling the cytotoxicity of infection related biomaterials [96].

**In 2018, Batebi et al.** studied a composite coating containing fluoride, silver and hydroxyapatite (Ag-FHA) was developed on titanium (Ti) substrate by sol-gel technique. Triethylphosphite, hydrated calcium nitrate, silver nitrate and ammonium fluoride were used respectively, as (P, Ca, Ag and F) precursors with a Ca:P ratio 1.67 and concentration of silver was 0.3 wt.%. Antibacterial activity of coatings against *Escherichia coli* indicated a significant enhancement in the antibacterial property of (Ag-FHA) nano composite with increasing the amount of fluoride. These coatings can prevent the bacterial infections of implants [97].

**In 2018, Gou et al.** studied antibacterial biomaterial such as nano silver or nano zinc oxide has been utilized on the surface of hydroxyapatite (HA) to promote its antibacterial activity. However, it is difficult to obtain a balance between antibacterial activity and biocompatibility. In this paper, an innovative strategy is presented to fabricate HA nanomaterial with a strong antibacterial activity and a good biocompatibility. HA generated with surface deposition of nano silver and nano zinc oxide was fabricated by a two-step liquid chemical reduction method. XRD confirmed the success of dual deposition. Ion release testing indicated the dual deposition increased silver ion release rate and zinc ion release rate simultaneously [98].

**In 2020, Dalavi et al.** studied microspheres (COS-Ag-Alg-HA) containing chitooligosaccharide (COS) coated silver nano particles (Ag NPs) with alginate (Alg) and hydroxyapatite as bone graft substitutes. Antimicrobial activity and biocompatibility of the developed microspheres were evaluated with pathogenic microbes and osteoblast-like cells, respectively. Results suggest that microspheres are rigid, and strong chemical interaction were observed between the materials. The size of the

microspheres was ranging from  $(1.5 \pm 0.5$  to  $4.0 \pm 0.5$  mm). Significant microbial inhibition was observed against *Staphylococcus aureus*, and the developed microspheres were biocompatible with osteoblast like cells. Based on the aforementioned and finding results, the developed microsphere was proposed to be a potential nominee for bone tissue repair and renewal [99].

### **2.15.2. Micro Arc Oxidation**

In 2012, Dicu et al. studied grow nano-structured  $\text{TiO}_2$  by micro-arc oxidation (MAO) on titanium surfaces. During the oxidation treatment, the titanium sample was immersed in electrolytic solution containing calcium acetate monohydrate ( $\text{CH}_3\text{COO})_2\text{CaH}_2\text{O}$ ) and sodium phosphate monobasic dihydrate ( $\text{NaH}_2\text{PO}_4 \cdot 2\text{H}_2\text{O}$ ). During the process of the simulated body fluid (SBF) immersion (3 day in SBF and 3 day in 5SBF), the Ca and P of the MAO coating dissolves into the SBF, increasing the supersaturation degree near the surface of the MAO coating, which could promote the formation and growth of apatite. The coatings were rough and porous, without apparent interface to the titanium substrates. All the oxidized coatings contained Ca and P as well as Ti and O, and the porous coatings were made up of anatase, rutile and hydroxyapatite [100].

In 2017, Aktug et al. studied hydroxyapatite [ $\text{HA}$ ,  $\text{Ca}_{10}(\text{PO}_4)_6(\text{OH})_2$ ] based coatings are used in biomaterial applications and biomedical industrial applications due to its bioactive and biocompatible properties. commercially pure zirconium was coated in the solution consisting of calcium acetate [ $\text{CA}$ ,  $(\text{CH}_3\text{COO})_2\text{Ca}$ ] and  $\beta$ -calcium glycerophosphate [ $\beta$ -Ca-GP,  $(\beta\text{-C}_3\text{H}_5(\text{OH})_2\text{PO}_4\text{Ca})$ ] by micro arc oxidation (MAO) in a single-step process for 1min, 10min and 30 min duration times to produce HA-based coatings. The surface morphologies of coatings produced by (MAO) technique at 1 min had very porous structures because of the existence of micro discharge

channels during the process. The surface coatings morphologically had HA microstructure owing to the crystallization of HA particles at 10 min and the existence of growing HA particles in (MAO) process at 30 min [101].

**In 2017, Wang et al.** studied micro-arc oxidation coatings were fabricated on 7E04 aluminum drillpipes materials in  $\text{Na}_2\text{SiO}_3$ -NaOH electrolyte system containing 3.0 g/L SiC particles at different current density (1, 5, 10, 15 and 20 A/dm<sup>2</sup>). The oxidation voltage, coating thickness, surface morphologies, surface micro-hardness, phase composition and potentiodynamic polarization curves of the MAO coatings were investigated. The results showed that the oxidation voltage increased and the coatings were thickened with the increment of current density. The coating surface morphologies got coarser gradually which led to the reduction of the surface micro-hardness. The phase composition of the coatings consisted of SiO<sub>2</sub> because the oxidation of SiC particles and the corrosion resistance of the coatings increased slightly [102].

**In 2018, Teker Aydogan et al.** studied the optimised silver Ag content of the coating synthesised on commercially pure titanium (Cp-Ti, Grade 4) for biomedical applications by micro-arc oxidation (MAO) process. The MAO process was conducted in electrolytes containing silver acetate ( $\text{AgC}_2\text{H}_3\text{O}_2$ ) at different concentrations between 0 and (0.002 mol L<sup>-1</sup>). When compared to the base electrolyte, coatings synthesised in  $\geq 0.001$  mol L<sup>-1</sup>  $\text{AgC}_2\text{H}_3\text{O}_2$  added electrolytes exhibited an antibacterial efficiency of 99.98% against Staphylococcus aureus "S. aureus" [103].

**In 2018, Du, Q., Wei et al.** studied the micro arc oxidation (MAO) coatings with different concentrations of Ca, Zn and p elements are successfully formed on the titanium (Ti) substrate at the various applied voltages. After MAO treatment, the MAO coating exhibits the porous

surface structure and composed of anatase and rutile (TiO<sub>2</sub>) phases. Meantime, the average size and density of micro-pores on the (MAO) coatings have been modified by the adjusting the applied voltages. In addition, the contents of the incorporated elements such as Zn, Ca and P elements in the MAO coatings have been optimized. The (MAO) coating containing Ca, Zn, and P elements have excellent antibacterial ability for "E.coli and S.aureus". Thus, the incorporation of Ca, Zn and P elements was an effective method to improve the antibacterial ability [104]

**In 2018, Huang et al.** studied the micro-arc oxidation (MAO) method was used to fabricate Cu- containing ceramic coatings on titanium(Ti) substrates. The macrophages cultured on cu-containing (MAO) fabricated surfaces were polarized to M1 phenotype, evidenced by the high expression levels of inducible nitric oxide synthase (iNOS), low expression levels of arginase1 (Arg1), enhanced pro-inflammatory cytokine interleukin-6 (IL-6) release and inhibited IL-4 and IL-10 (anti-inflammatory cytokines) release. The MAO treated surface incorporated with larger amounts of Cu (referred as Cu(h)-MAO) modulated a favorable inflammatory microenvironment for osteoblast-like cell differentiation. Moreover, the macrophages cultured on Cu(h)-MAO surface exhibited enhanced bacteria uptake and killing rate, indicating that the Cu(h)-MAO surface promoted the bactericidal capacity of macrophages. Together, Cu could be used as a promising modulatory agent for macrophage functions. The integration of Cu in biomaterials led to enhanced macrophage mediated osteo genesis and bactericidal capacity [105].

*Chapter Three**Experimental Work***3.1 Introduction**

This chapter deals with search equipment and the experimental procedure required to accomplish the objectives of the current work which are mentioned in chapter one. As well as the evaluation and testing methods includes surface modification of the pure titanium by composite coating (HA, HA/Ag) by MAO. The practical part includes the determination of basic materials that are used in MAO process, preparation of specimens and suitable concentrations for suspension that are used in deposition process. In this study coating thickness measurements, light Optical Microscope (LOM) analysis, field emission Scanning electron microscopy (FESEM) analysis, Atomic force microscopy (AFM) analysis, Energy Dispersive X-ray (EDX) analysis, corrosion rate measurements and antibacterial test was used to evaluate coating and uncoating specimens features. Contact angle test were used to know wettability of the electrolyte. Surgical procedure and implantation test were used to know biocompatibility of specimens.

### 3.2 Flowchart of Experiment Work

The experiment work to deposition composite coating (HA, HA/nAg) layers on (CP-Ti) substrate by MAO is illustrated by figure (3.1).

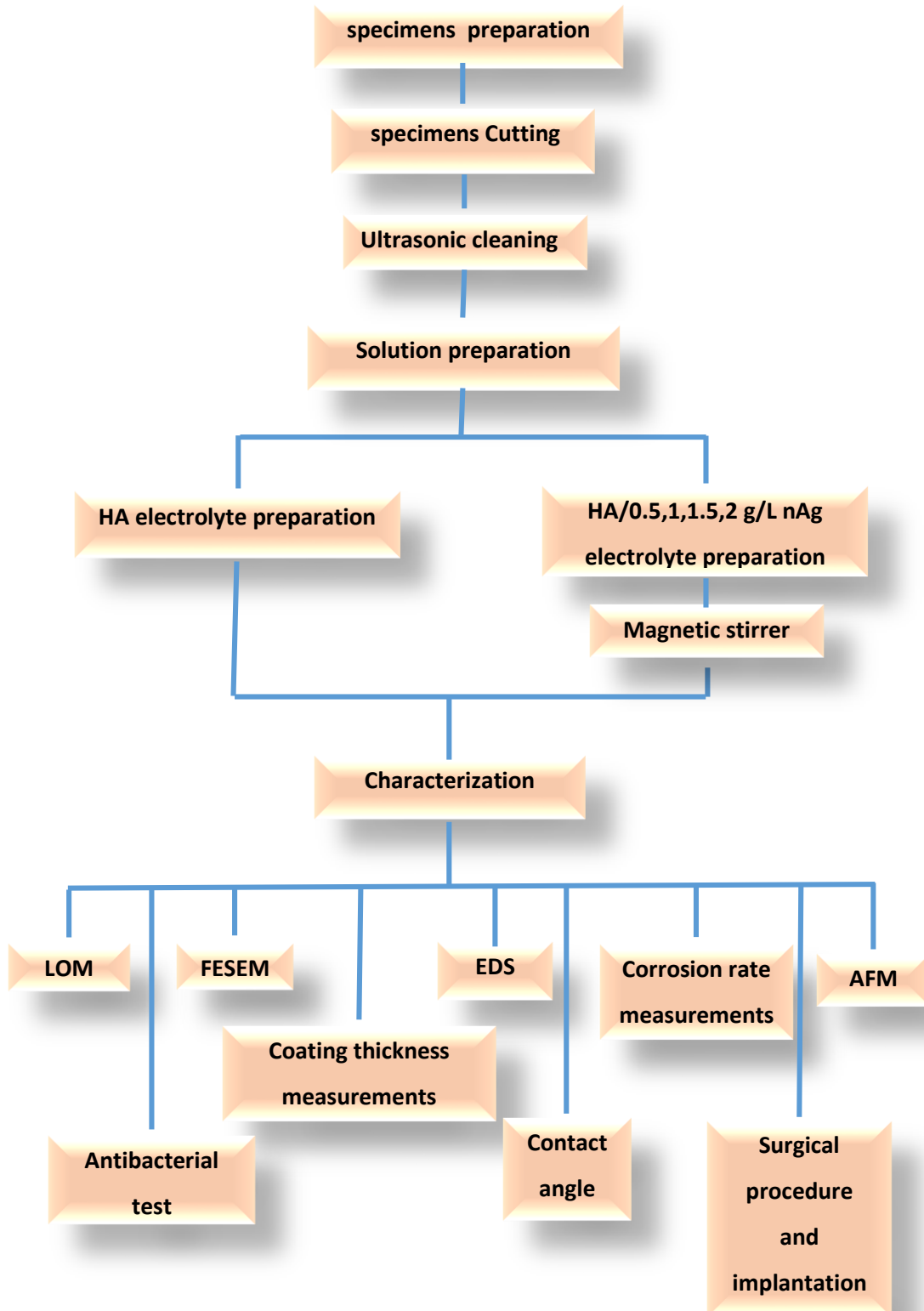


Figure (3.1): Flowchart of experiment work

### 3.3. Preparation of Commercial Pure Titanium (CP-Ti) Substrate

In this work, a plate of titanium with thickness of 0.1mm was cut into (1cm,1cm). Table (3.1) shows the chemical analysis of (CP-Ti) substrate and the result of it test in state Company for Inspection and Engineering Rehabilitation (SIER)/Ministry of Industry and Minerals by spectroscopy device. Before coating, Specimens were ultrasonically cleaned in ethanol alcohol for 10 min using ultrasonic cleaning device in College of Engineering Material/Ceramic Department / University of Babylon and dried with warm air.

Table (3.1): Chemical analysis of (CP-Ti) substrate

No	element	concentration %	No	element	concentration %
1	Mg	< 0.0040	13	Cu	0.0161
2	Al	< 0.00090	14	Zn	0.00480
3	Si	< 0.0032	15	As	< 0.00048
4	P	< 0.0016	16	Zr	< 0.050
5	S	< 0.00026	17	Nb	< 0.0019
6	Ti	98.84	18	Mo	0.0443
7	V	< 0.062	19	Ag	0.0030
8	Cr	< 0.0050	20	Cd	< 0.00081
9	Mn	0.0116	21	Sn	< 0.00092
10	Fe	0.0507	22	Sb	0.0015
11	Co	0.0035	23	W	< 0.0019
12	Ni	0.0191	24	Pb	< 0.00083

**3.4. Materials**

To prepare composite coating on titanium substrate the following materials were used:-

1- hydroxyapatite electrolyte: Preparation of the electrolyte in the electrolyte cell were an aqueous solution containing 0.13 mol/l calcium acetate monohydrate ( $(\text{CH}_3\text{-COO})_2\text{Ca.H}_2\text{O}$ ) and 0.06 mol/l sodium biphosphate dihydrate ( $\text{NaH}_2\text{PO}_4.2\text{H}_2\text{O}$ ) in distilled water [100], PH of electrolyte was 2.3.

2- nano silver: the particle size and purity of nano silver was 20 nm, 99.9% respectively. Nano silver was added to hydroxyapatite electrolyte in proportions (0.5, 1, 1.5, 2)g/L. Magnetic stirrer was used to disperse nano silver in hydroxyapatite electrolyte for 30 min.

**3.5. Equipments and Apparatus**

To complete the titanium coating process with HAp, HAp/nAg by micro arc oxidation, a set of equipments and apparatus were used.

**3.5.1. Preparation Before Coating**

- 1- Cutting tool (scissors)
- 2- Ultrasonic cleaner (MTI Corporation)
- 3- Electronic sensitive balance type (ABS 220-4, KERN) calibrated with ( $\pm$  0.0001% accuracy)
- 4- Magnetic stirrer (IKA<sup>TM</sup> RH basic 2)
- 5- PH meter (HI9811-5, HANNA).

**3.5.2. Characterizations of Deposited Specimens**

- 1- The thickness measuring device (TT260).

2- Light Optical Microscope.

3- Field Emission Scanning Electron microscopy (FESEM)( ZEISS, SIGMA Company).

4- Atomic Force Microscopy (SPMAA3000, Angstrom Advanced Inc., USA).

5- Water Bath device for Corrosion Rate Measurements.

### **3.6. Micro Arc Oxidation (MAO)**

By using micro arc oxidation process obtained pores and coherent coating and the spark was very clear. In addition, the nano silver was dispersed and remained suspended in the electrolyte during the coating process. The Coating layer served as an insulating layer and became specimens that did not have an electrical connection after the coating.

The temperature was measured by mercury thermometer of the coating process and its was between (65-75) C° and the spark was obtained at a voltage of magnitude (200 V) as illustrated in figure (3.2)

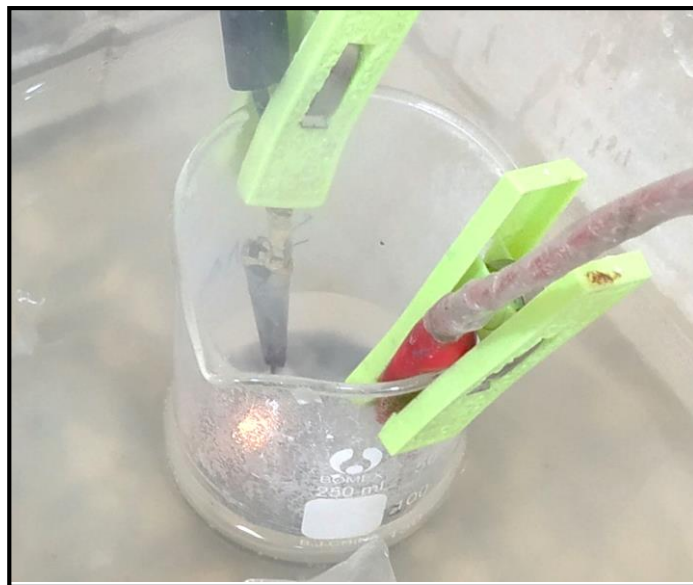


Figure (3.2) The spark during coating process.

### **3.6.1. Micro Arc Oxidation Requirements**

- 1- A power supply (DC) was used to determine the voltages.
- 2- A container consisting of water pump was connected with a source for warm water output a second source for cold water input and glass includes the electrolyte, thermometer, cathode electrode (pace of stainless steel) and anode electrode (specimen). The distance between electrodes is (4 cm).
- 3- Cooling system. The requirements for micro arc oxidation process are shown in figure (3.3) in College of Engineering Material / University of Babylon.

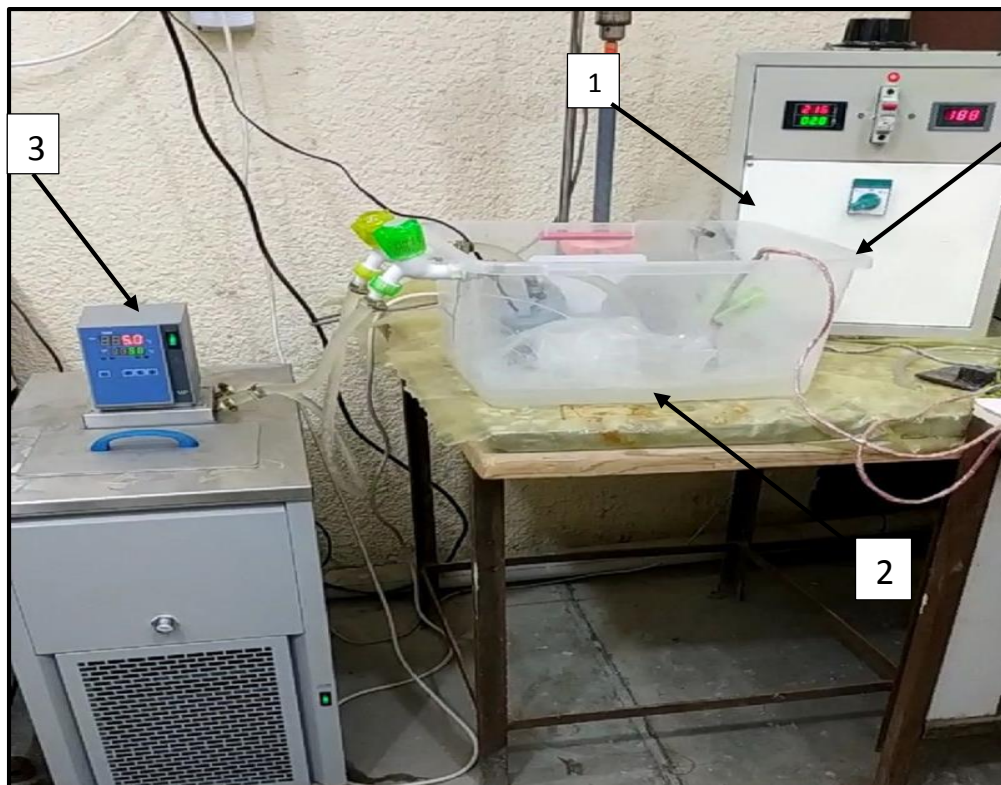


Figure (3.3) Schematic of the MAO coating system (1) A power supply (DC), (2) A container or electrical cell and (3) Cooling system.

### **3.6.2 Experimental Procedure**

In micro arc oxidation process, Ti specimen was used as counter electrodes (anode) and stainless steel as the working electrode (cathode).

The deposition was done by drenching the electrodes inside 100 ml beaker filled with solution. Ti specimen with the dimensions of  $10 \times 10 \text{ mm}^2$  was used as the substrates; and the distance between two electrodes in the cell was 4 cm at 200 V. Several voltage were used (100,150) V, but no coating was obtained. Parameters of MAO process shows in table (3.1).

Table (3.2) parameters of MAO process

No	Specimen	Time (sec)	Proportion nAg (g/L)	Code
1	HA	30	—	HA30
2	HA	45	—	HA45
3	HA	60	—	HA60
4	HA / nAg	30	0.5 g/L	HA30Ag0.5
5	HA / nAg	45	0.5 g/L	HA45Ag0.5
6	HA / nAg	60	0.5 g/L	HA60Ag0.5
7	HA / nAg	30	1 g/L	HA30Ag1
8	HA / nAg	45	1 g/L	HA45Ag1
9	HA / nAg	60	1 g/L	HA60Ag1
10	HA / nAg	30	1.5 g/L	HA30Ag1.5
11	HA / nAg	45	1.5 g/L	HA45Ag1.5
12	HA / nAg	60	1.5 g/L	HA60Ag1.5
13	HA / nAg	30	2 g/L	HA30Ag2
14	HA / nAg	60	2 g/L	HA60Ag2

### **3.7. Testing and Characterization**

To know and analyze the properties of the composite coating HA, HA/Ag layers on titanium by micro arc oxidation and compare them with substrate titanium, a number of tests were applied.

### 3.7.1. Coating Thickness Measurements

The thickness measuring device (TT260) as shown in figure (3.4) was used to measure the thickness of HA thin film, in (College of Material Engineering / University of Babylon).



Figure (3.4) Thickness measuring device

### 3.7.2. Light Optical Microscope (LOM) Analysis

The microstructure was evaluated with (200x) magnification using microscope device as shown in Figure (3.5) to identify the phases, shape and grain size of grain boundaries, in College of Engineering Material / University of Babylon.



Figure (3.5) Light optical microscope device

### **3.7.3. Field Emission Scanning Electron Microscopy (FESEM) Analysis**

SEM is one of the most commonly used surface analysis techniques to get information about the surface topography, particle size and composition of the nano silver powder.

Figure (3.6) shows (FESEM) device (ZEISS, SIGMA Company). It is an analytical technique used in materials science to investigate molecular surface structures such as the morphology, porosity, cracks and homogeneity of composite coating at Rostac center/ Tehran / Iran.



Figure (3.6) Field Emission Scanning Electron Microscopy (FESEM) system

To analyze the chemical composition of titanium substrate, energy Dispersive X-ray (EDX) at Rostac center/ Tehran / Iran was used.

#### **3.7.4. Atomic Force Microscopy (AFM) Analysis**

To observe the morphology (the nano roughness, surface image feature, depth morphology of film and particle size of the HA & HA/nAg composite coating) atomic force microscopy (SPMAA3000, Angstrom Advanced Inc., USA) was used as shown in figure (3.7) at college of Material engineering /University of Babylon.

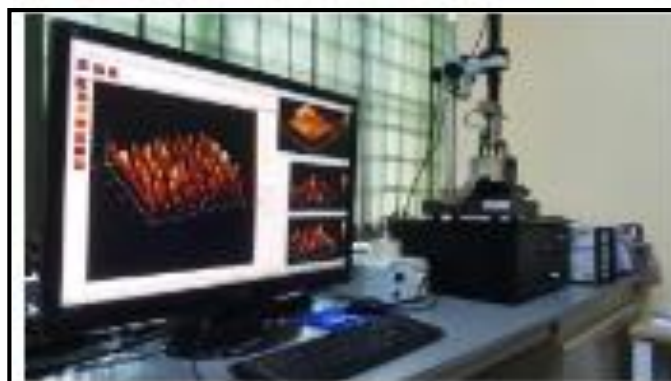


Figure (3.7) Atomic force microscopy system.

### **3.7.5. Antibacterial Test**

When biomaterials especially metallic implants are used inside the human body, they are exposed to types of bacteria that cause infections in the adjacent living cells to the metallic implant. Therefore, it must be known if there are bacteria present or not on Ti substrate and composite coating (HA, HA/nAg) specimens by the antibacterial test. This test was performed by washing the specimen in petridish with mannitol salt agar and it stayed in dish for 5 minutes. Then 0.5 ml of the solution was taken and placed in another petri dish to be incubated for 24 h at 37 C° at College of Girls science / University of Babylon.

### **3.7.6. Corrosion Rate Measurements**

The simplest method of measuring the corrosion rate of a metals is to immerse the specimen to the test medium (Ringer's solution) with components that are shown in table (3.3) and measure the loss of weight of the material as a function of time. From the initial and final thus the loss in this obtained and corrosion rate (CR) is found from the formula given below [106].

$$CR = \frac{W_o - W_i}{A * t}$$

Where:

CR is corrosion rate (mdd).

W<sub>o</sub> is original weight (mg) and W<sub>i</sub> is the weight after immersion where (i) express the number of days.

A is area of specimen (dcm)

t is time at days.

Table 3.3. Composition of Ringer's solution [87].

Component	Concentration(g/L)
NaCl	8.60
KCl	0.30
CaCl <sub>2</sub> .2H <sub>2</sub> O	0.33
Ph	5-7.5

In this work, as ASTM each specimen was placed in 100 ml of Ringer's solution for 32 day at a temperature of 37 °C in a water bath device shown in figure (3.8) at college of Material engineering /University of Babylon.

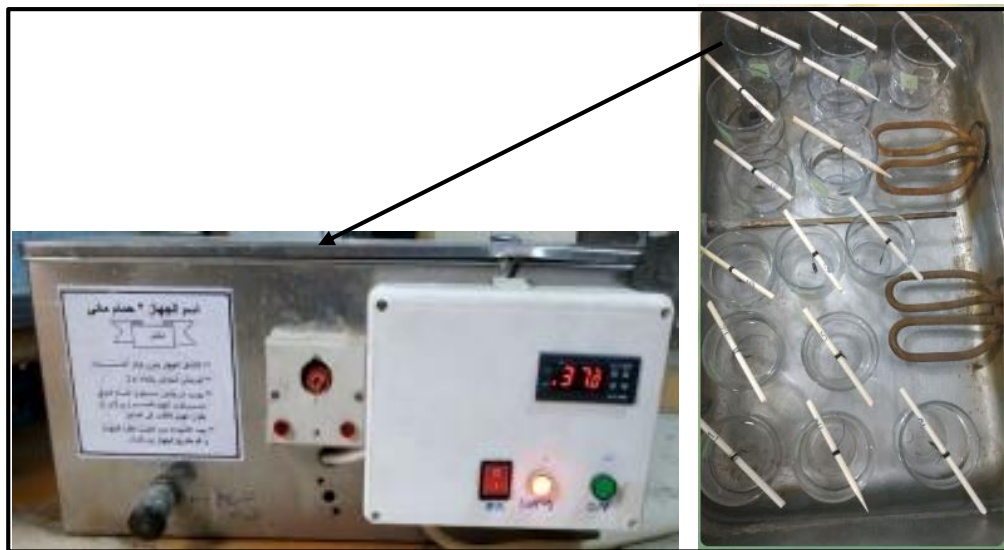


Figure (3.8) Water Bath Device

### **3.7.7. Contact Angle Test**

Contact angle inspection device measure the angle of contact between the liquid (HA, HA/ 0.5g/1 nAg, HA/1g/1 nAg, HA/1.5g/1 nAg, HA/2g/1 nAg) and soild (CP-Ti) substrate to know the wettability of the electrolyte to the surface of the base specimen as shown in figure (3.9). This test done at college of Material engineering /University of Babylon.

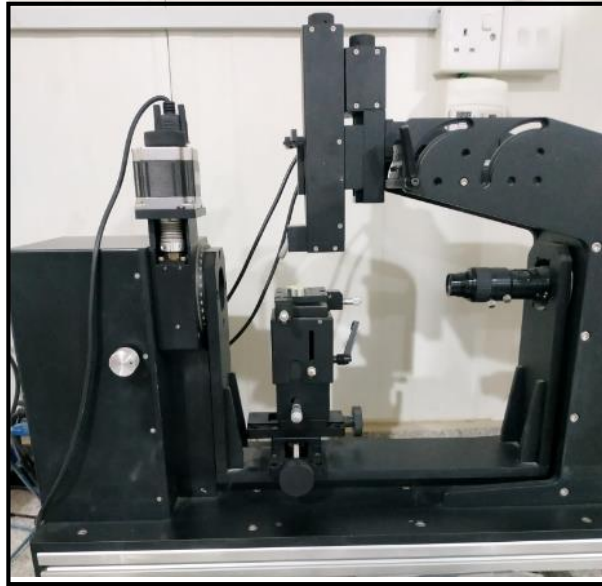


Figure (3.9) Contact Angle Inspection Device

### **3.7.8. Surgical Procedure and Implantation Test**

#### **3.7.8.1. Methodology**

Six local origin adult male rabbits with weight (2 – 3) kg were utilized. These animals were kept in a standard separate cage and had free access to tap water, and were fed with standard pellets and vegetables. They were left for 3 days in the same environment before the surgical operation.

Before the surgical operation, implants and instruments must be sterilized as a preliminary step. Anesthesia was created by an intramuscular injection of ketamine and xylazine. The surgery was achieved under a sterile state and a careful surgical method. The left leg for each rabbit was shaved from all sides. The surgical towel was placed around the operation site. The skin was cleaned with ethanol and then iodine. The leg was wrapped with a surgical towel. An incision was done about (3.5 cm) length to exhibit the femur bone. The skin and fascia were reflected. The periosteum (vascular connective tissue) was carefully reflected, figure (3.10).



Figure (3.10) Surgical clips and towels around the surgical site, reflection of skin and reflection fascia and muscles

Figures (3.11) and (3.12) show a drilling operation which was performed by means a round bar with an interrupted pressure. The hole enlargement was done in a gradual manner with a drill of 2 mm in diameter.

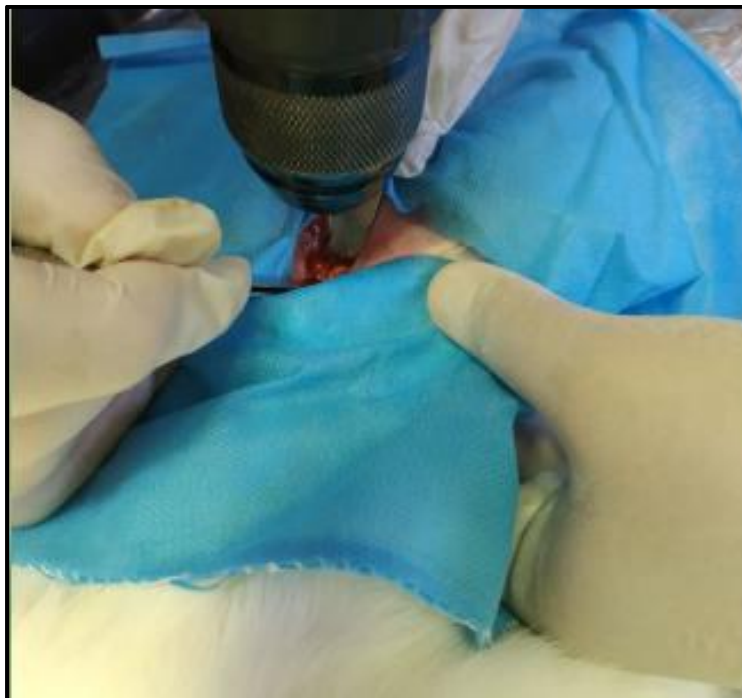


Figure (3.11) Preparation of the holes



Figure (3.12) The hole

The implants with dimensions (5, 2, 0.1) mm was placed in hole with a slight pressure completely introduced into the bone, figure (3.13)



Figure (3.13) Insert the Implants

Post-operative care was performed by giving an antibiotic (ceftriaxone) and voltaren injection for 3 days after surgery.

### **3.7.8.2. Histological Testing**

Bone sectioning was conducted after the animal was sacrificed with an overdose of general anaesthesia at 40 days interval. Following that, an optical microscope was used to examine the implant's histology. A cutting tool was used to get bone-implant block. The bone-implant block was placed in 10% newly produced formalin and kept for 3 weeks.

The histological specimen fixative in 10% formalin for 48 hours at room temperature and then washed with tap water for two hours, after that decalcification of specimen by used formic acid-sodium citrate method, until decalcification is complete washed the specimen with tap water 4 hours [107,108]. The specimen send to processed by routine histological processing methods including:

1) Dehydration. 2) Clearing. 3) Infiltration. 4) Embedding. 5) Sectioning  
6) Mounting. 7) Staining by Hematoxylin & Eosin. 8) Cover slipper and labeling [108].

Dehydration by using series spiraling of alcohol beginning with 50%, 60%,70%, 80%, 90% and 100% for 2 hours for each concentration. Clearing by using Xylen twice 10-50 minutes for each solution. Infiltration by putting the tissue specimens in paraffin wax on (56.5-58°C) for overnight. Embedding the specimens within paraffin wax for to made blocks. Sectioning the specimens to 5-7µm by using rotary microtome.

Rehydration by alcohol abdicable series beginning by 100%, 90%, 80%, 70%, 60% and 50%. Finally staining the specimens by Mayer's hematoxylin and eosin and massons trichrome stains. Mounting was the

process of adding the amount of DPX and then putting the cover slide on the sections strip on glass slides to cover it [107]. Finally examine the histological slides under the light microscope.

## *Chapter Four*

### *Results and Discussion*

#### **4.1. Introduction**

This chapter presents experimental results for HA and HA/nAg depositions on Ti specimen which includes the results of coating thickness measurements. Light optical microscope (LOM), field emission scanning electron microscopy (FESEM), energy dispersive X-ray (EDX), atomic force microscopy (AFM). Antibacterial test, contact angle test, corrosion rate measurements and surgical procedure and implantation with their discussions.

#### **4.2. Coating Thickness**

Table (4.1) represent results of the coating thickness of composite coating (HA/nAg) on (CP-Ti) substrate.

Table (4.1) Result of coating thickness

Specimens	Coating thickness ( $\mu\text{m}$ )
HA30	43.77
HA45	45.47
HA60	50.8
HA30/Ag0.5	28.67
HA45/Ag0.5	43.77
HA60/Ag0.5	57.73
HA30/Ag1	30.3
HA45/Ag1	33.8
HA60/Ag1	48.7
HA30/Ag1.5	32.1
HA45/Ag1.5	18.27
HA60/Ag1.5	44.67

HA30/Ag2	12.87
HA60/Ag2	17.43

It is clear from table (4.1) that there was an increase in the thickness of the coating with the increase in the coating time because there was enough time for the hydroxyapatite particles to grow. At the same time, the thickness of the coating layer decreases with the increase in the proportion of nano silver, as its deposition limits the growth of hydroxyapatite particles.

### **4.3. Light Optical Microscope (LOM)**

The microstructure of composite coating (HA & HA/nAg) on titanium plate with a change proportion the nano silver and coating time using the magnification of the microscope (200X) are shown in Figure (4.1).

Compared with the (CP-Ti) specimen surface, the formation pores and the distribution of hydroxyapatite particles is not homogeneous.

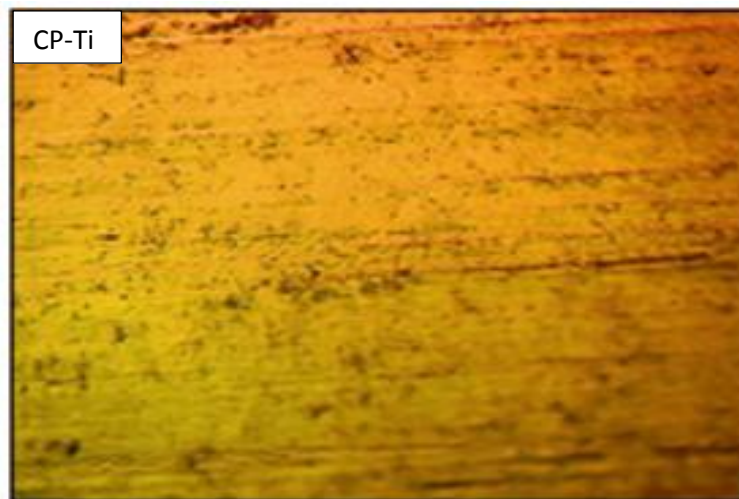


Figure (4.1) Microstructures of CP-Ti, HA, HA/nAg specimens

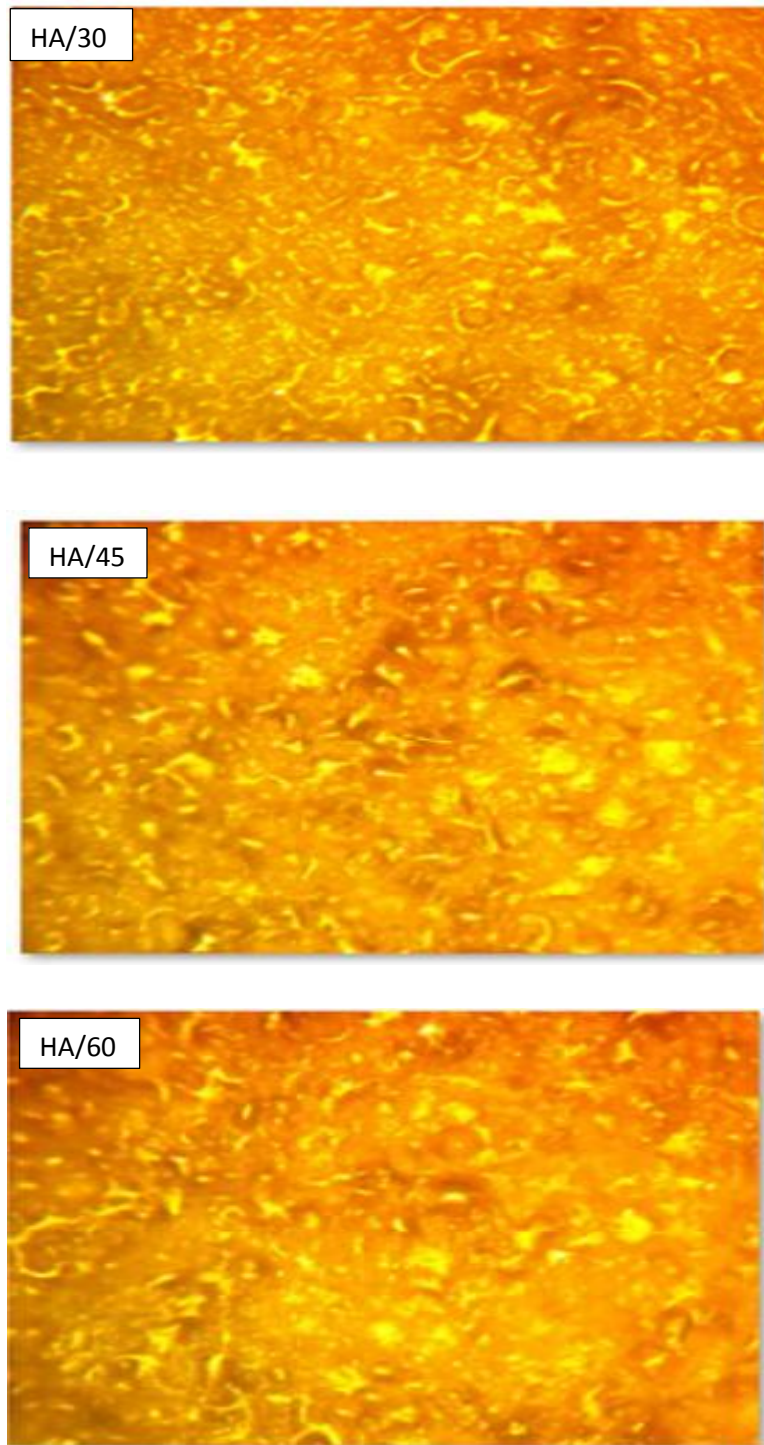


Figure (4.1): Microstructures of CP-Ti, HA, HA/nAg specimens (Contd)

With the addition of nano silver, the topography of the surface has changed, becoming smoother and fewer pores but in the (HA30Ag0.5) specimen, it did not have enough time to precipitate the nano silver.

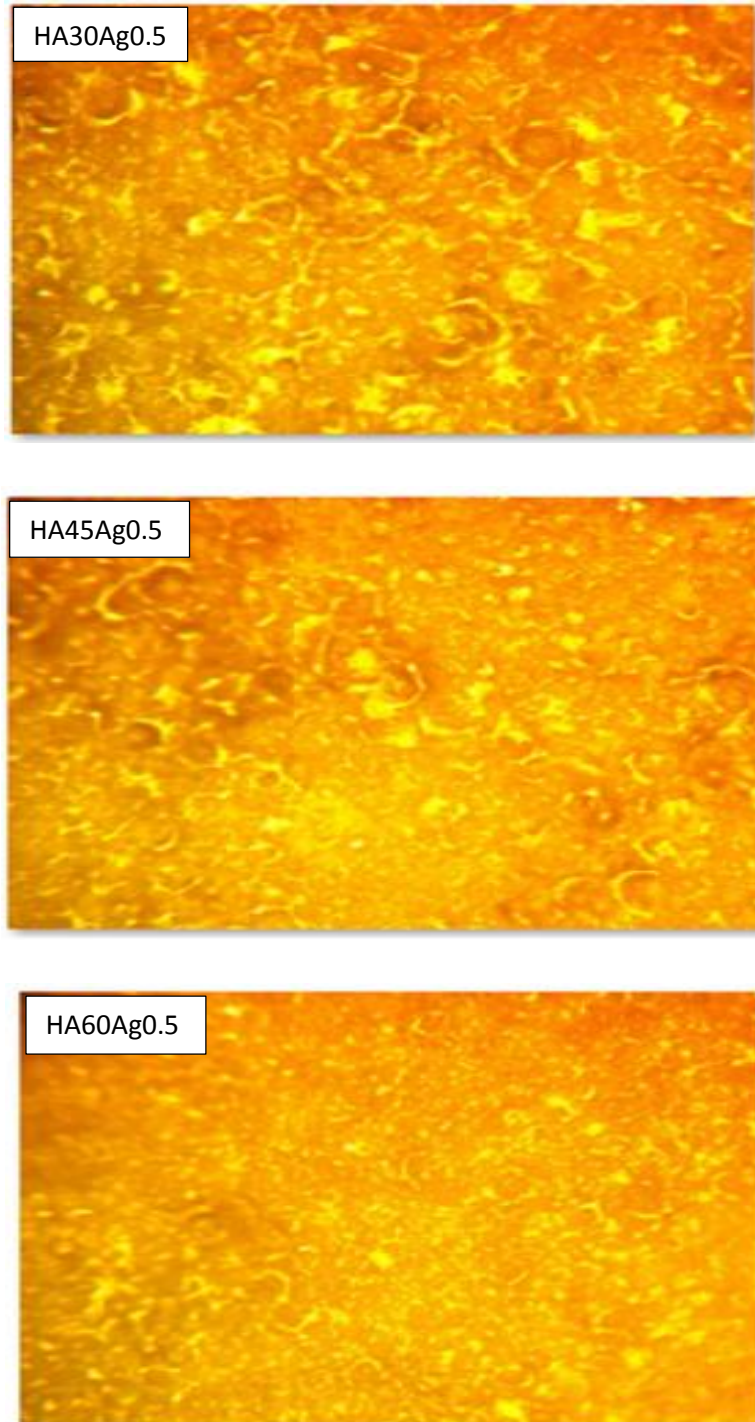


Figure (4.1): Microstructures of CP-Ti, HA, HA/nAg specimens (Contd)

The morphology of the surface changed with the addition of nano silver, becoming smoother and with fewer pores, although the (HA30Ag0.5) specimen did not have enough time to precipitate the nano silver.

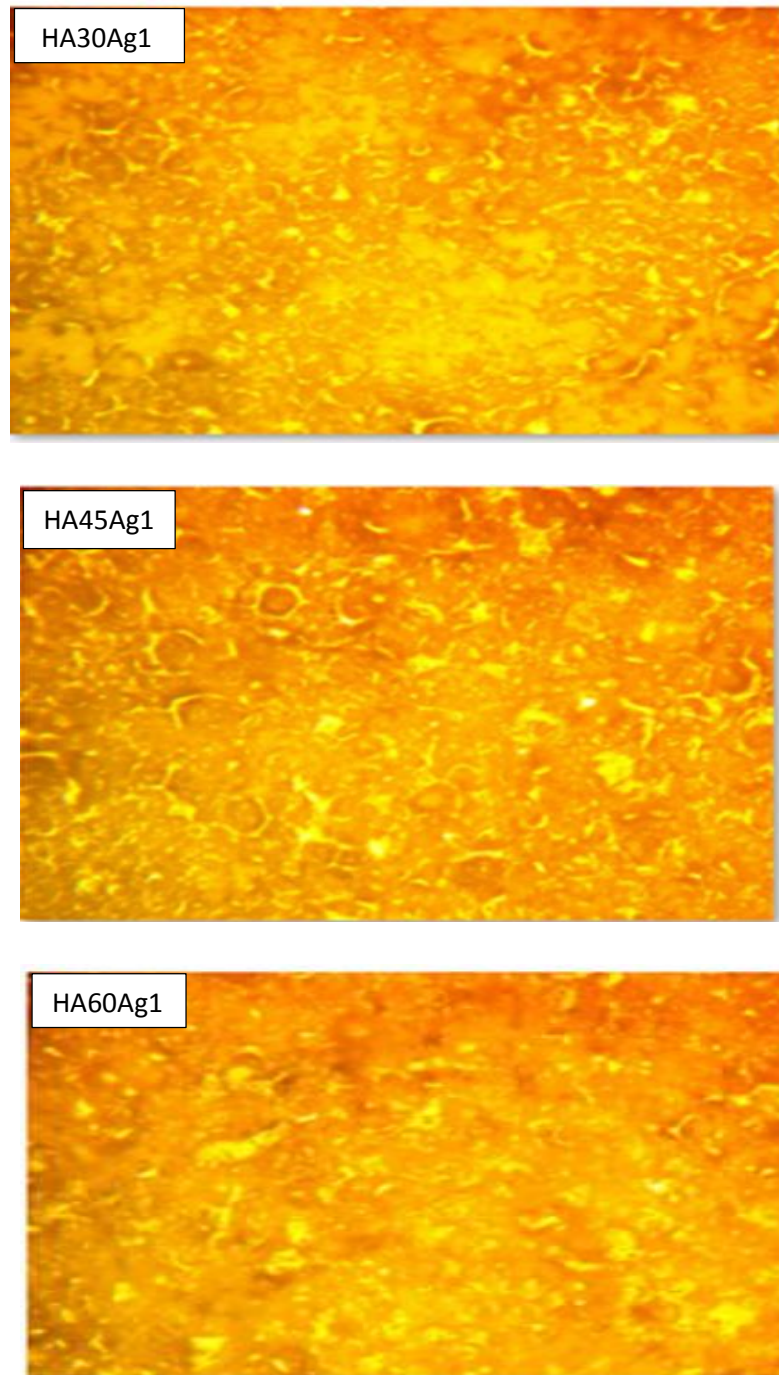


Figure (4.1): Microstructures of CP-Ti, HA, HA/nAg specimens (Contd)

The addition of nano silver changed the surface topography, making it smoother and with fewer pores, but the (HA30Ag0.5) specimen did not have enough time to precipitate the nano silver.

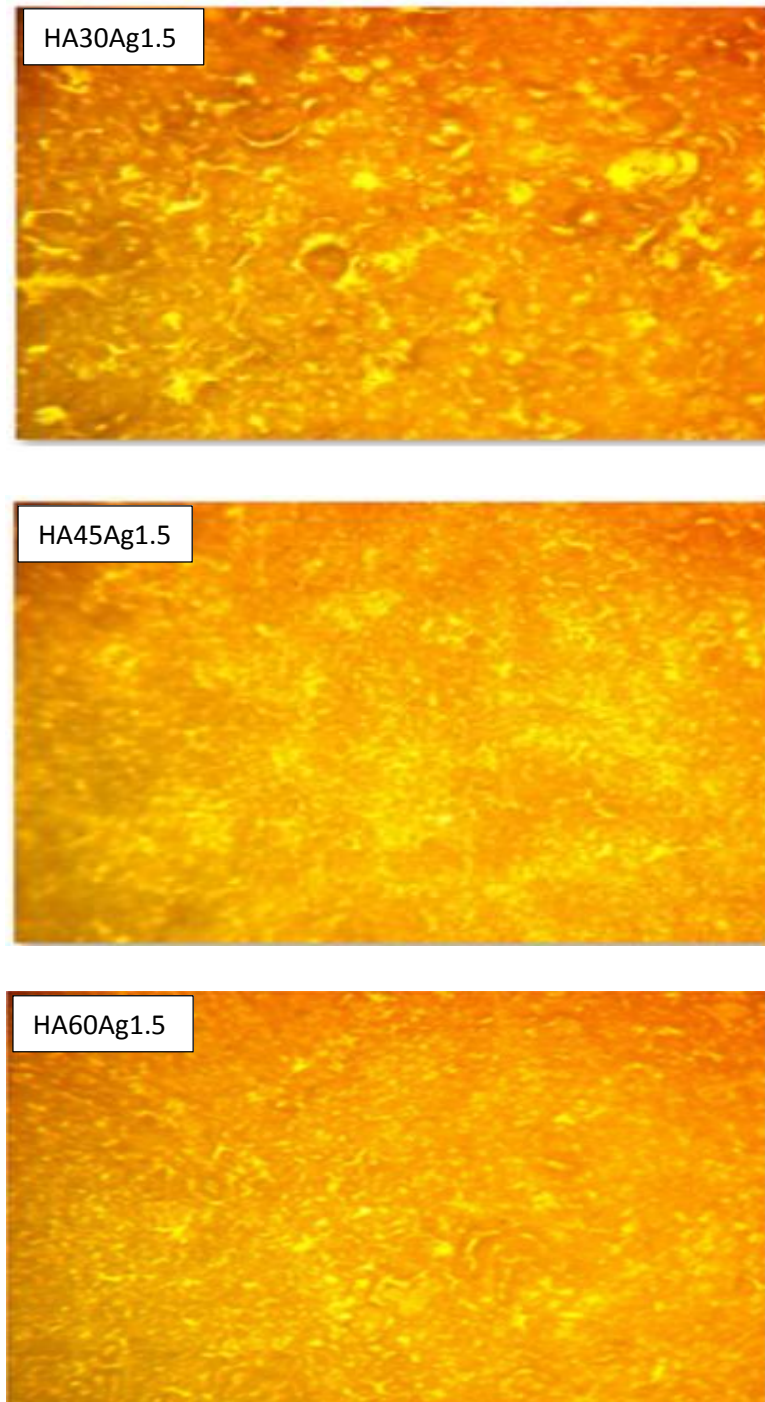


Figure (4.1): Microstructures of CP-Ti, HA, HA/nAg specimens (Contd)

The topography of the surface changed with the addition of nano silver, becoming smoother and with fewer pores, but the nano silver did not precipitate in the (HA30Ag0.5) specimen.

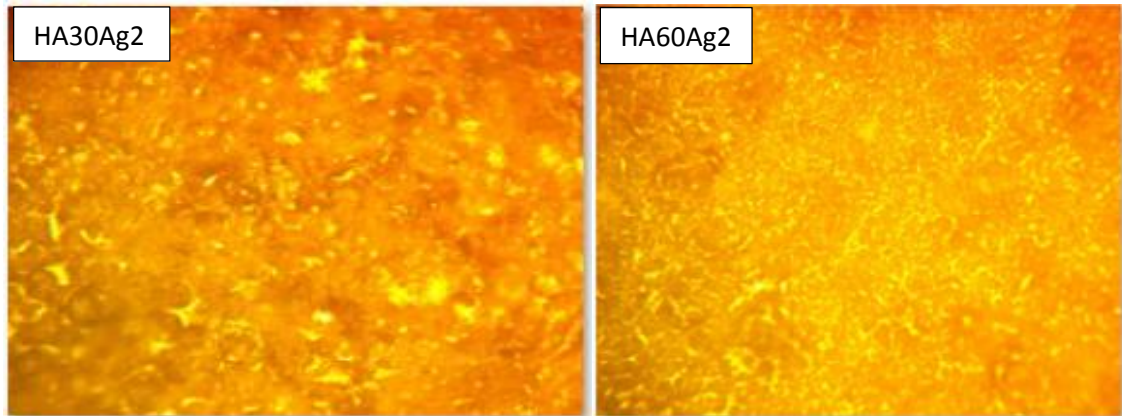


Figure (4.1): Microstructures of CP-Ti, HA, HA/nAg specimens (Contd)

#### **4.4. Field Emission Scanning Electron Microscopy (FESEM)**

Figure (4.2) illustrates Scanning Electron Microscopy (SEM) micrographs of nano silver powder. It is clear from the figure that particle size of nAg is 20 nm. Table (4.2) shows chemical composition of nAg and it is clear from the table that the purity of nAg is 99.99%. China was the country of origin of nano silver.



Figure (4.2) SEM of Nano Silver 20 nm.

Table (4.2) Chemical Composition of nAg.

element	Ag	Cu	Bi	Fe	Pb	Sb	Se	Te
Content	>=	<=	<=	<=	<=	<=	<=	<=
%	99.99	0.0002	0.0003	0.0001	0.0001	0.0003	0.0001	0.0003

The Figure (4.3) below show FESEM micrographs of CP-Ti specimen which proves that its surface was clean and free from the remnants of the cutting process after cleaning it with ultrasonic cleaning device.

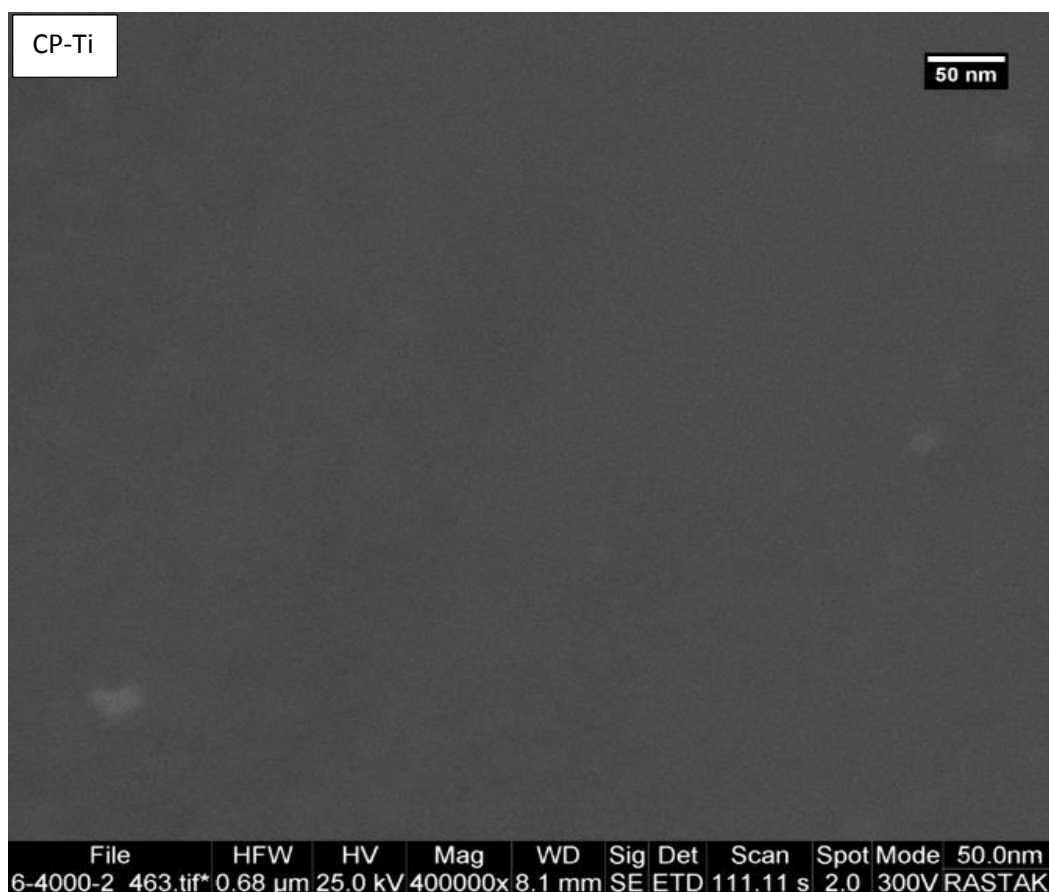


Figure (4.3) FESEM micrographs of CP-Ti specimen

The Figure (4.4 a, b, c) below show FESEM micrographs of HA30 specimen on CP-Ti specimen at constant voltage (200) V with different magnification. It is clear from the figure that the hydroxyapatite particles are deposited, forming the coating layers one on top of the other in the form of flakes through the titanium oxide ( $\text{TiO}_2$ ) layer in a heterogeneous of pores and cracks.

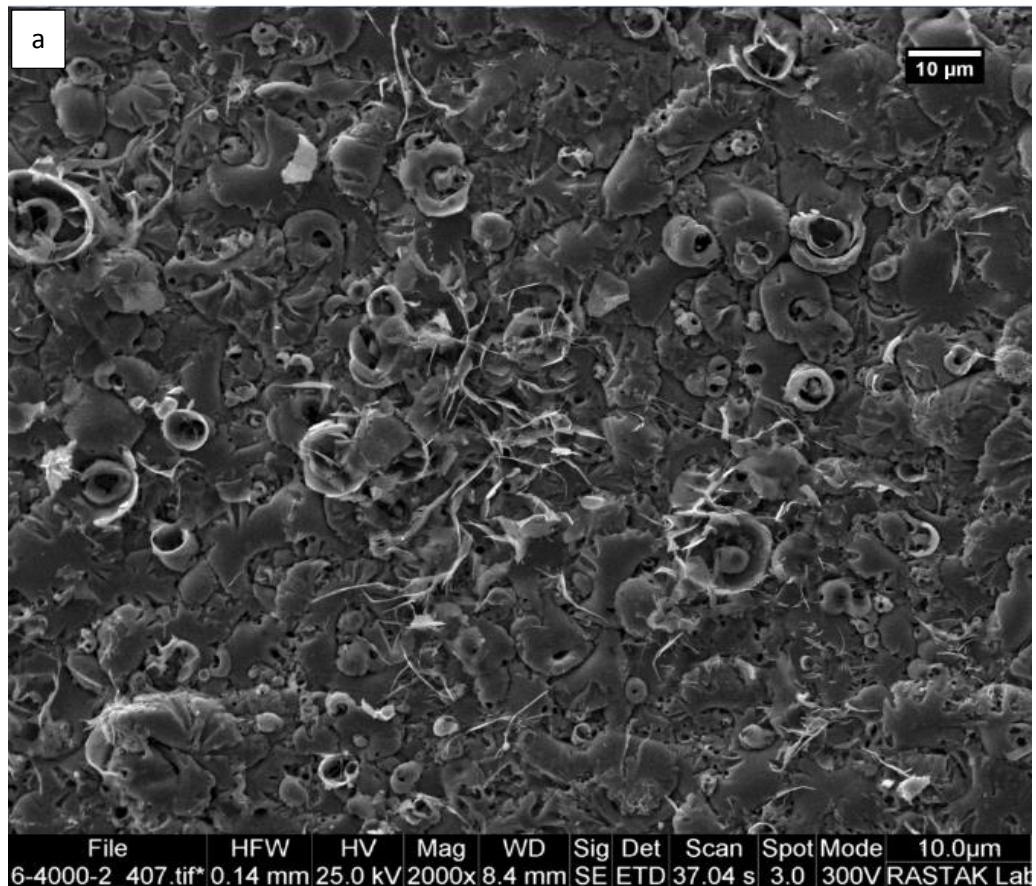


Figure (4.4 a,b,c) FESEM micrographs of HA30 specimen.

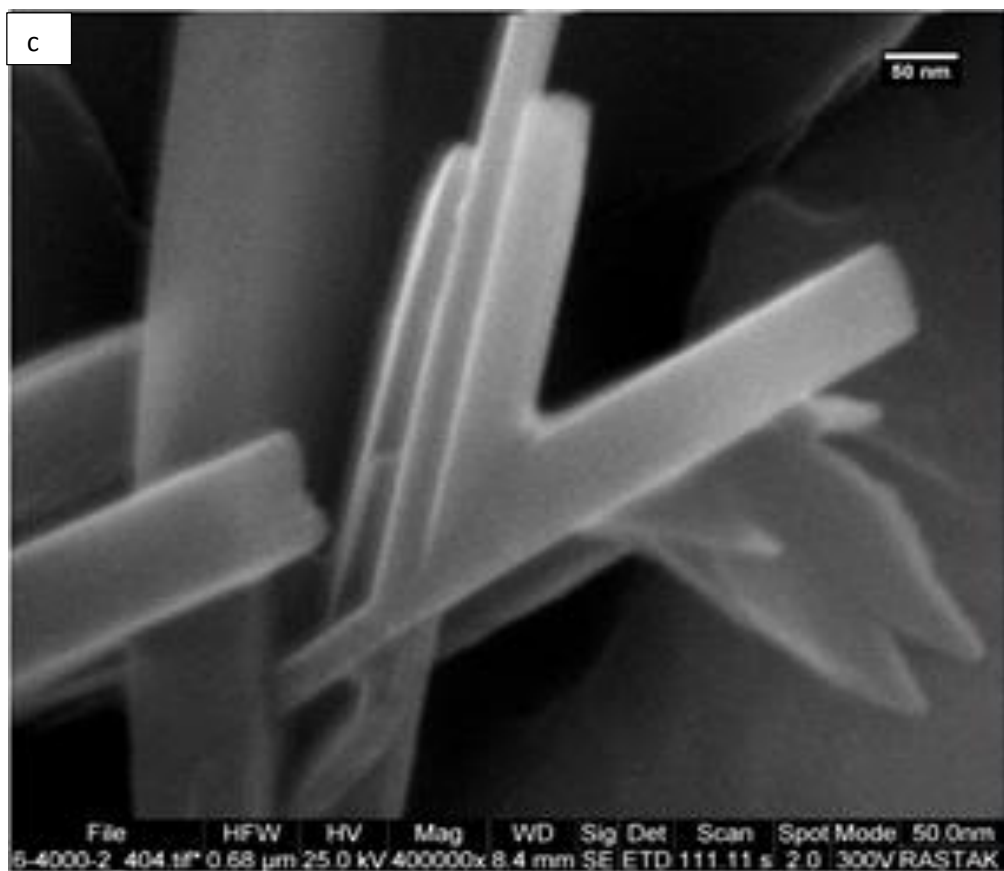
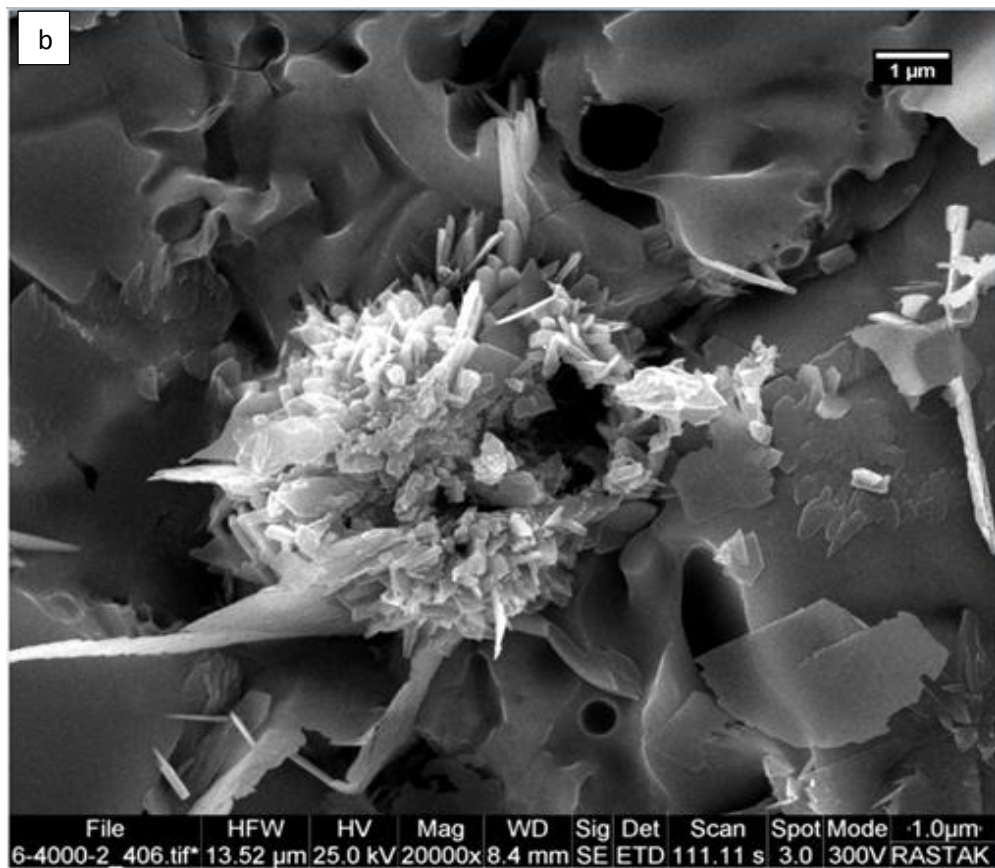


Figure (4.4 a, b, c): FESEM micrographs of HA30 specimen (Contd)

The Figure (4.5 a, b, c) below show FESEM micrographs of HA45 specimen on CP-Ti specimen at constant voltage (200) V with different magnification. The longer the coating time, the growth of hydroxyapatite particles increased and remained a heterogeneous distribution, there are also cracks and pores.

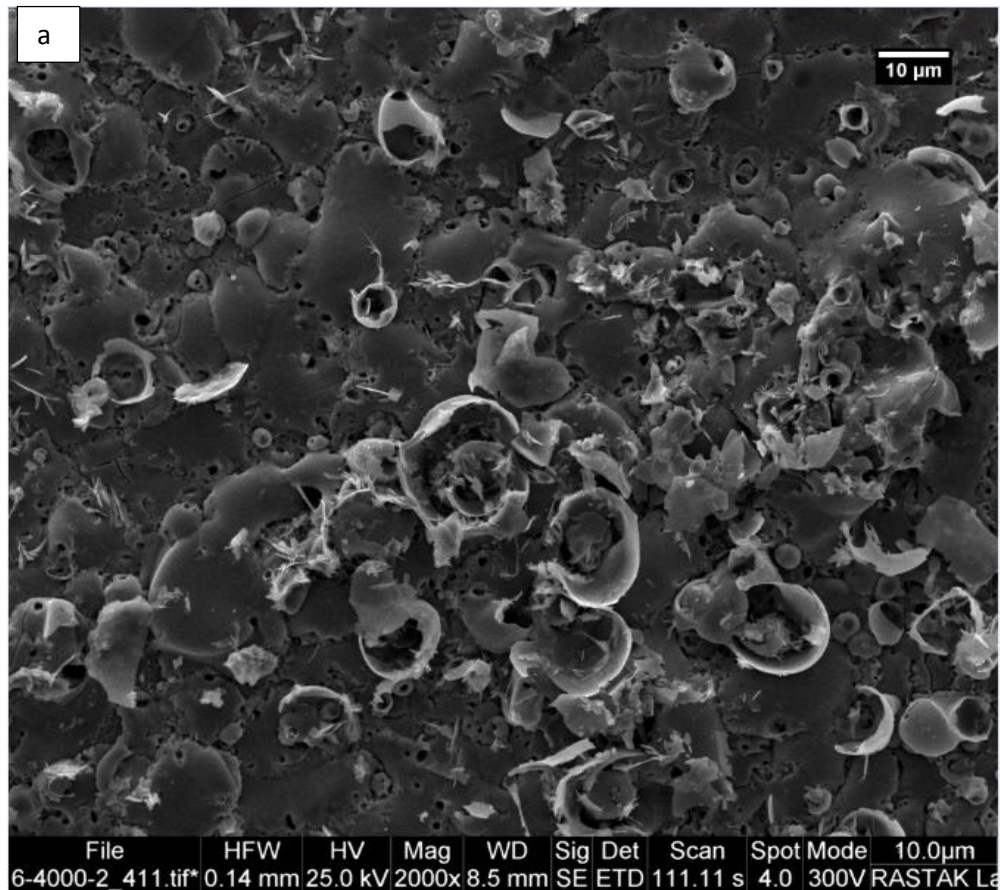


Figure (4.5 a, b, c) FESEM micrographs of HA45 specimen

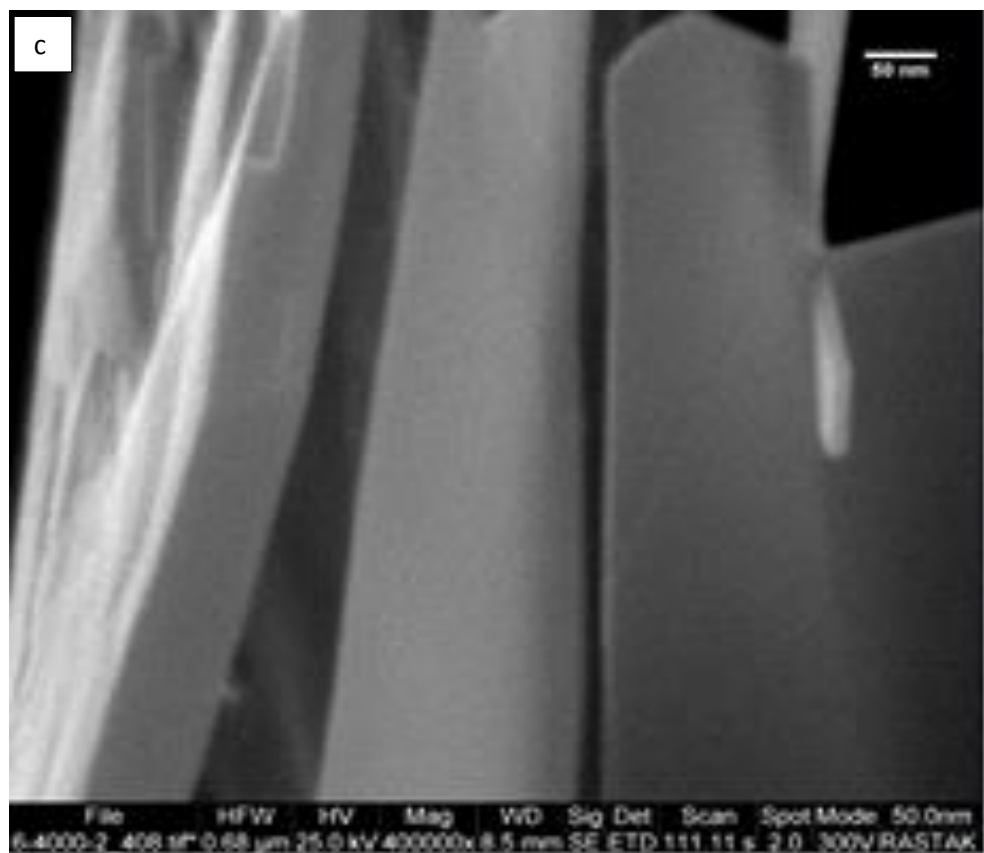
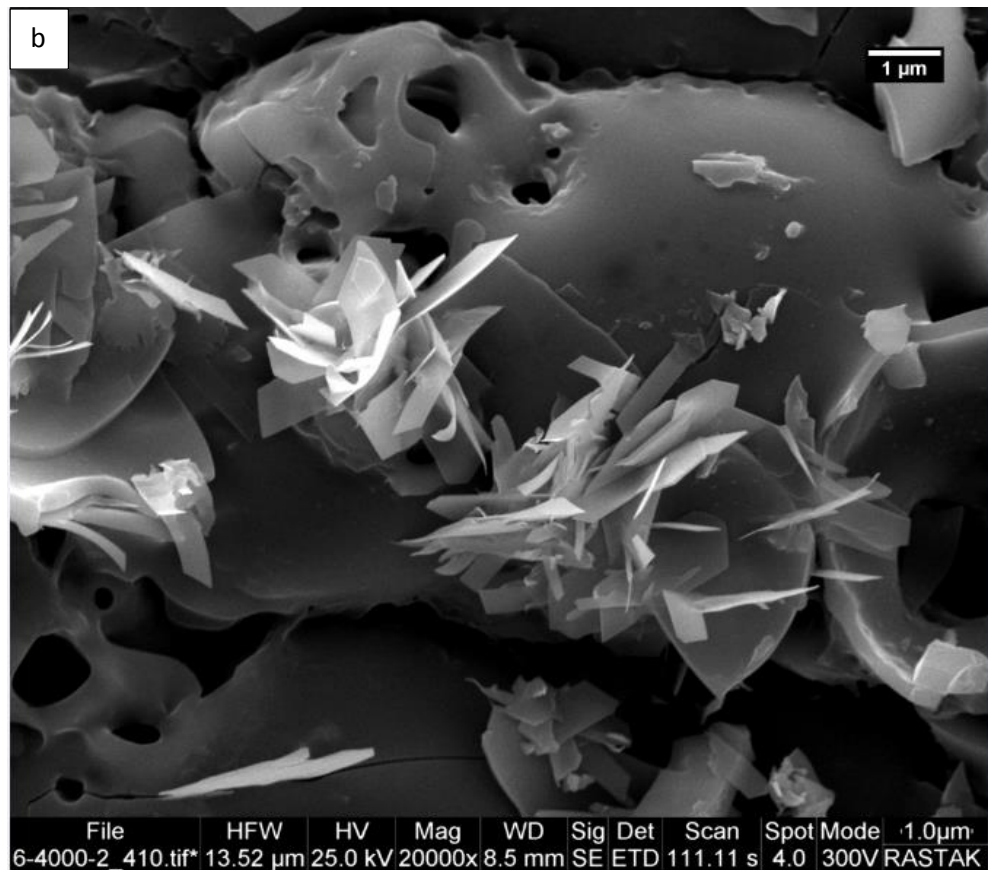


Figure (4.5 a, b, c): FESEM micrographs of HA45 specimen (Contd)

The Figure (4.6 a, b, c) below show FESEM micrographs of HA60 specimen on CP-Ti specimen at constant voltage (200) V with different magnification. The longer the coating time, the more hydroxyapatite particles grew and remained in a heterogeneous distribution with cracks and pores and that matches [100].

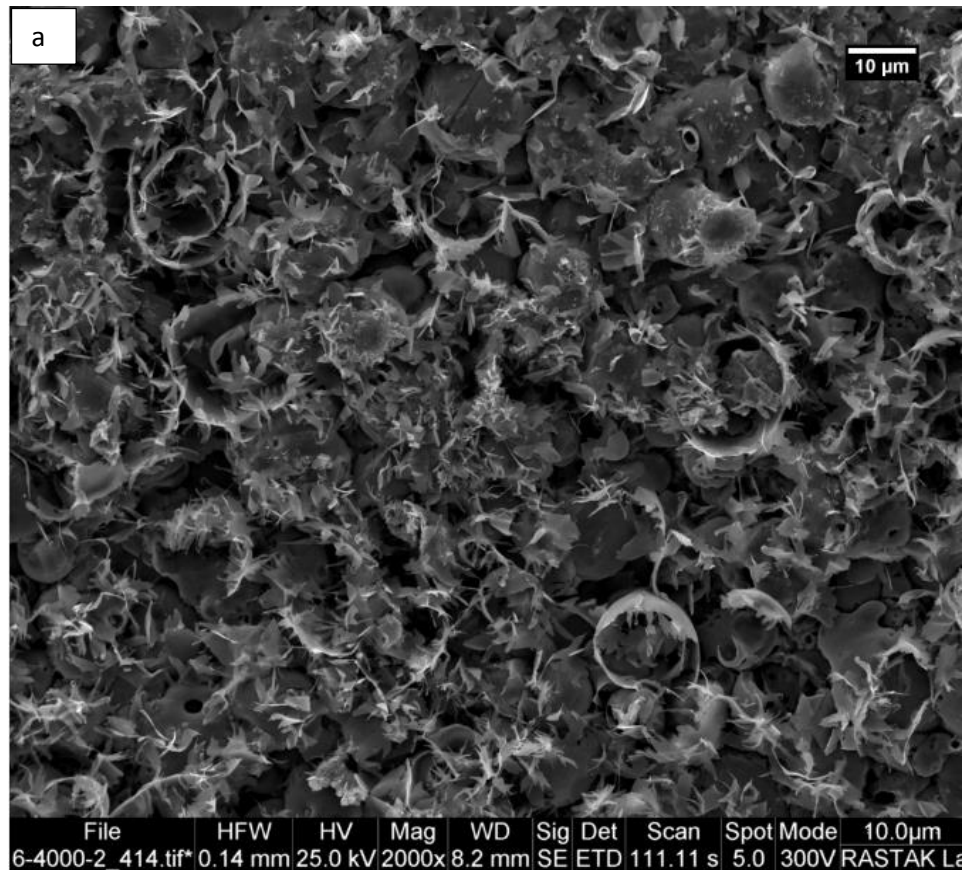


Figure (4.6 a, b, c) FESEM micrographs of HA60 specimen

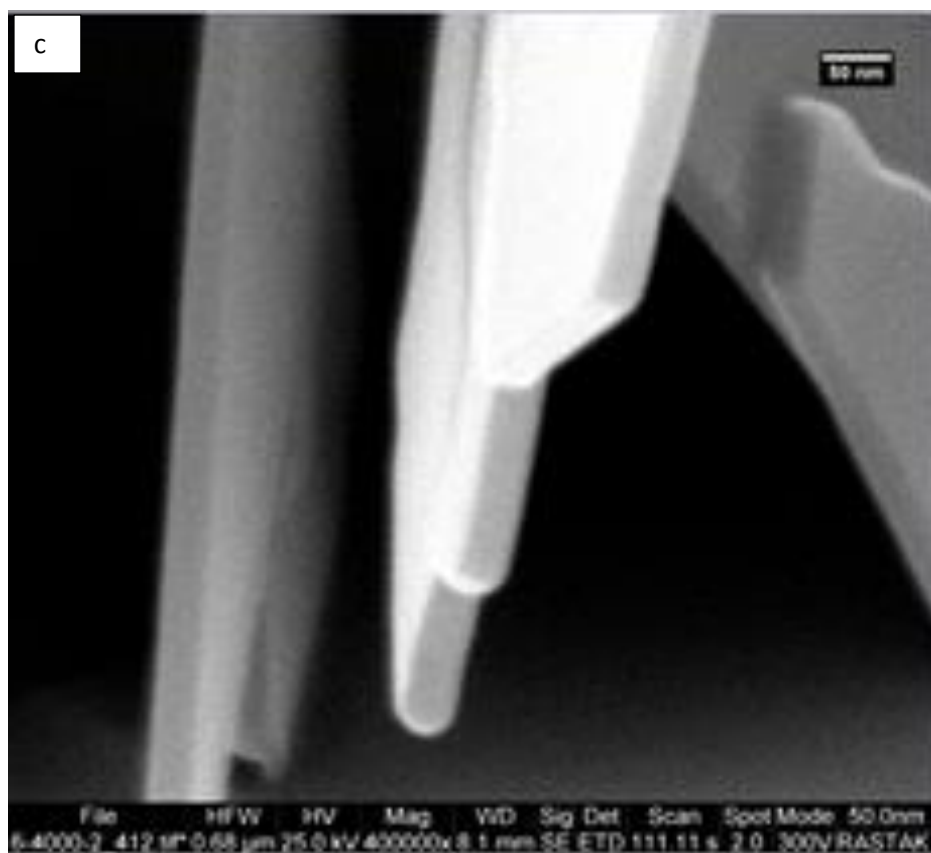
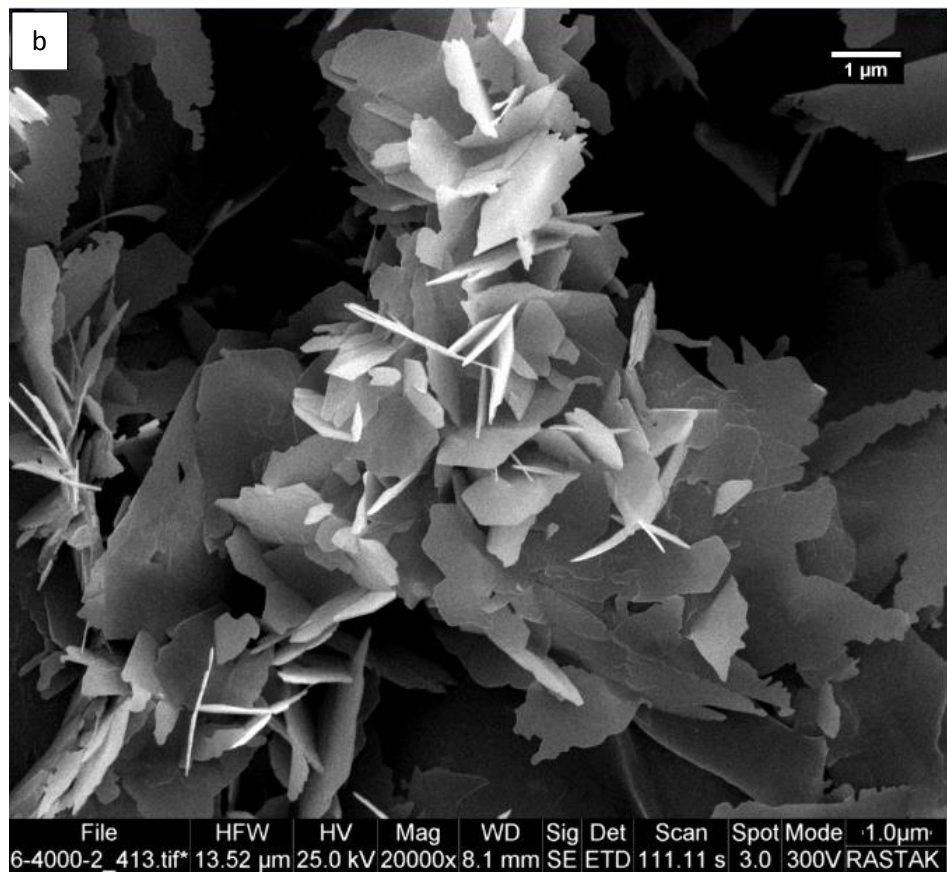


Figure (4.6 a, b, c): FESEM micrographs of HA60 specimen (Contd)

The Figure (4.7 a, b, c) below show FESEM micrographs of HA30Ag0.5 specimen on CP-Ti specimen at constant voltage (200) V with different magnification. Although nano silver is added to the hydroxyapatite electrolyte, it will not precipitate because there is not enough time to precipitate it.

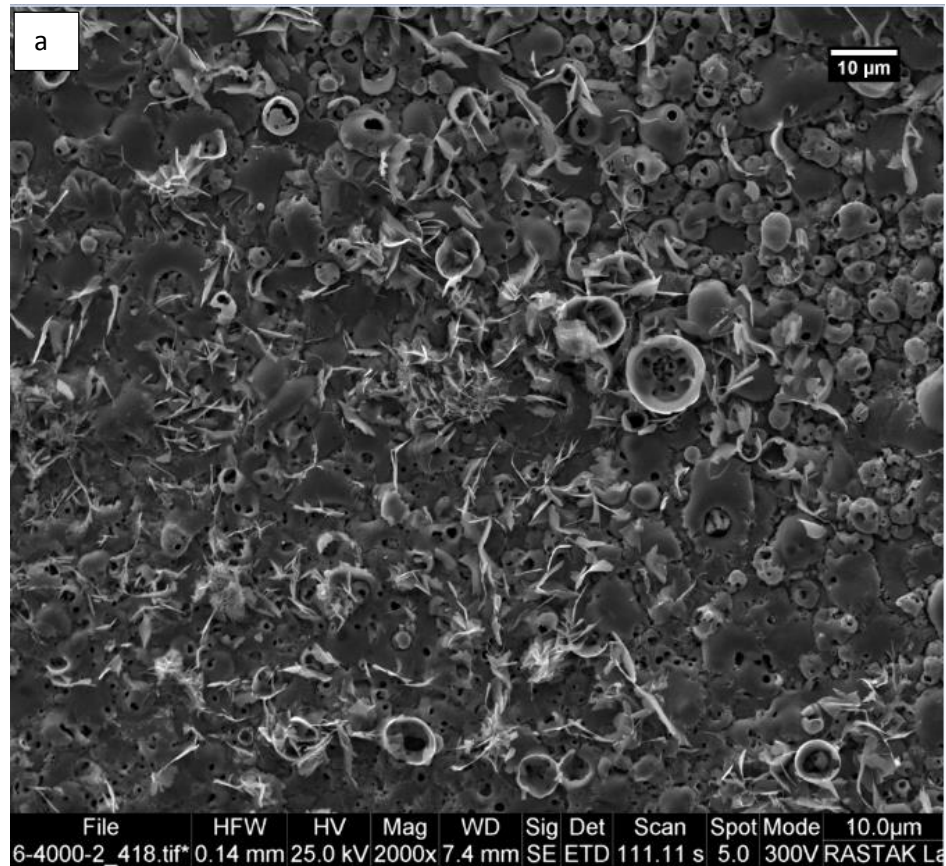


Figure (4.7 a, b, c) FESEM micrographs of HA30Ag0.5 specimen.

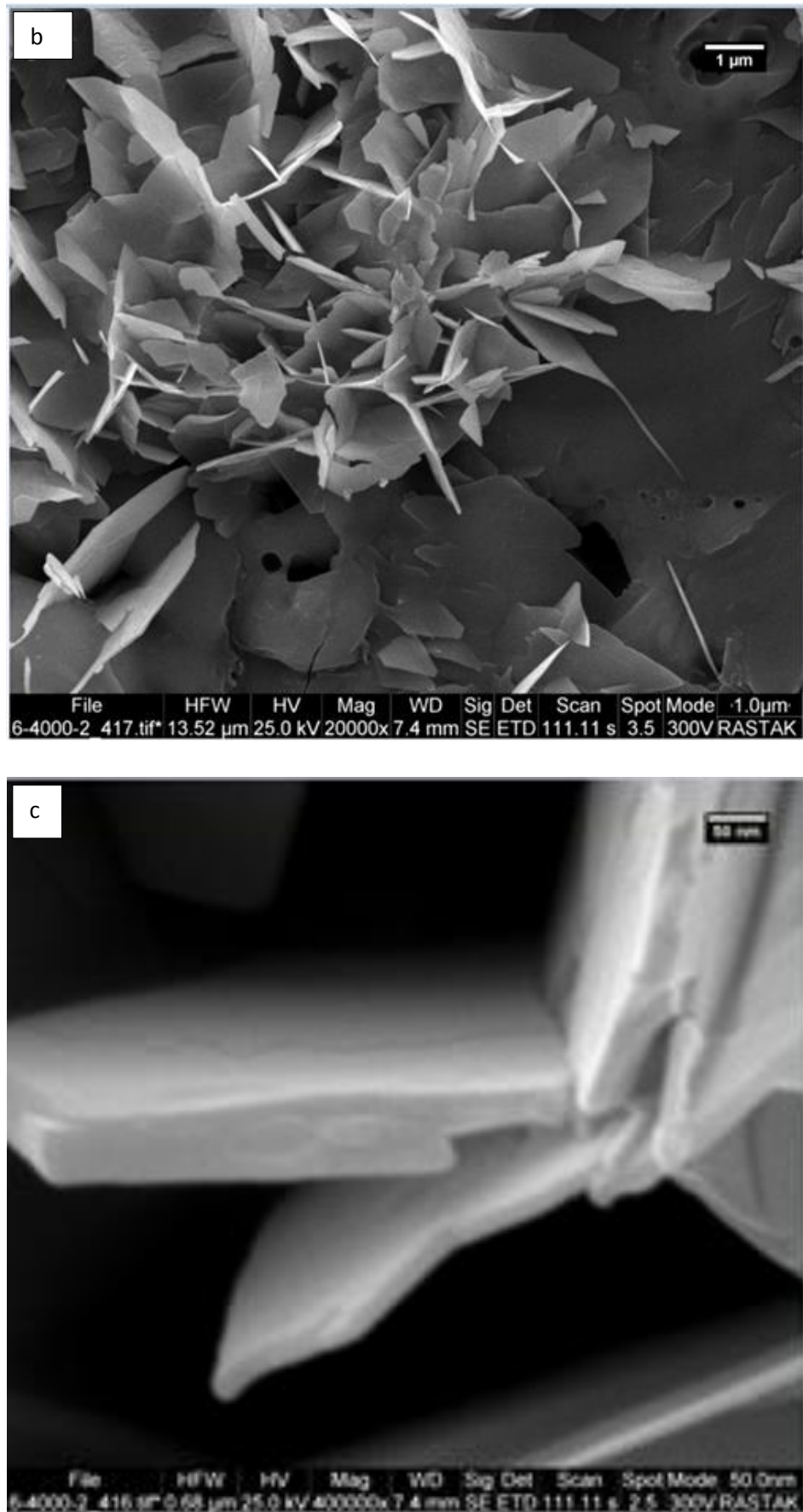


Figure (4.7 a, b, c): FESEM micrographs of HA30Ag0.5 specimen (Contd)

The Figure (4.8 a, b, c) below show FESEM micrographs of HA45Ag0.5 specimen on CP-Ti specimen at constant voltage (200) V with different magnification. Silver nanoparticles were deposited by increasing the coating time. The presence of nano silver was inferred from the figure (4.2), where the size of the nano silver particles is 20nm and the magnification by FESEM analysis was 50nm.

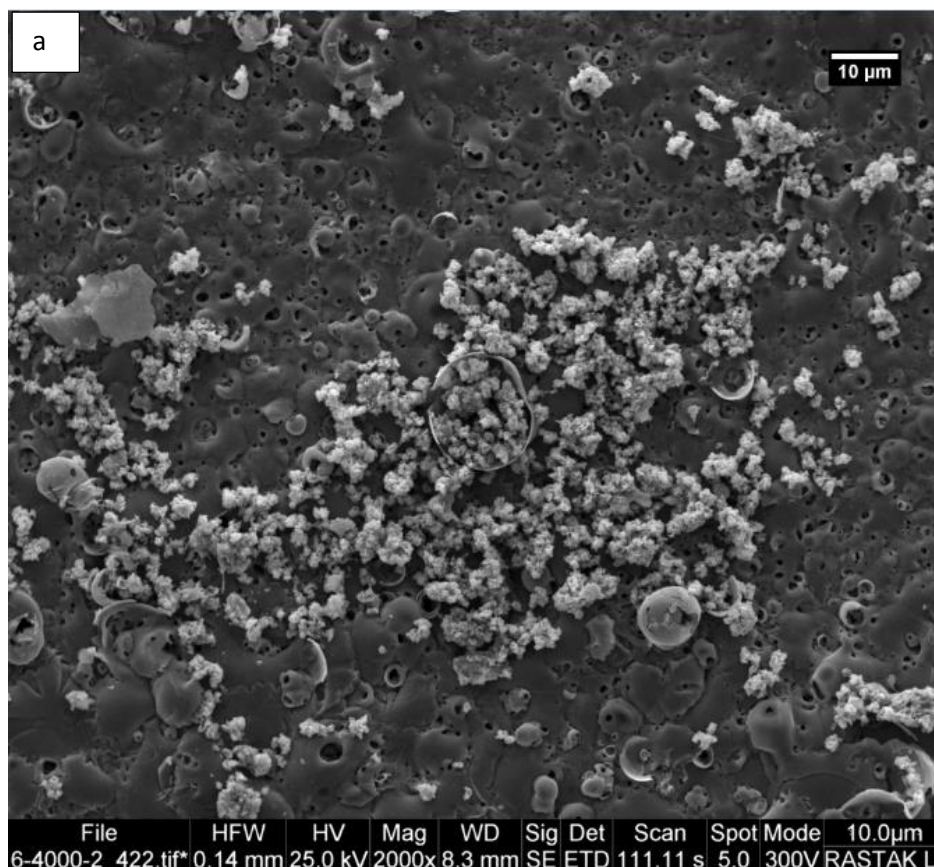


Figure (4.8 a, b, c) FESEM micrographs of HA45Ag0.5 specimen

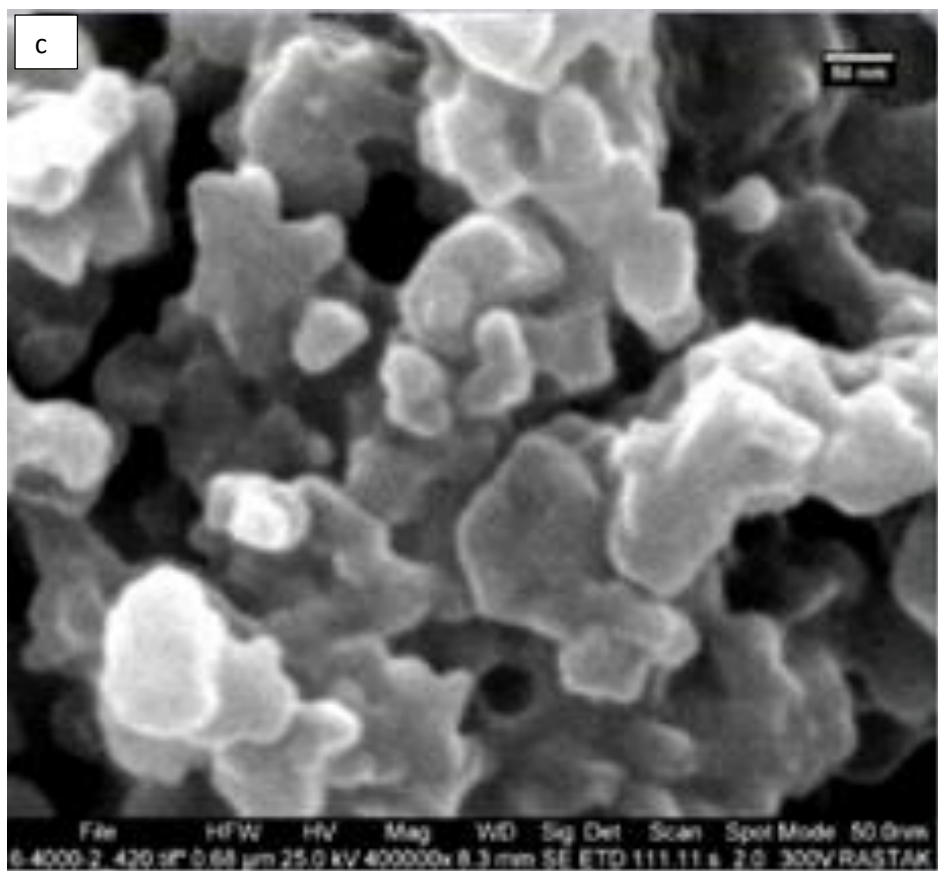
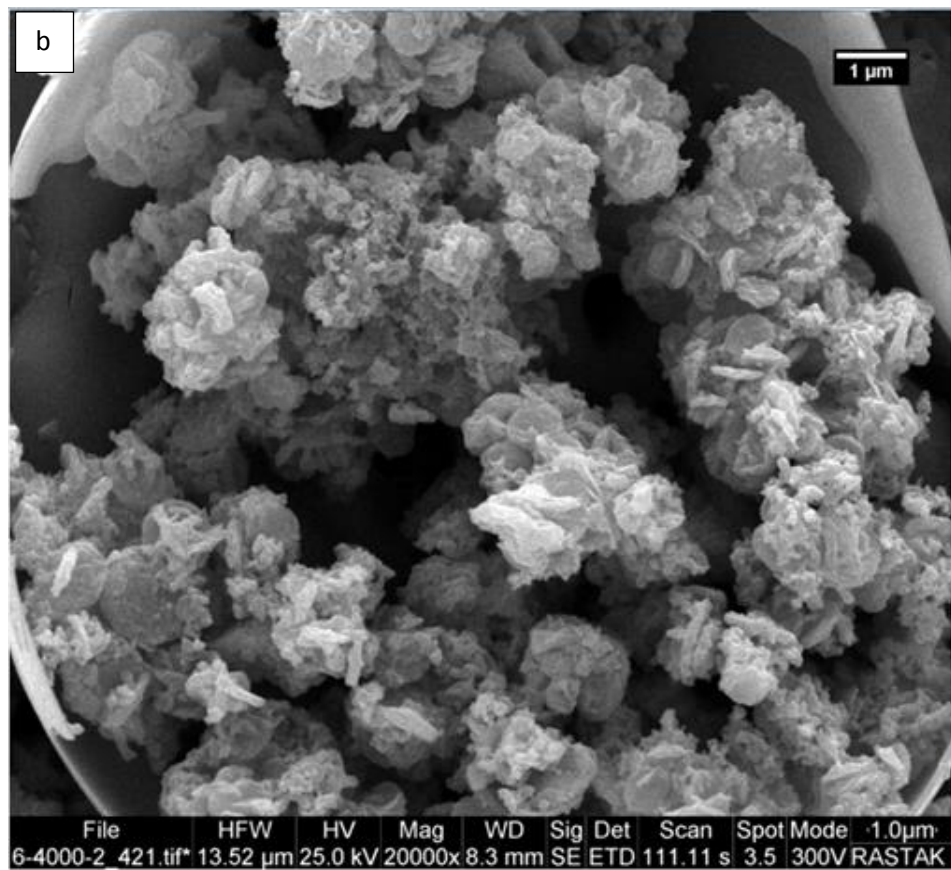


Figure (4.8 a, b, c): FESEM micrographs of HA45Ag0.5 specimen (Contd)

The Figure (4.9 a, b, c) below show FESEM micrographs of HA60Ag0.5 specimen on CP-Ti specimen at constant voltage (200) V with different magnification. By increasing the coating time, silver nanoparticles were deposited. The presence of nano silver was deduced from figure (4.2), where the nano silver particle size is 20nm and the magnification by FESEM analysis is 50nm.

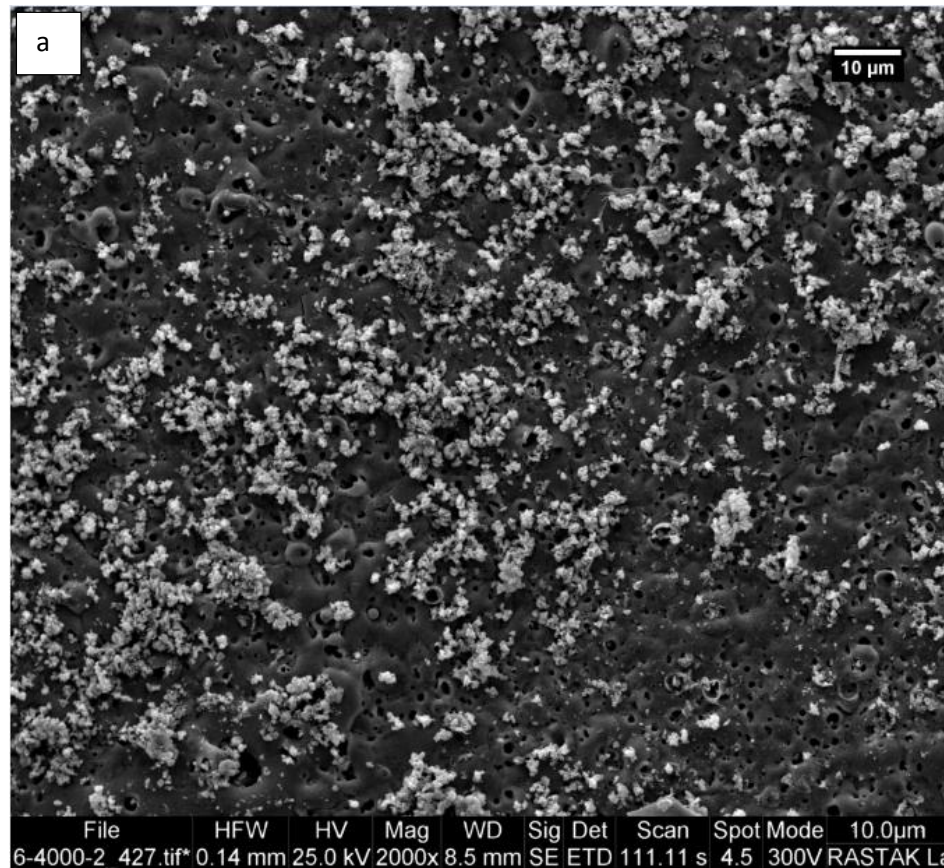


Figure (4.9 a, b, c) FESEM micrographs of HA60Ag0.5 specimen

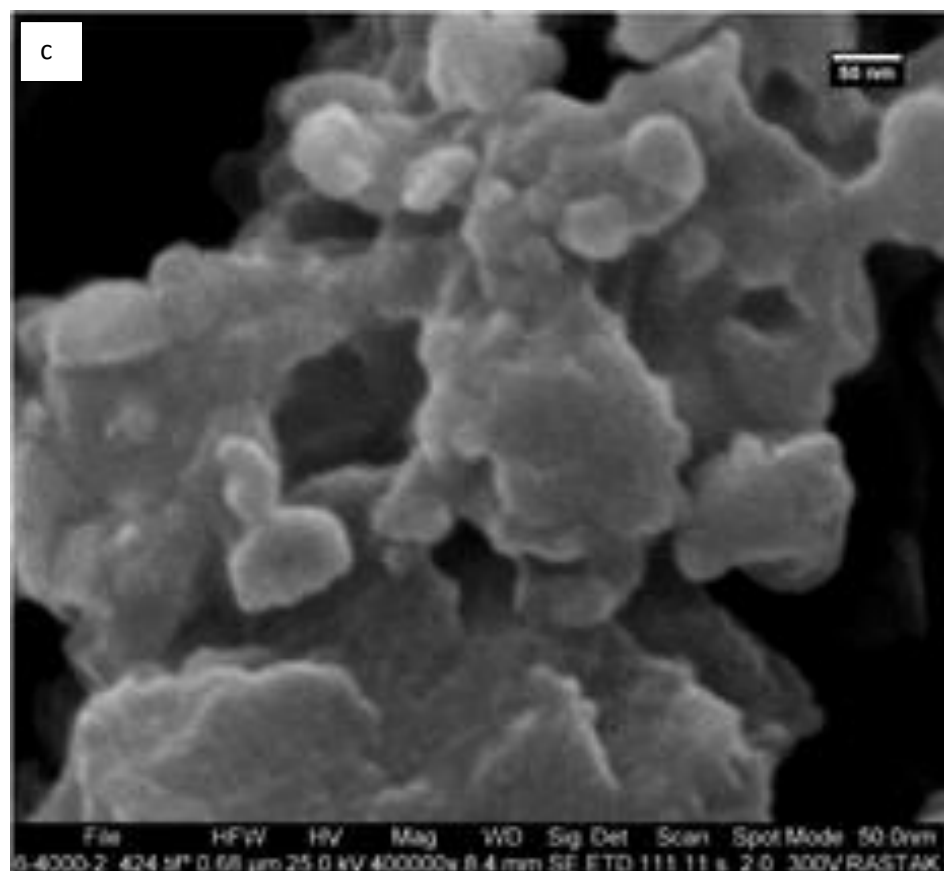
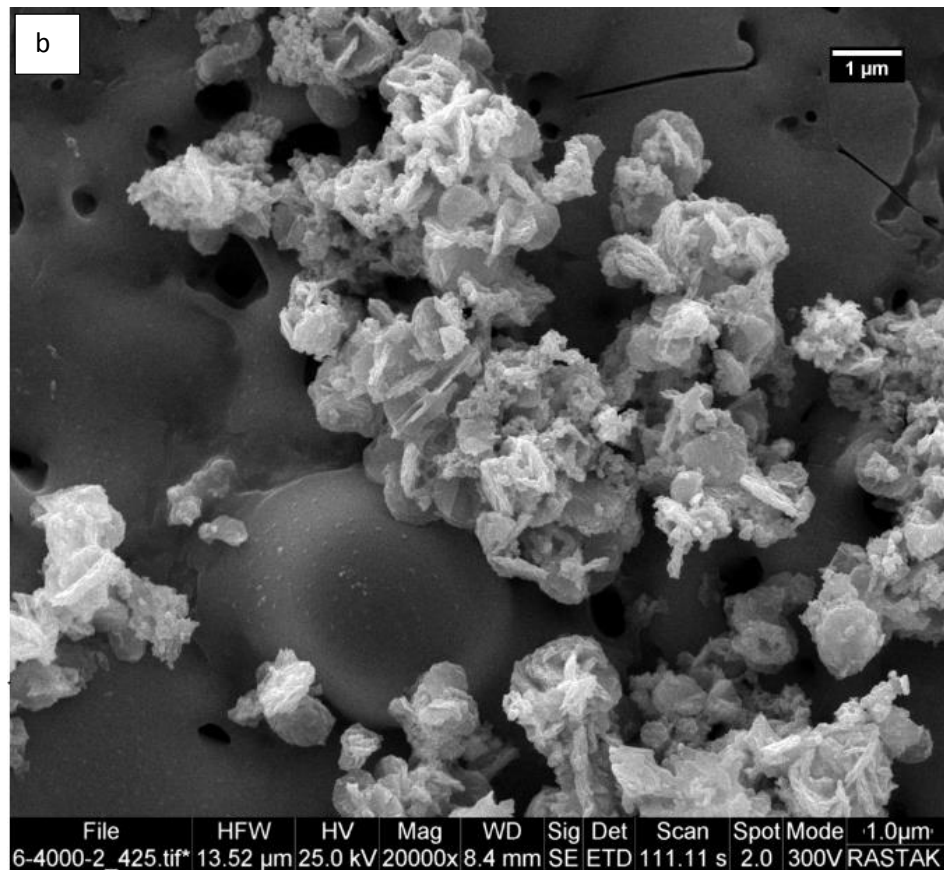


Figure (4.9 a, b, c): FESEM micrographs of HA60Ag0.5 specimen (Contd)

The Figure (4.10 a, b, c) below show FESEM micrographs of HA30Ag1 specimen on CP-Ti specimen at constant voltage (200) V with different magnification. Despite the increased in the proportion of nano silver to the hydroxyapatite electrolyte, it does not precipitate because there is insufficient time. The specimen contains holes and is visible in the examination distance 1 $\mu$ m, 2 $\mu$ m and this, for example, occurs due to the plasma that leads to the generation of another layer on the first layer.

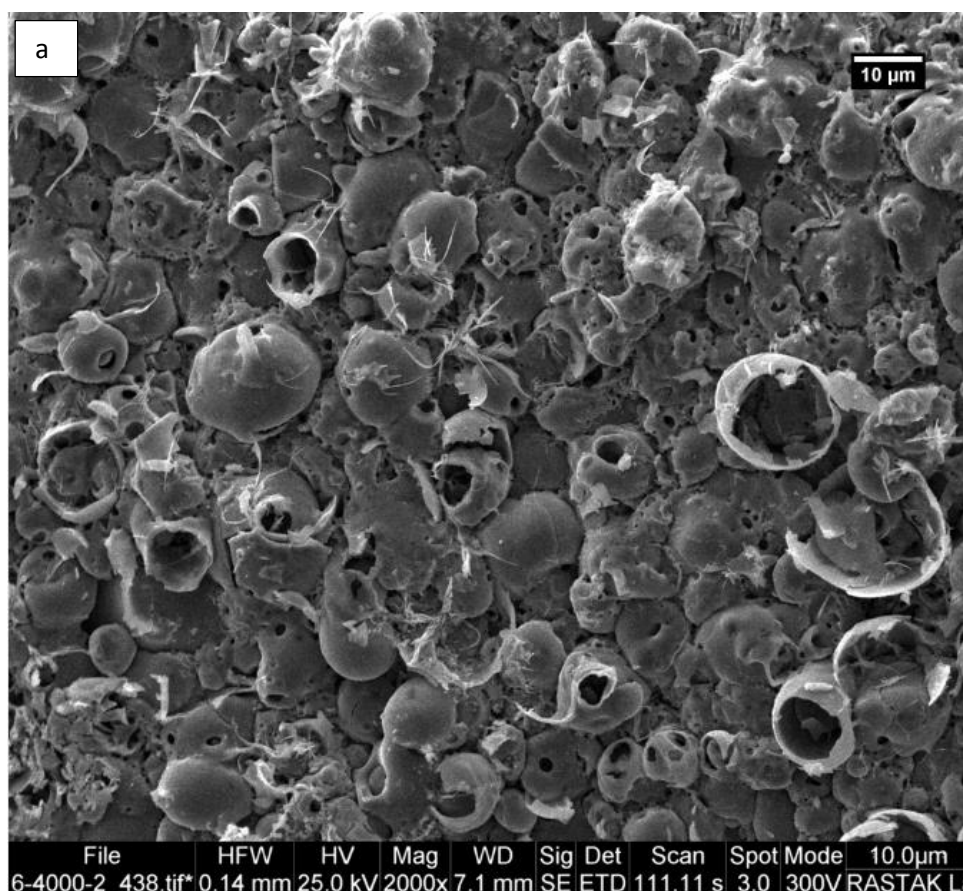


Figure (4.10 a, b, c) FESEM micrographs of HA30Ag1 specimen

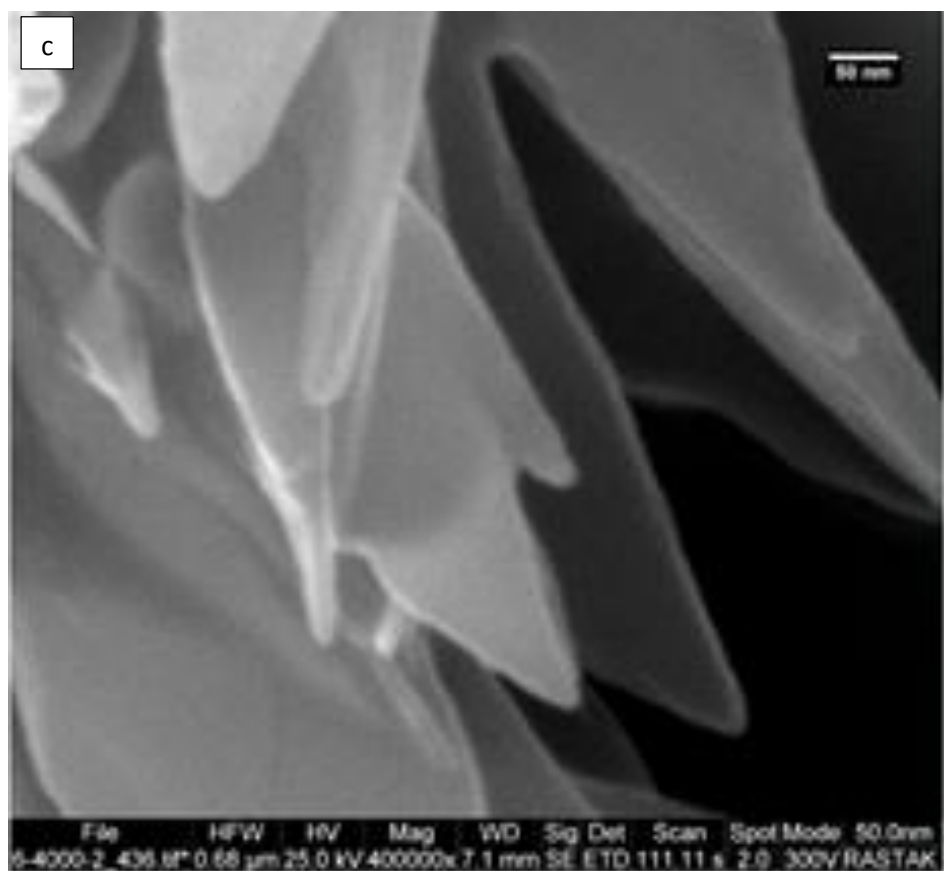
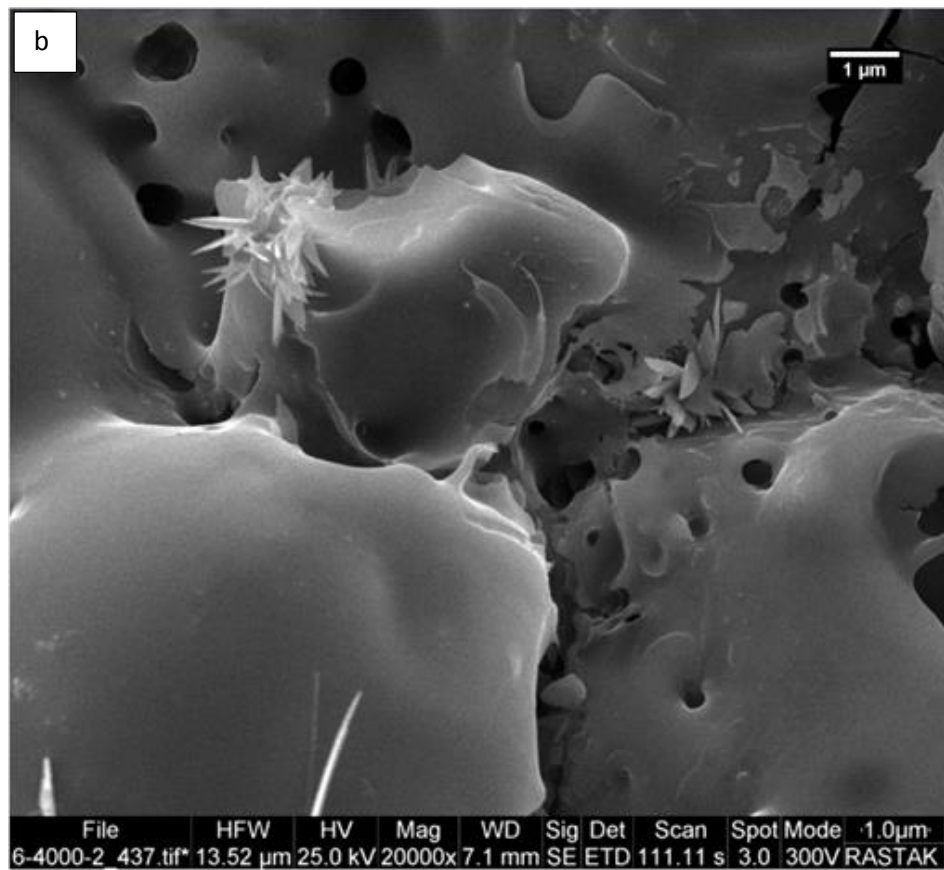


Figure (4.10 a, b, c): FESEM micrographs of HA30Ag1 specimen (Contd)

The Figure (4.11 a, b, c) below show FESEM micrographs of HA45Ag1 specimen on CP-Ti specimen at constant voltage (200) V with different magnification. Fracture of the TiO<sub>2</sub> layer due to high temperature and plasma formed, which appears to grow HA/Ag on the oxide layer, but the increase in the percentage of silver led to the formation of a different shape from the previous one, and at 50 nm it appears as continuous layers.

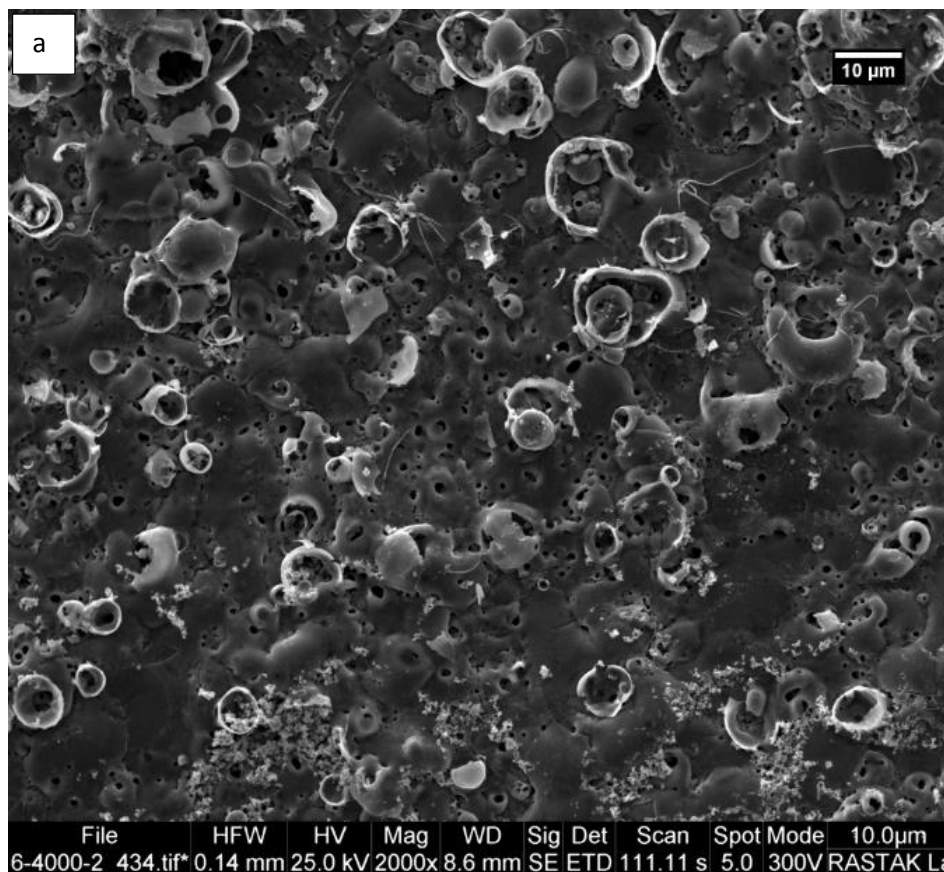


Figure (4.11 a, b, c) FESEM micrographs of HA45Ag1 specimen

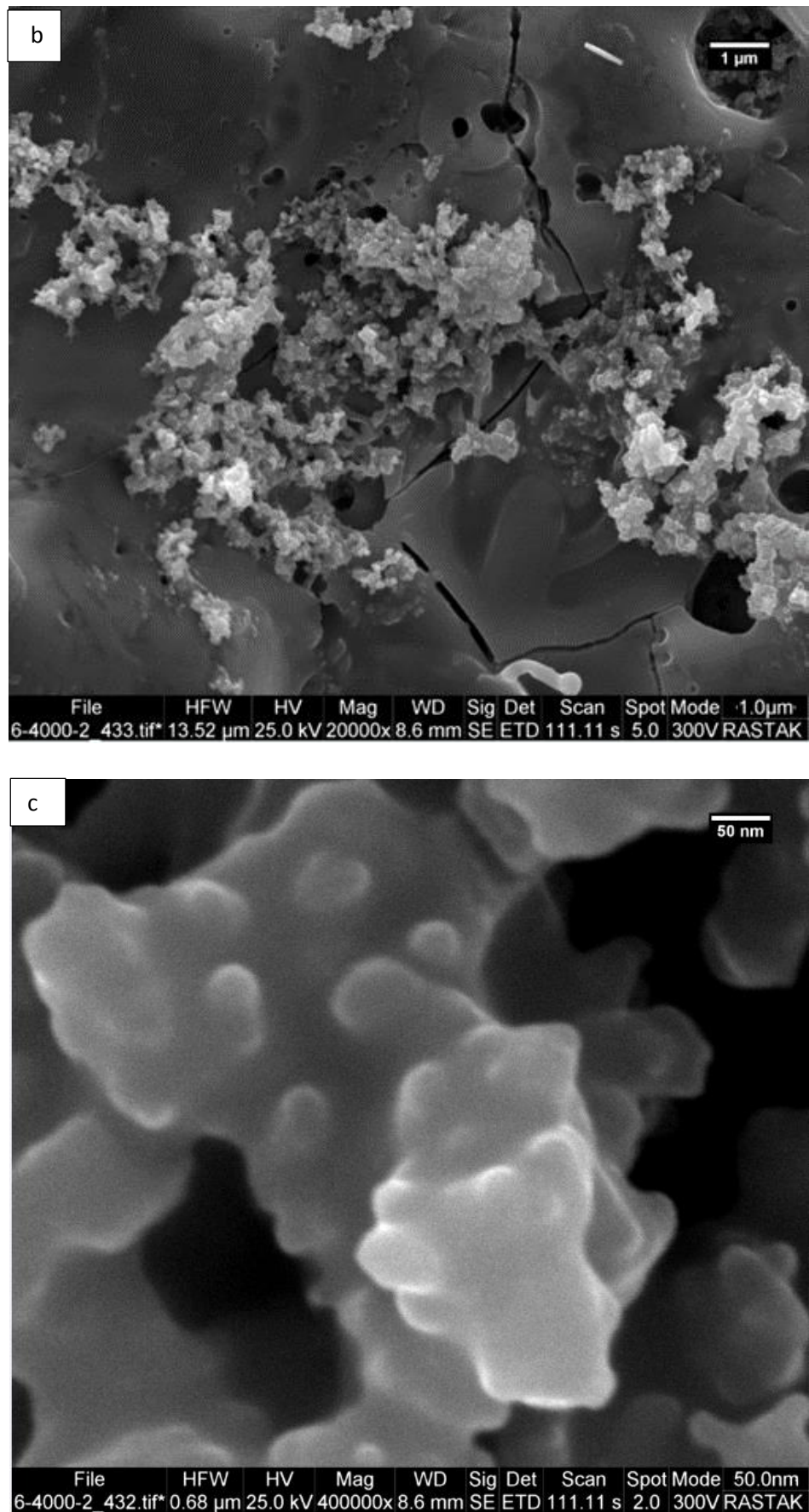


Figure (4.11 a, b, c): FESEM micrographs of HA45Ag1 specimen (Contd)

The Figure (4.12 a, b, c) below show FESEM micrographs of HA60Ag1 specimen on CP-Ti specimen at constant voltage (200) V with different magnification. Clear holes on each specimen because the time period is long.

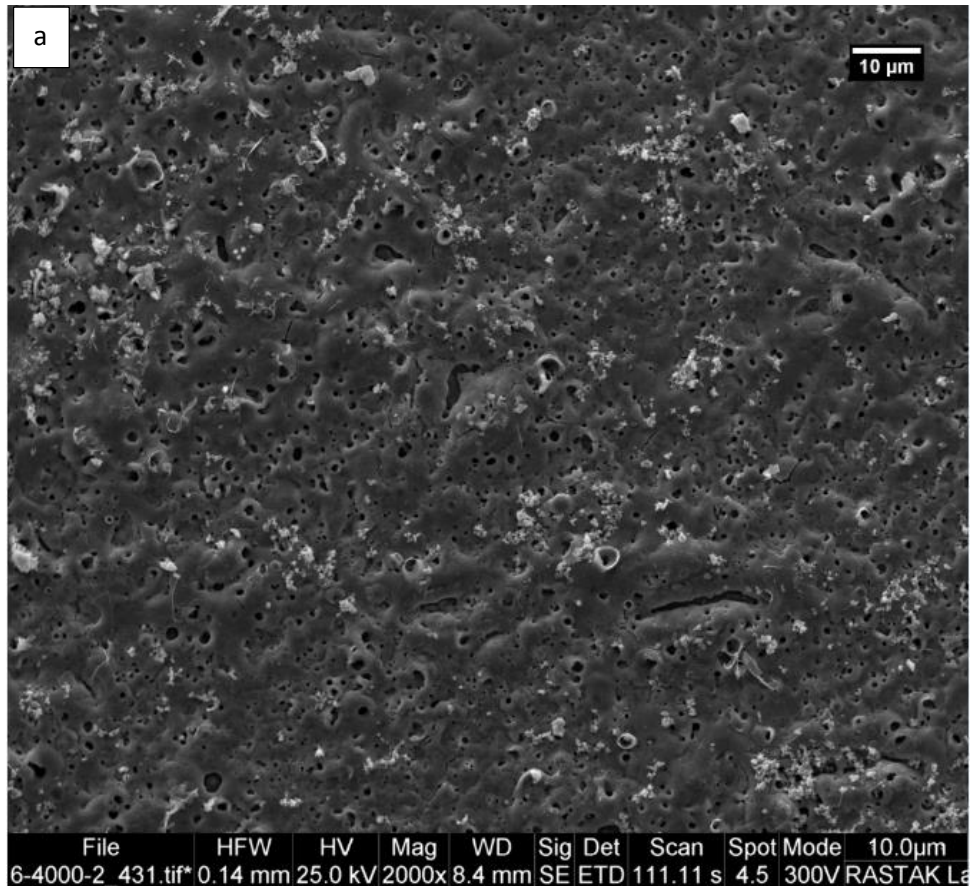


Figure (4.12 a, b, c) FESEM micrographs of HA60Ag1 specimen

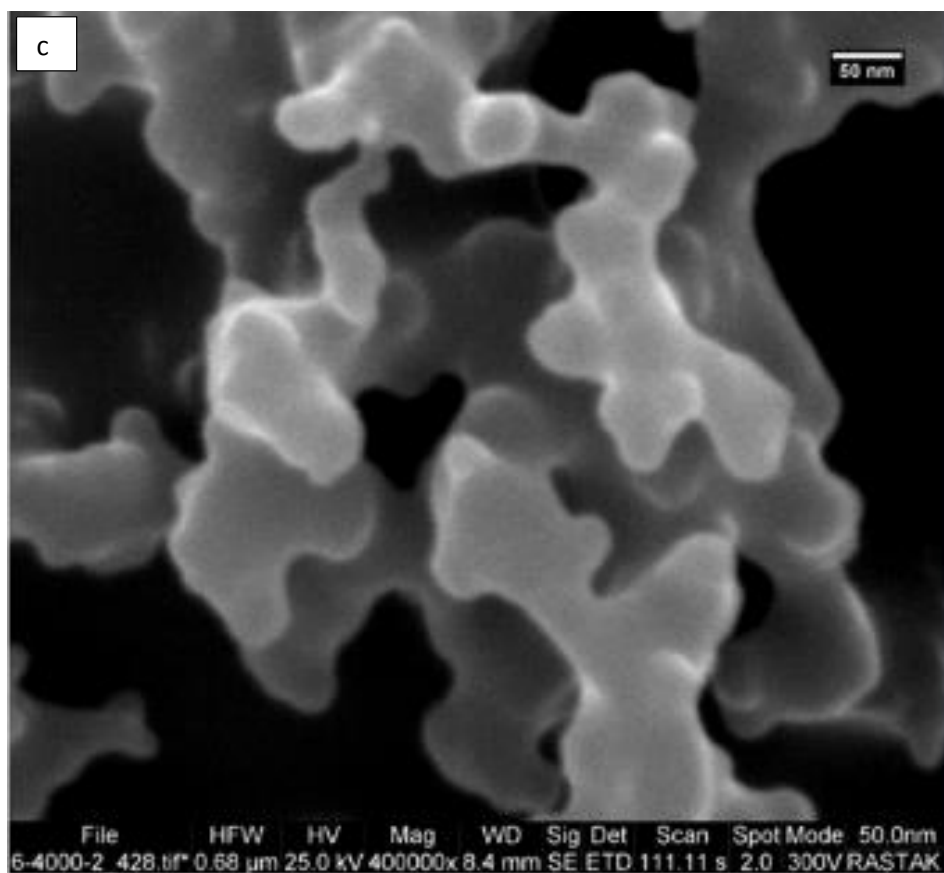
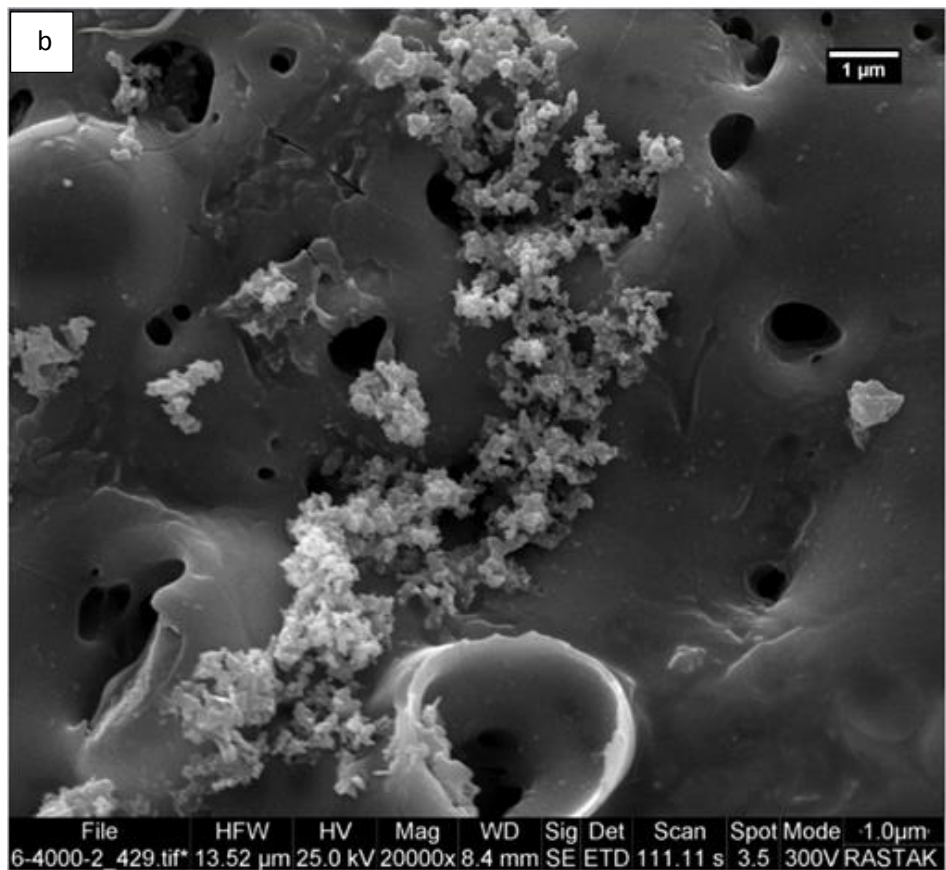


Figure (4.12 a, b, c): FESEM micrographs of HA60Ag1 specimen (Contd)

The Figure (4.13 a, b, c) below show FESEM micrographs of HA30Ag1.5 specimen on CP-Ti specimen at constant voltage (200) V with different magnification. The shape of the structure of the deposited layer and at 50 nm the deposited layer is different and the growth of the deposited layer in two directions.

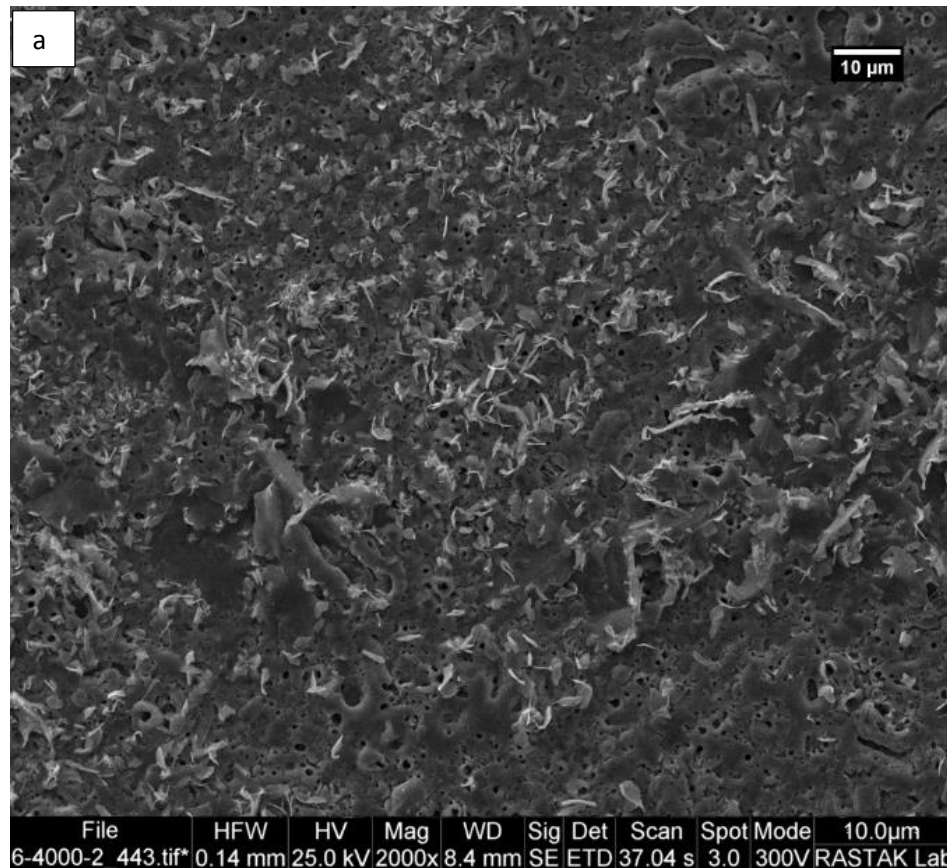


Figure (4.13 a, b, c) FESEM micrographs of HA30Ag1.5 specimen

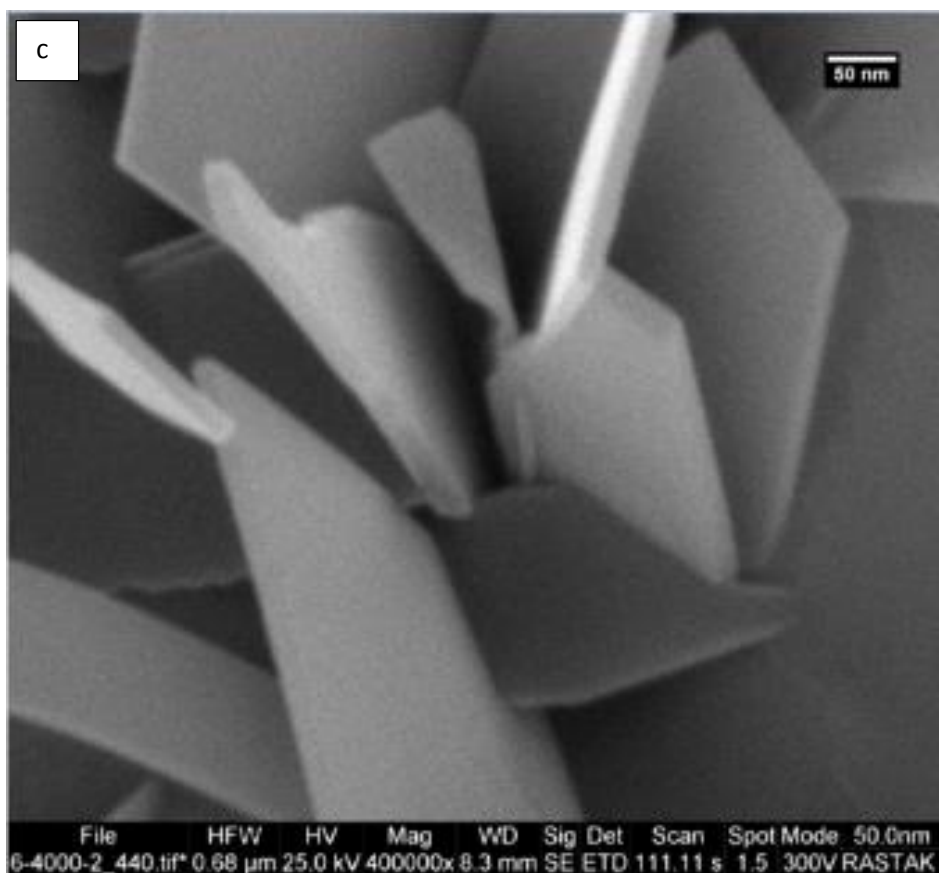
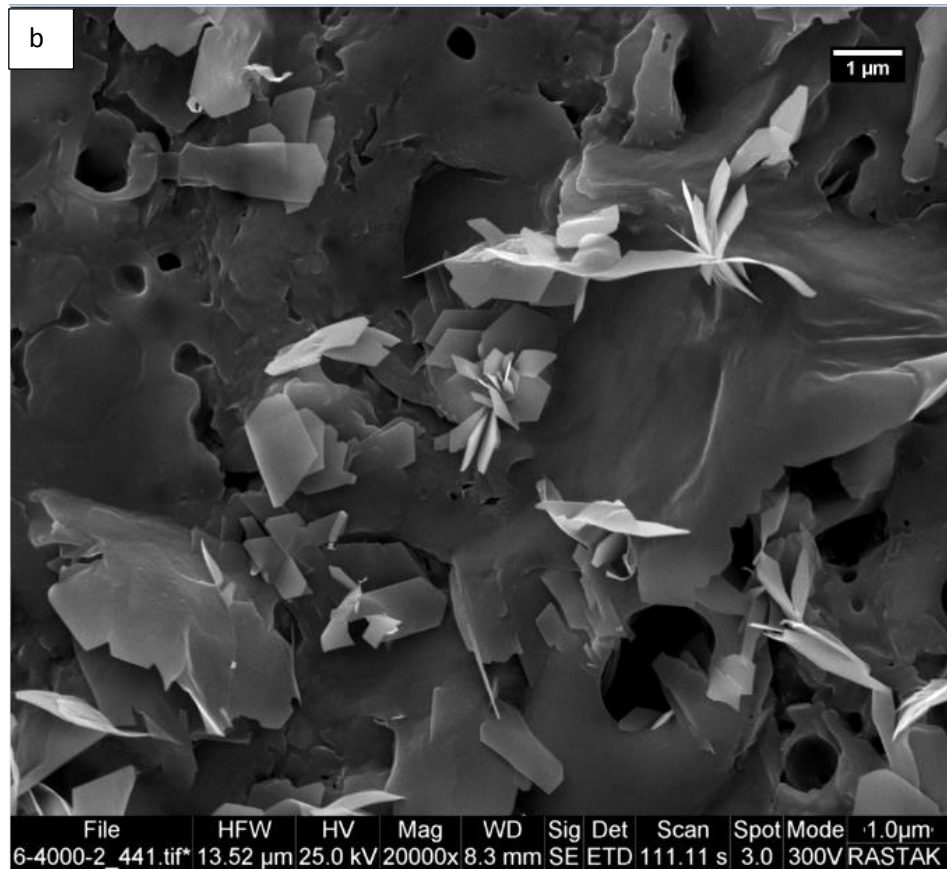


Figure (4.13 a,b,c): FESEM micrographs of HA30Ag1.5 specimen (Contd)

The Figure (4.14 a, b, c) below show FESEM micrographs of HA45Ag1.5 specimen on CP-Ti specimen at constant voltage (200) V with different magnification. It is clear that there is growth in separate sites and other sites with holes. The reason for the appearance of cracks is due to the high temperature during MAO process.

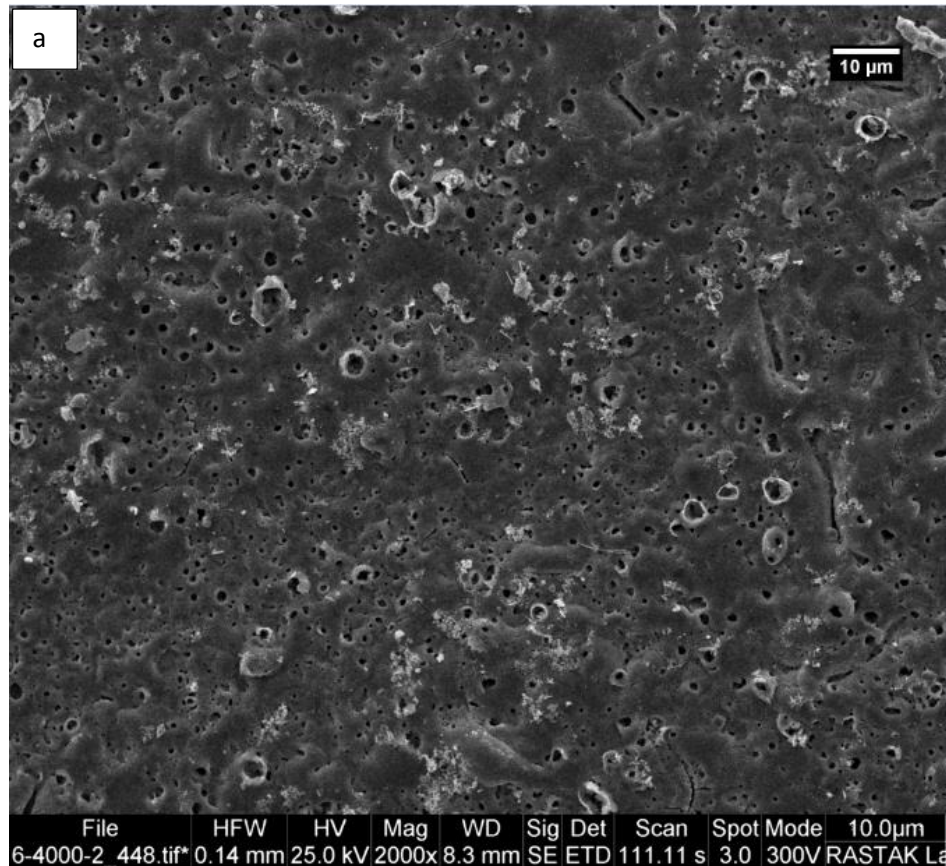


Figure (4.14 a, b, c) FESEM micrographs of HA45Ag1.5 specimen

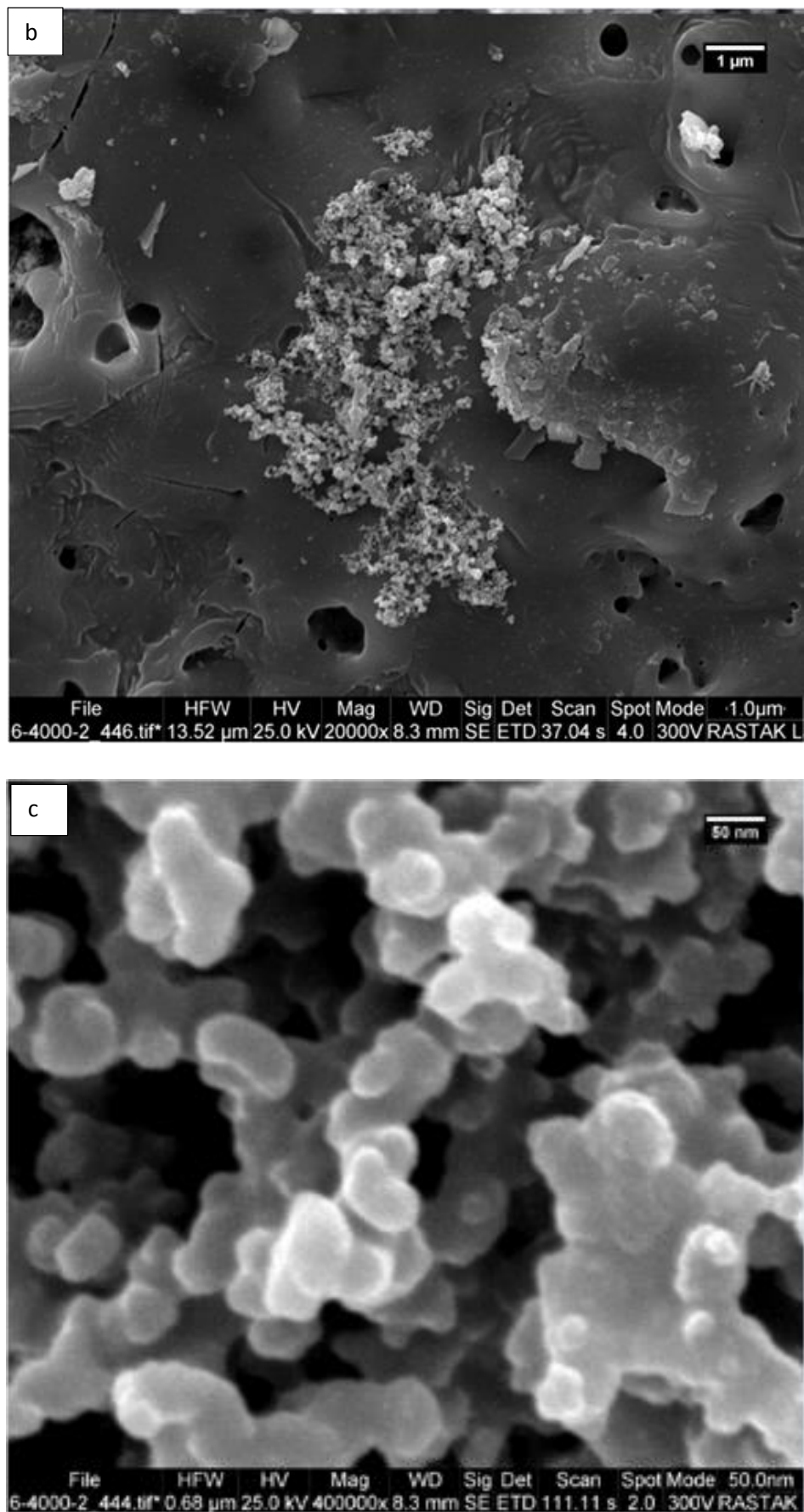


Figure (4.14 a, b,c): FESEM micrographs of HA45Ag1.5 specimen(Contd)

The Figure (4.15 a, b, c) below show FESEM micrographs of HA60Ag1.5 specimen on CP-Ti specimen at constant voltage (200) V with different magnification. At 50 nm there are clear areas of HA as well as silver because an increase in its ratio led to its deposition with HA on the surface of CP-Ti.

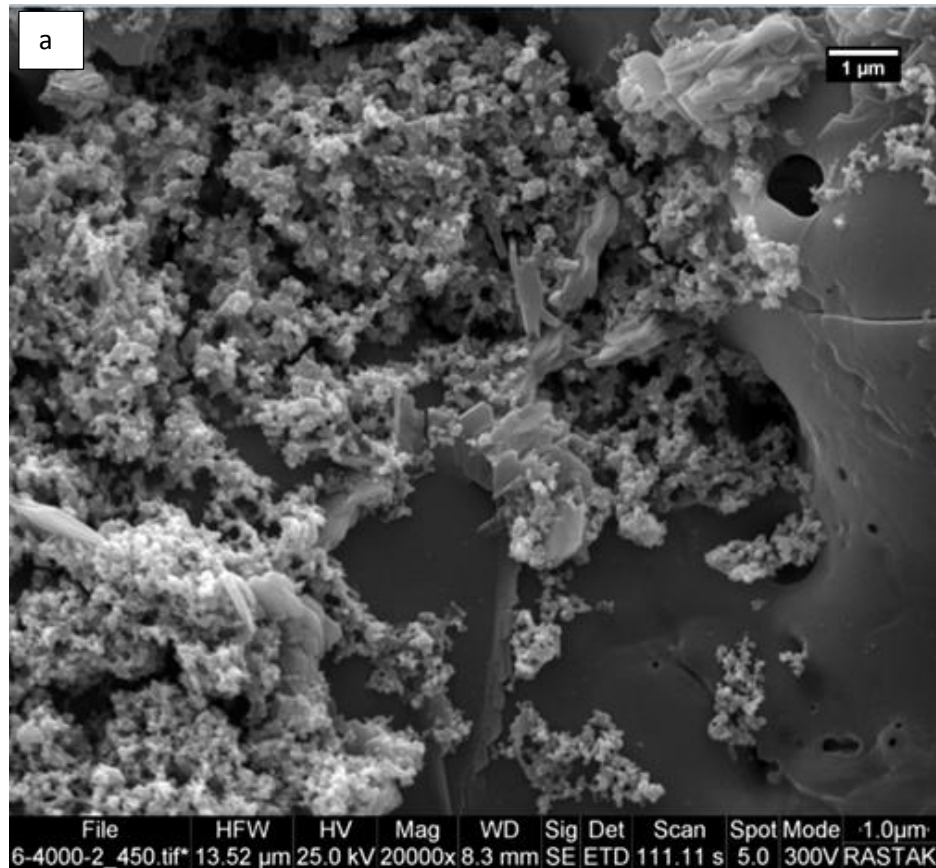


Figure (4.15 a, b, c) FESEM micrographs of HA60Ag1.5 specimen

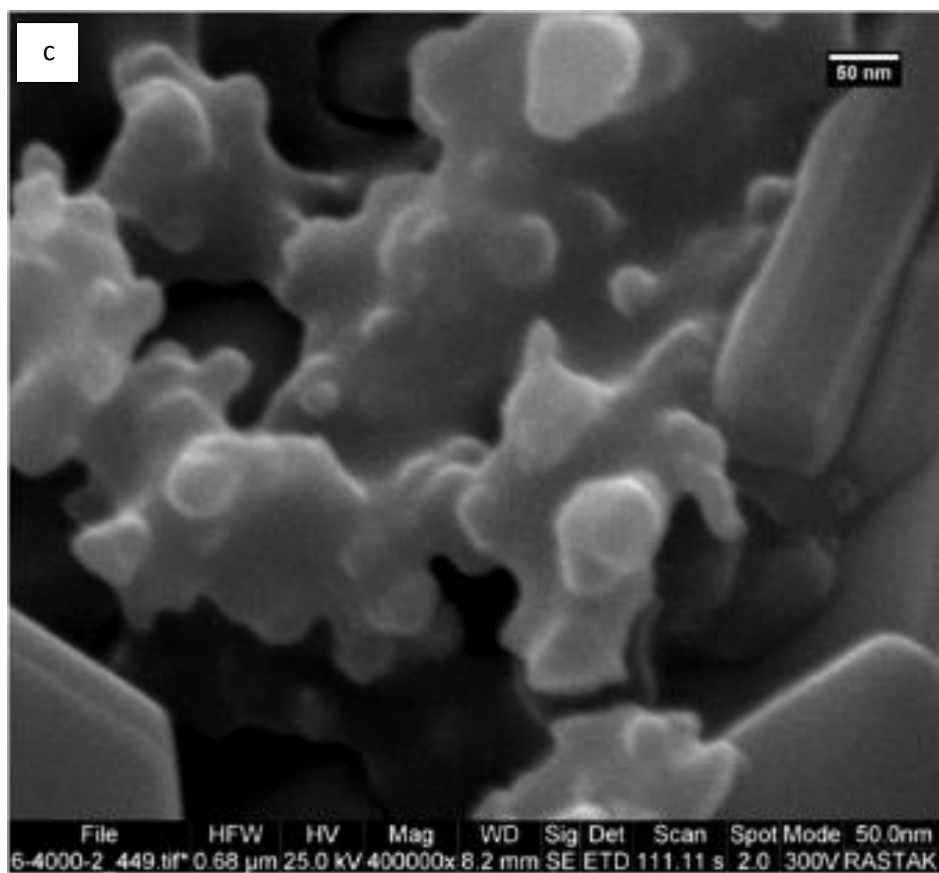
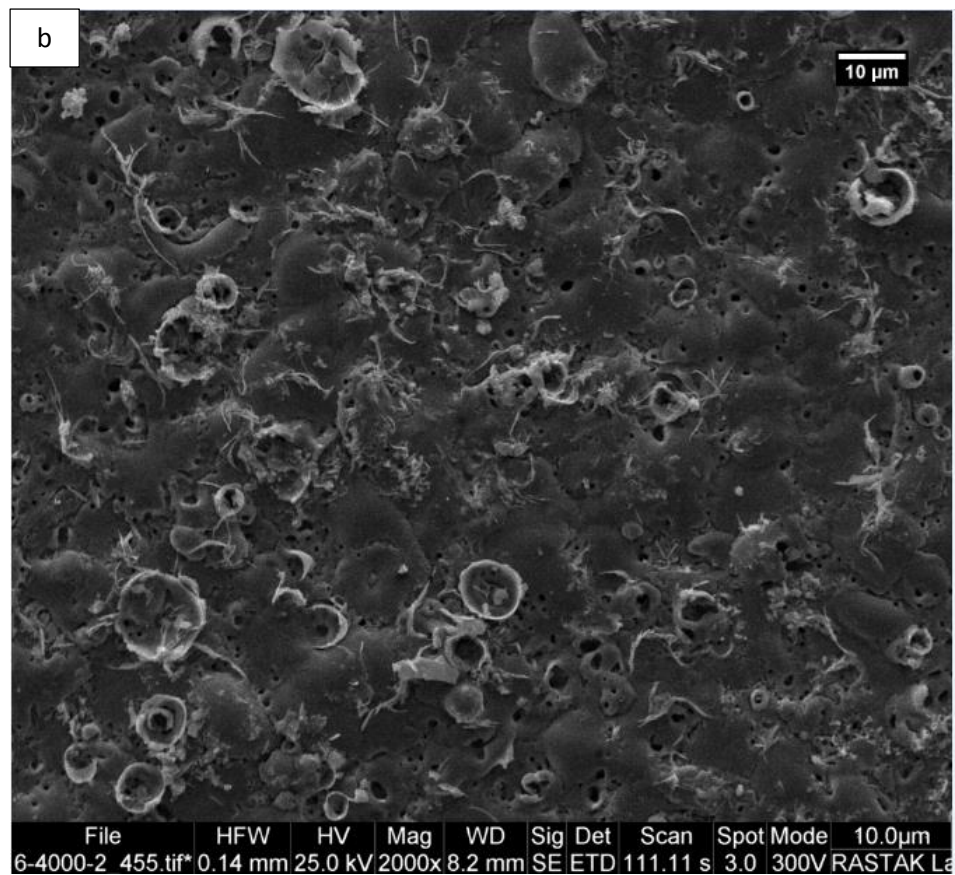


Figure (4.15 a, b,c): FESEM micrographs of HA60Ag1.5 specimen (Contd)

The Figure (4.16 a, b, c) below show FESEM micrographs of HA30Ag2 specimen on CP-Ti specimen at constant voltage (200) V with different magnification. There are clear areas of HA as well as silver at 50 nm although the silver did not precipitate at this time in the previous cases but an increase in its ratio led to its deposition with HA on the surface of CP-Ti.

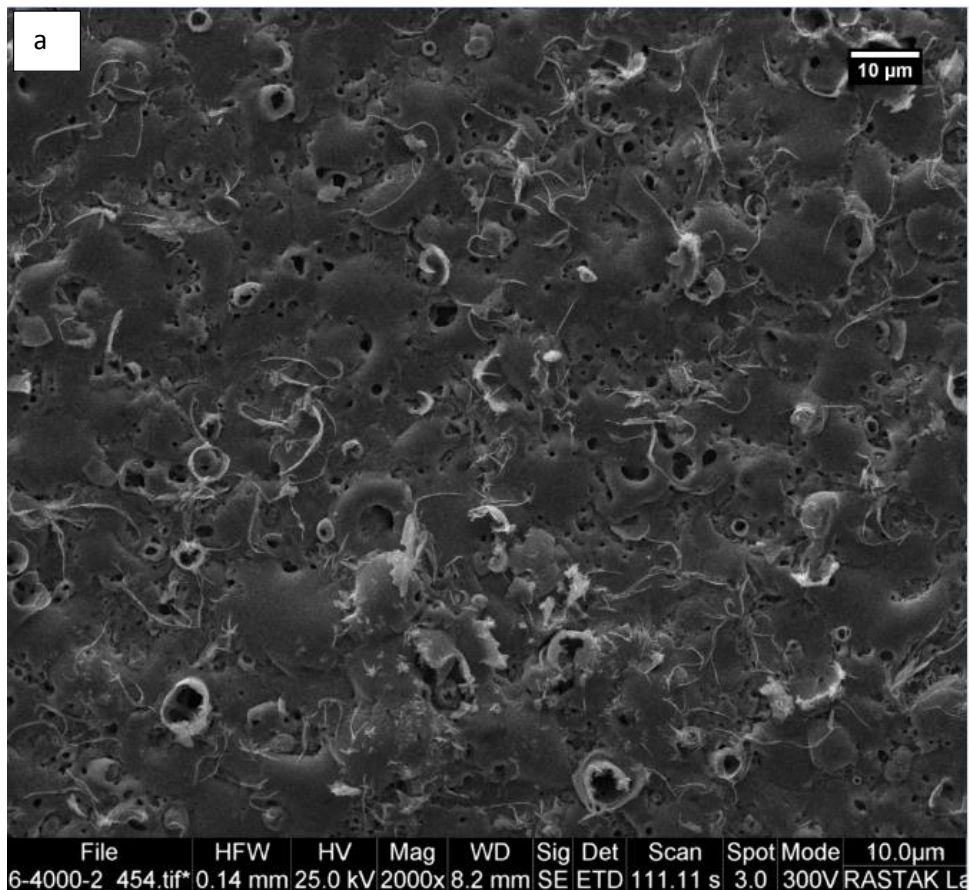


Figure (4.16 a, b, c) FESEM micrographs of HA30Ag2 specimen

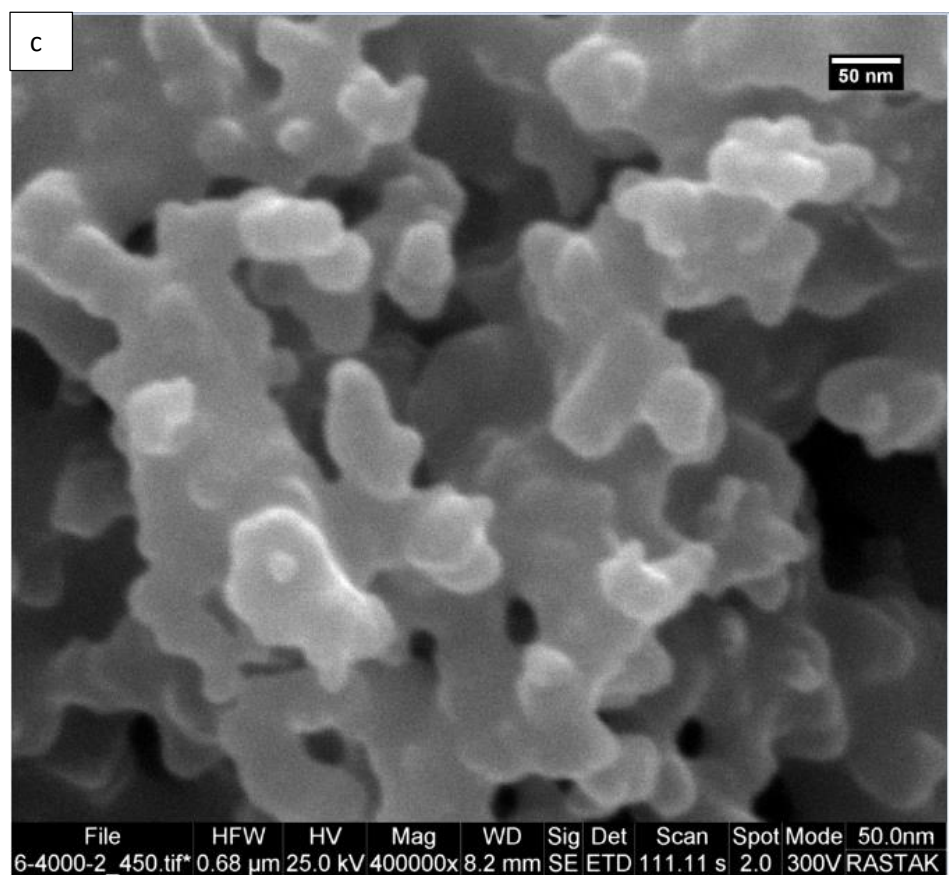
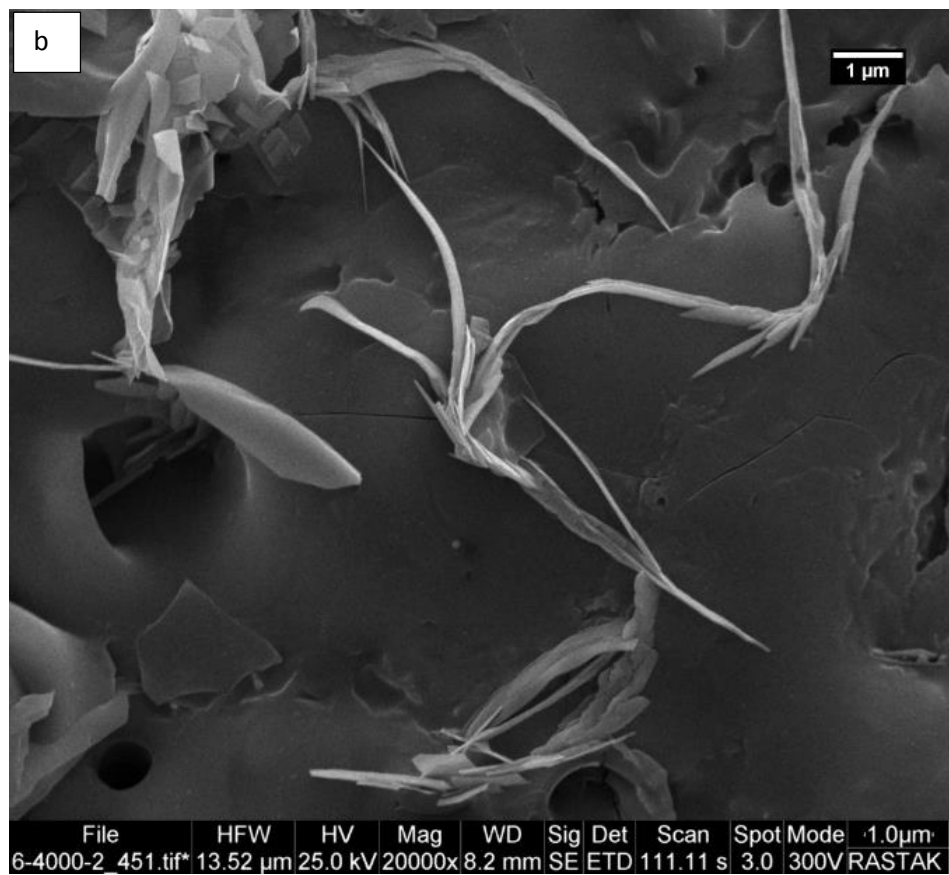


Figure (4.16 a, b, c): FESEM micrographs of HA30Ag2 specimen (Contd)

The Figure (4.17 a, b, c) below show FESEM micrographs of HA60Ag2 specimen on CP-Ti specimen at constant voltage (200) V with different magnification.

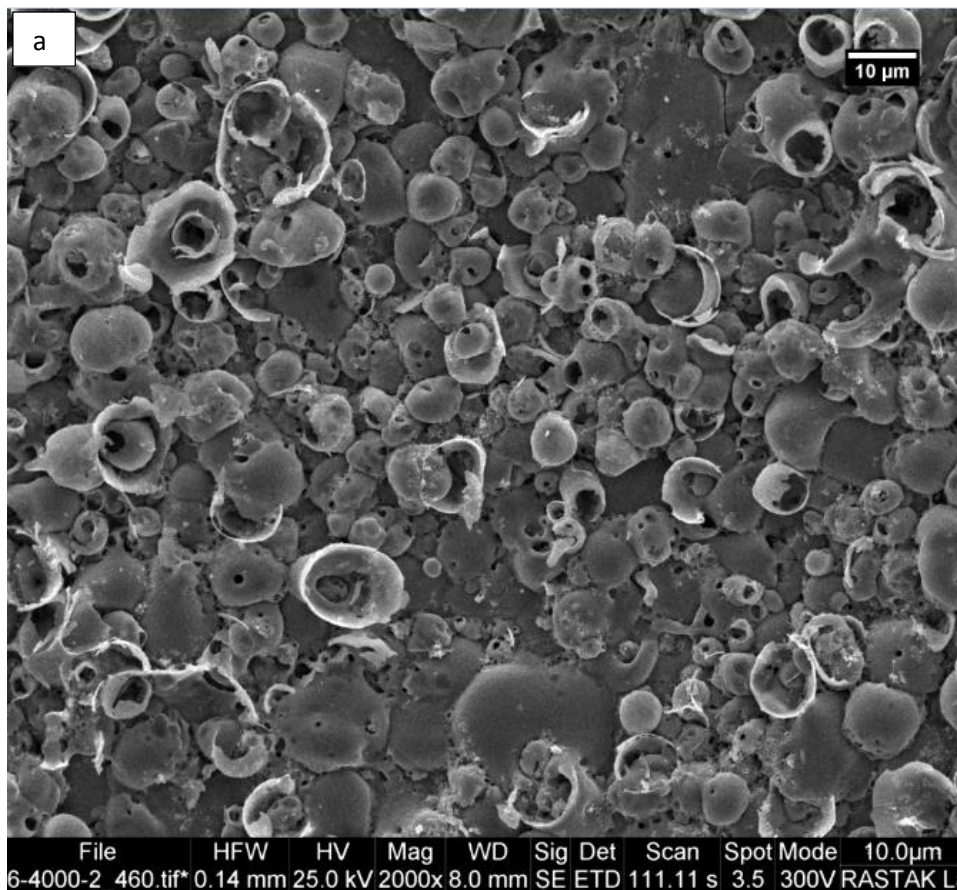


Figure (4.17 a, b, c) FESEM micrographs of HA60Ag2 specimen

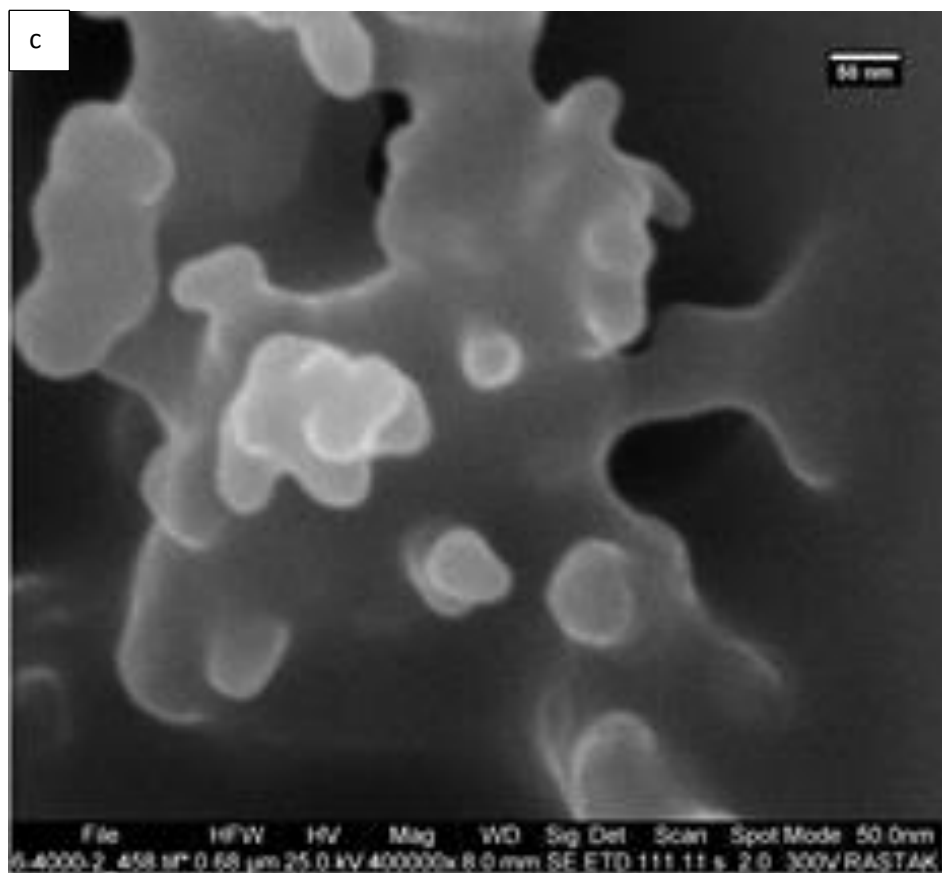
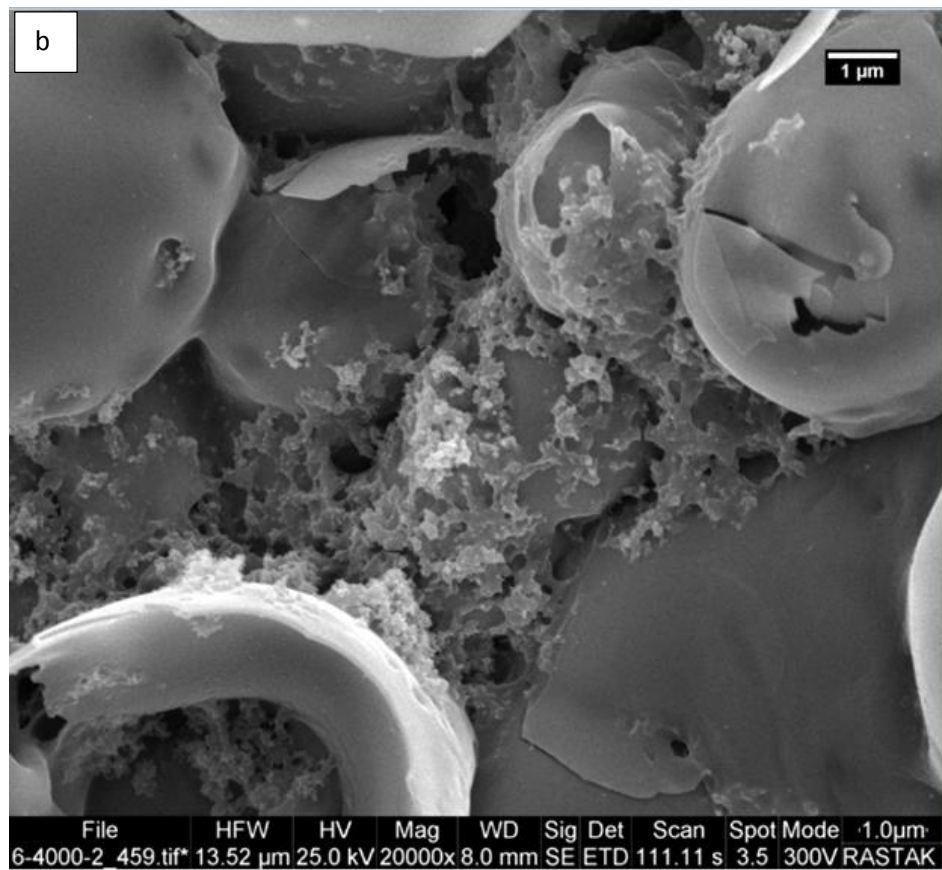


Figure (4.17 a, b, c): Continue

It can be observed that the microstructure in some figures was not densely packed, this is due to the HA/nAg particles at relatively 30sec. During MAO, which cannot properly migrate and therefore contain agglomeration with nonhomogeneous particles distribution within them, as they appeared in the deposition which produced a porous structure as a result when increased coating time. The use of longer coating time values during MAO process led to a considerable increase in the porosity of deposition. Moreover, coarse particles would deposit and cause an increase in the roughness and thickness of coating and that would promote the cracking to be more dominant for the thick layer [74]. Finally, if the MAO potential goes high, the nanoparticles will move quickly toward the opposite charge electrode which do not have an enough time to go in the favorable position to form a homogenous coating.

From figure (4.18) can be seen only titanium peaks this illustrated the pure titanium plate which was used in this research. It is clear from figures (4.19) & (4.20) that the deposition of HA, HA/nAg on the substrate titanium, as well as the presence of the stabilizing elements of the phase  $\beta$ .

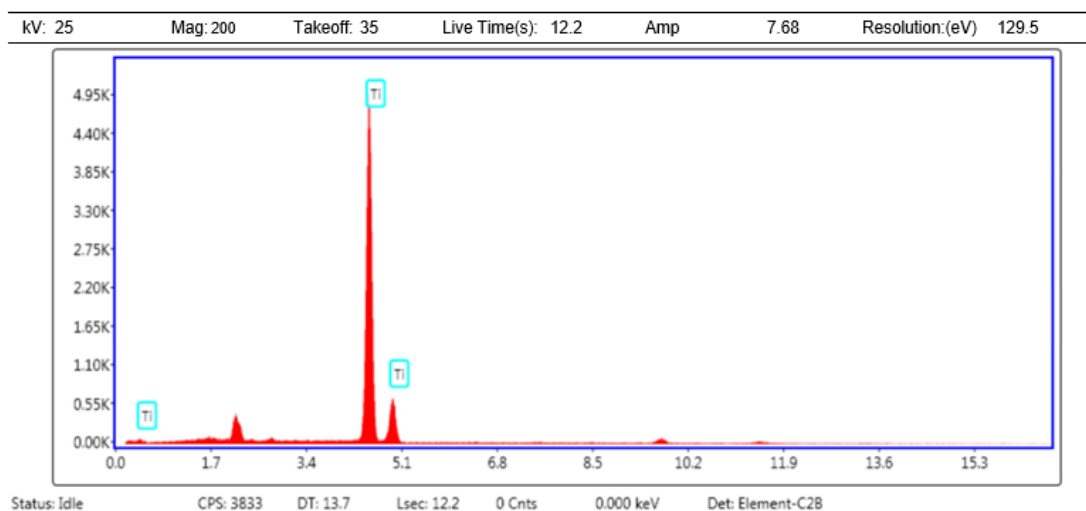


Figure (4.18) EDX Analysis for Ti.

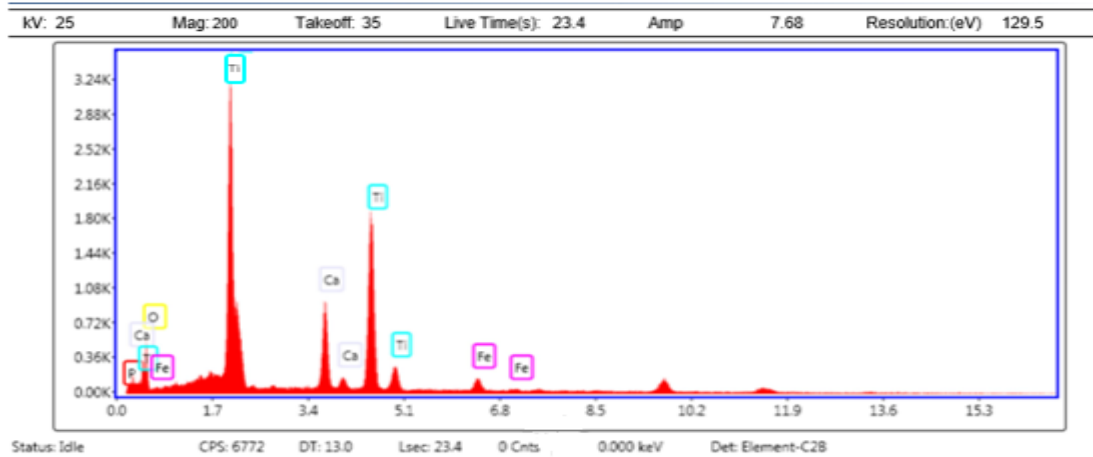


Figure (4.19) EDX Analysis for composite coating (HA) on CP-Ti.

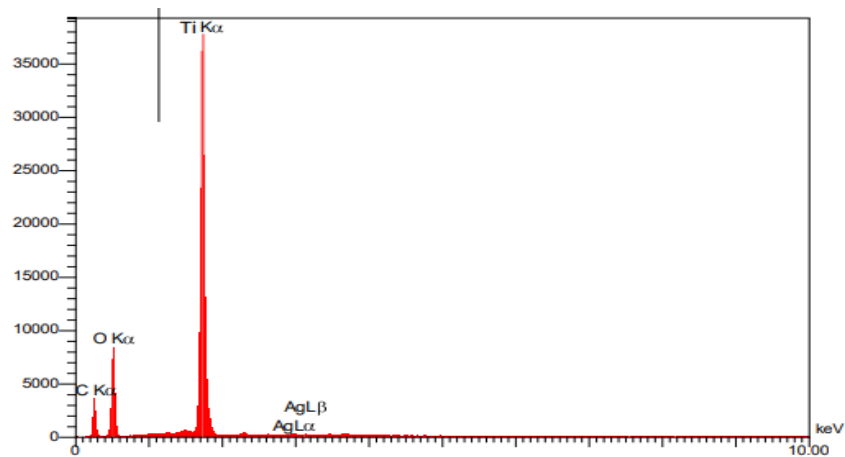


Figure (4.20) EDX Analysis for composite coating (HA/nAg) on CP-Ti.

#### **4.5. Atomic Force Microscopy (AFM)**

The Figures below shows the results AFM of specimen at (30, 45, 60) sec; it is clear there is decrease of roughness by increasing the coating time. Table (4.3) show roughness (HA & HA/nAg) specimens.

Table (4.3) Roughness of specimens

No	Specimens	Roughness (nm)	No	Specimens	Roughness (nm)
1	HA30	242.19	8	HA45Ag1	160
2	HA45	215.28	9	HA60Ag1	19.38
3	HA60	30.75	10	HA30Ag1.5	100

4	HA30Ag0.5	340.56	11	HA45Ag1.5	94.5
5	HA45Ag0.5	227.94	12	HA60Ag1.5	19.38
6	HA60Ag0.5	30.75	13	HA30Ag2	258.34
7	HA30Ag1	430.5	14	HA60Ag2	19.00

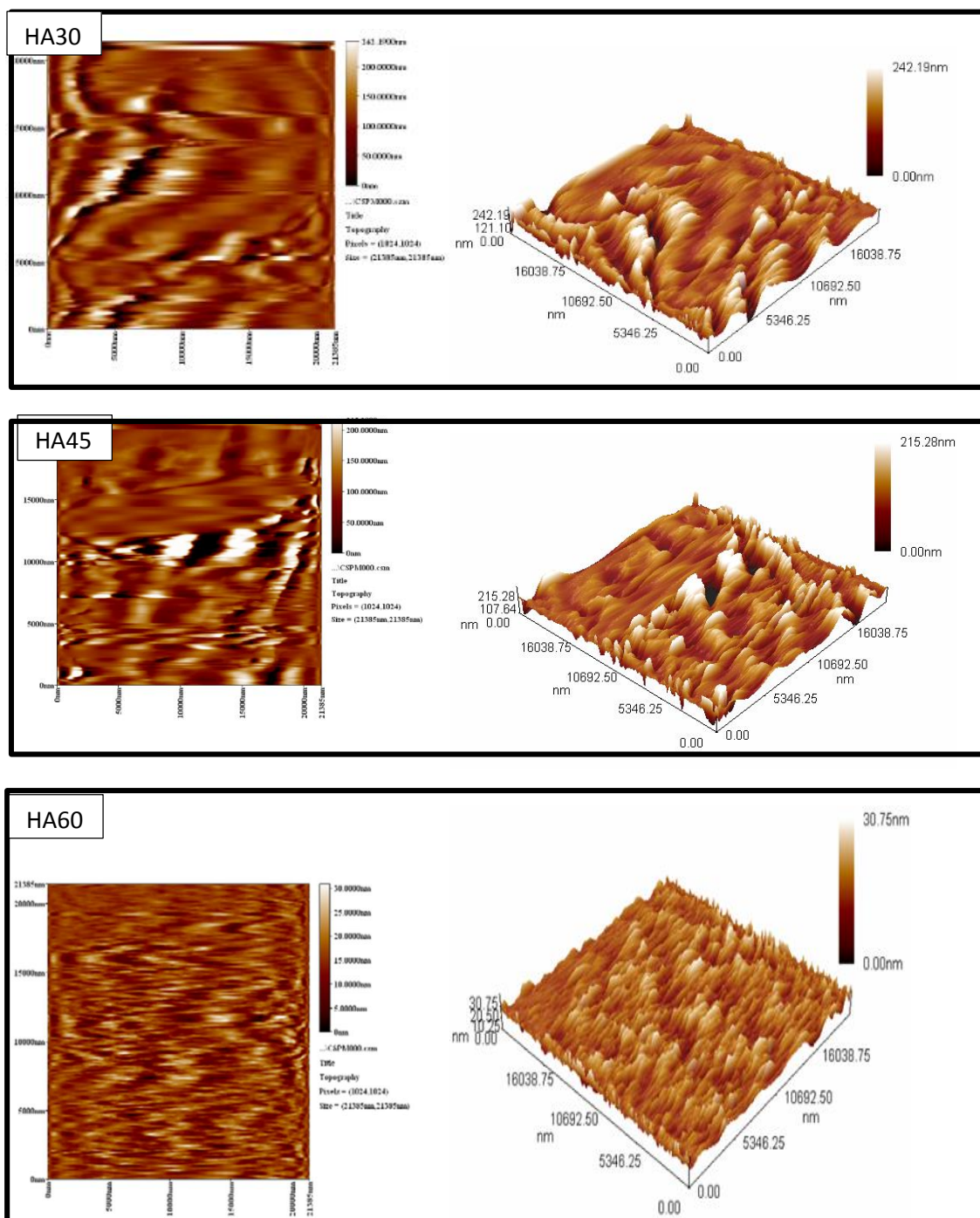


Figure (4.21) AFM of HA specimens

Surface roughness of HA60 < HA45 < HA30 this is due to an increase in the accumulation of particles and filling the pores, and this leads to making the surface topography more homogeneous.

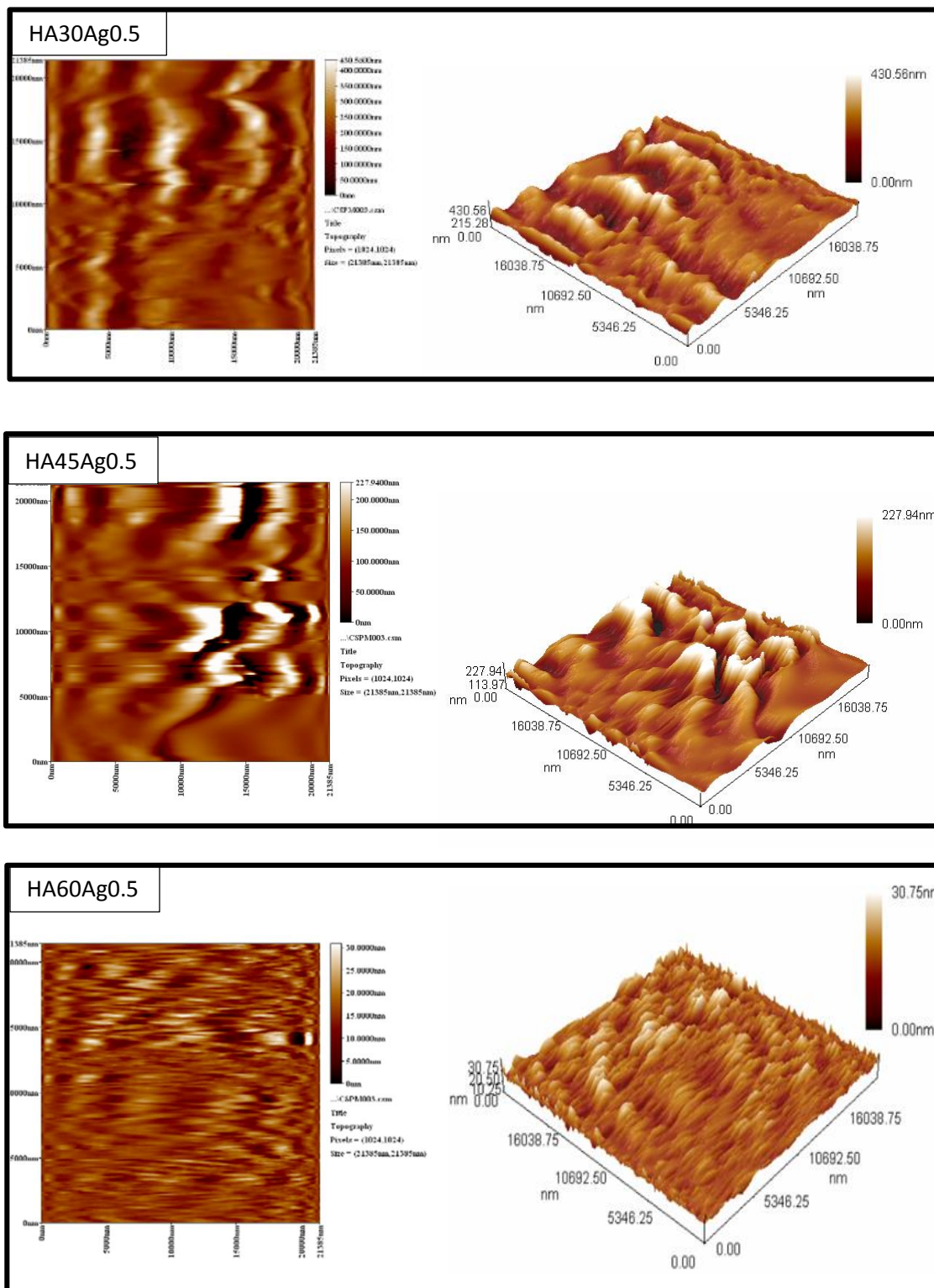


Figure (4.22) AFM of HA/Ag0.5 specimens

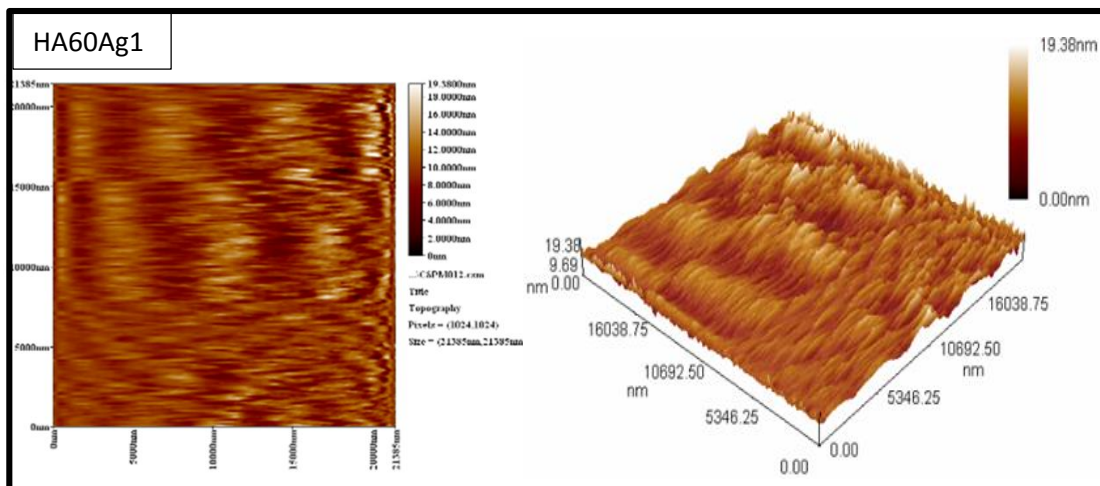
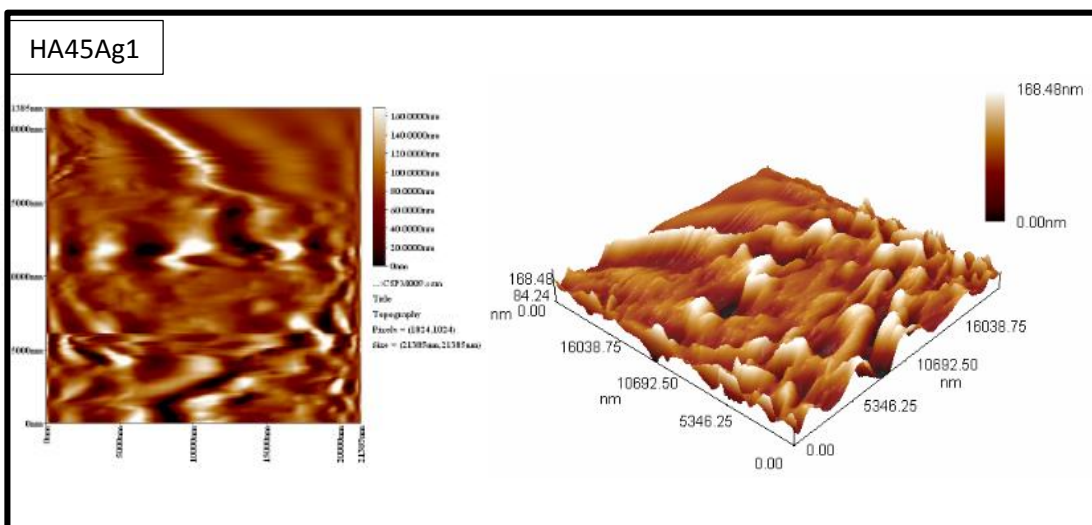
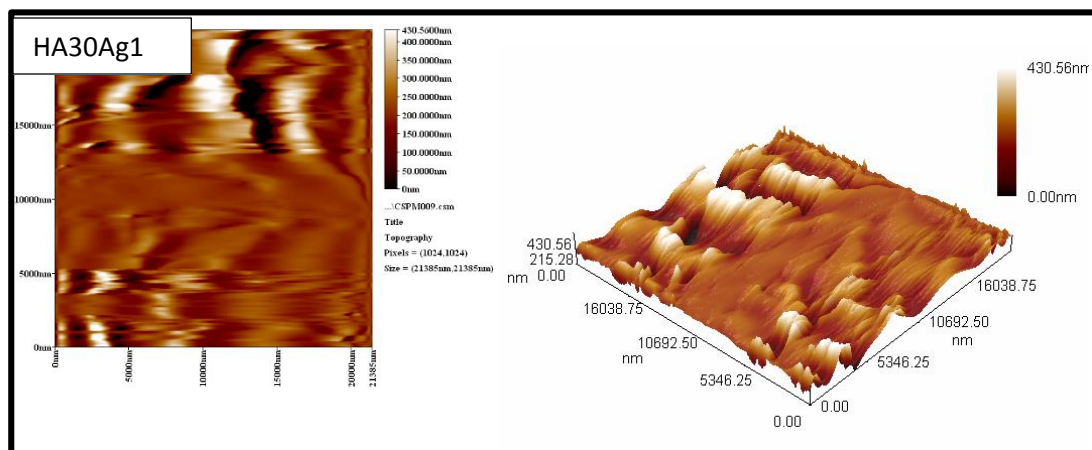


Figure (4.23) AFM of HA/Ag1 specimens

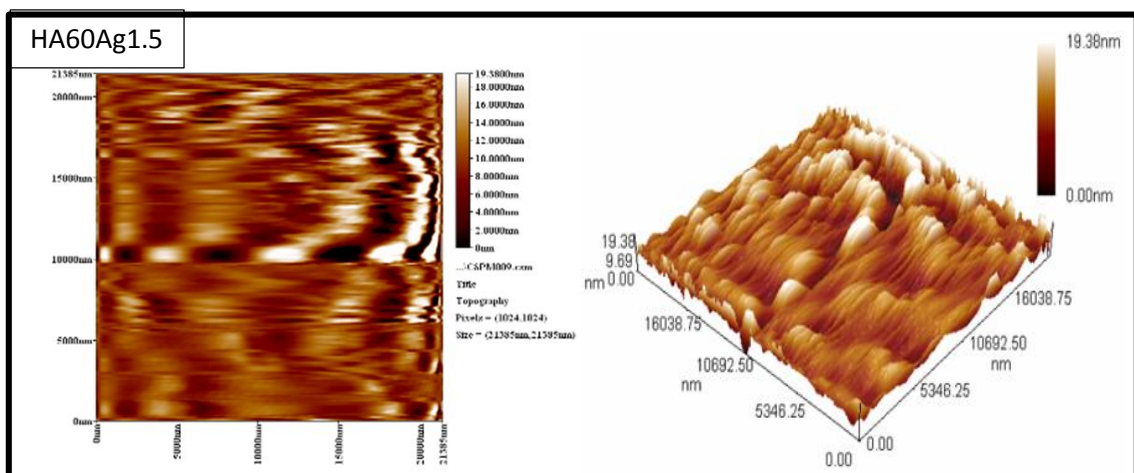
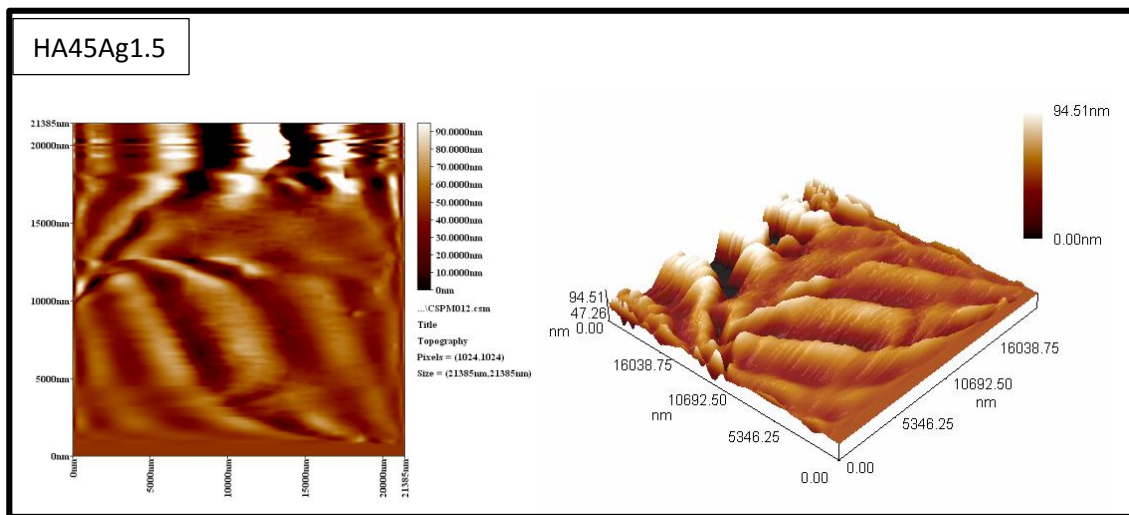
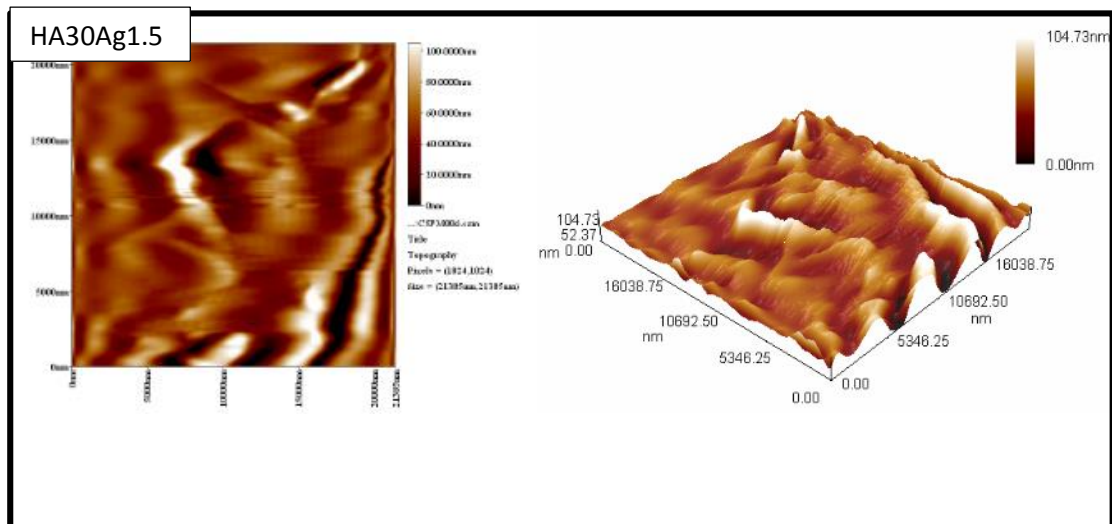


Figure (4.24) AFM of HA/Ag1.5 specimens

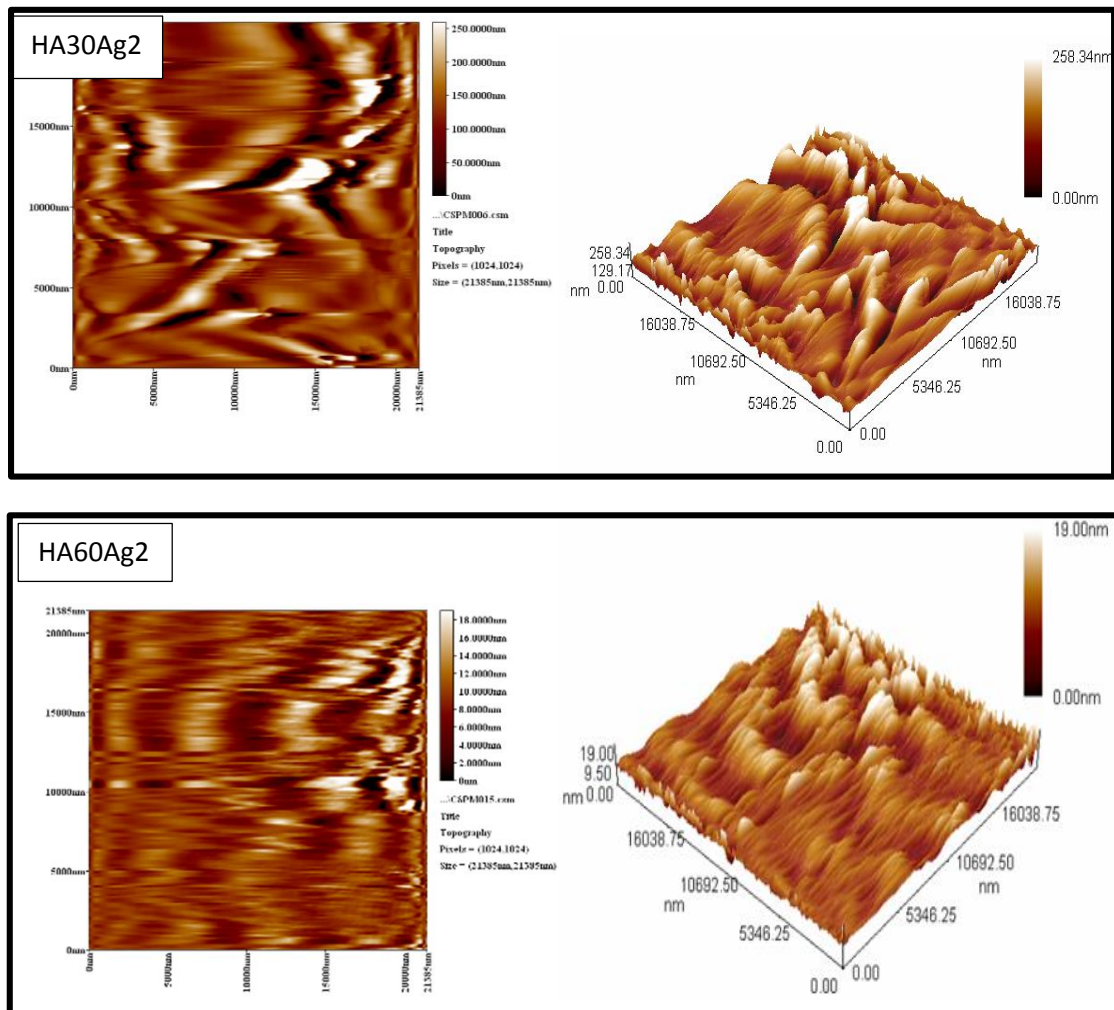


Figure (4.25) AFM of HA/Ag<sub>2</sub> specimens.

The results clearly show the higher the break down ( $V_b$ ) and final voltage ( $V_f$ ) of the coatings lower the surface roughness and vice versa. The different electrolyte environment determines the different breakdown and final voltage of the MAO coatings. If the break down voltage is low, micro arcs (dielectric break downs) are initiated at the earlier stage which eventually results in higher porosity in the stipulated duration and vice versa, [74]. Reducing the accumulation is also explained by the fact that there is enough time to fill the pores.

**4.6. Antibacterial**

Table (4.4) and Figure (4.26) represent results of the antibacterial test of control specimen (CP-Ti) and composite coating (HA, HA/nAg) on titanium samples.

Table(4.4)Antibacterial results.Notice + presence bacteria and - not presence

Specimen	The result	Specimen	The result
Ti (control)	+	HA45Ag1	-
HA30	-	HA60Ag1	-
HA45	-	HA30Ag1.5	-
HA60	-	HA45Ag1.5	+
HA30Ag0.5	-	HA60Ag1.5	-
HA45Ag0.5	-	HA30Ag2	-
HA60Ag0.5	-	HA60Ag2	-
HA30Ag1	-		



Figure (4.26) results of the antibacterial test (A) coating specimens, (B) uncoating specimen (control) and (C) coating specimen (HA45Ag1.5).

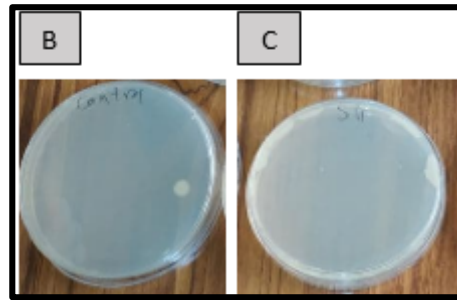


Figure (4.26): Figure (4.26) results of the antibacterial test (A) coating specimens, (B) uncoating specimen (control) and (C) coating specimen (HA45Ag1.5).(Contd)

The effect composite coating (HA, HA/nAg) on (CP-Ti) substrate was clearly effective against bacteria where this type of coating killed bacteria compared to the base sample. There was a growth of bacteria on uncoating specimen (CP-Ti) due to minimum level of roughness but there was no presence of it on coating sample as shown in table (4.4) and Figure (4.26) except for one specimen (HA45Ag1.5), the reason for this is breakage of the coating layer within parts of a second and it caused the solution to penetrate through the cracks and reach the base metal and the FESEM of this specimen was showing many holes and cracks.

#### 4.7. Corrosion Rate (CR)

Table (4.5) shows corrosion rate measurements and figure (4.27) shows relationship between corrosion rate, time (t) of (CP-Ti) and composite coating (HA& HA/nAg) on (CP-Ti) specimens.

Table (4.5) Corrosion rate measurements

No	Specimen	CR1(mdd) t=8 days	CR2(mdd) t=12 day	CR3(mdd) t=18 day	CR4(mdd) t=19 day
A	CP-Ti	2.678	0.595	-9.524	-8.271
B	HA30	12.5	19.643	1.984	3.008

C	HA45	10.714	0.595	0.794	3.383
D	HA60	63.393	61.309	25.396	25.564
E	HA30Ag0.5	16.071	8.333	3.175	5.639
F	HA45Ag0.5	12.5	3.571	3.175	3.383
G	HA60Ag0.5	0	5.357	2.777	4.135
H	HA30Ag1	8.929	2.976	3.571	3.759
I	HA45Ag1	-50	-28571	-18.254	-17.293
J	HA60Ag1	8.929	3.571	-9.921	3.008
K	HA30Ag1.5	13.393	5.357	6.349	6.015
L	HA45Ag1.5	7.143	6.548	3.175	4.135
M	HA60Ag1.5	21.429	11.309	9.524	6.767
N	HA30Ag2	8.036	3.571	3.175	3.383
O	HA60Ag2	-3.572	7.143	4.365	4.511

No	Specimen	CR5(mdd)	CR6(mdd)	CR7(mdd)
		t=20 day	t=25 day	t=32 day
A	CP-Ti	-2.5	-3.714	-1.562
B	HA30	3.571	1.714	1.339
C	HA45	1.786	1.143	3.571
D	HA60	20.714	18.286	13.616
E	HA30Ag0.5	4.286	3.429	3.571
F	HA45Ag0.5	2.5	2.286	1.563
G	HA60Ag0.5	2.143	3.143	3.125
H	HA30Ag1	3.929	2.857	1.563
I	HA45Ag1	-15.714	-12	-9.152
J	HA60Ag1	3.214	1.714	1.563
K	HA30Ag1.5	4.643	3.714	2.009

L	HA45Ag1.5	3.571	1.429	2.455
M	HA60Ag1.5	8.571	6.857	4.911
N	HA30Ag2	2.5	3.429	0.669
O	HA60Ag2	4.643	3.143	1.786

It is clear from the table (4.5) that the corrosion rates for the specimen (I- HA45Ag1) are all less than zero due to the increase in the weight of the specimen after immersion in Ringer’s solution, meaning that there is adsorption of solution ions on its surface. While the corrosion rates for the specimen (D-HA60) all more than zero this shows indicated that they lose from their weight after the immersion but over time its corrosion rates decrease and stabilizes.

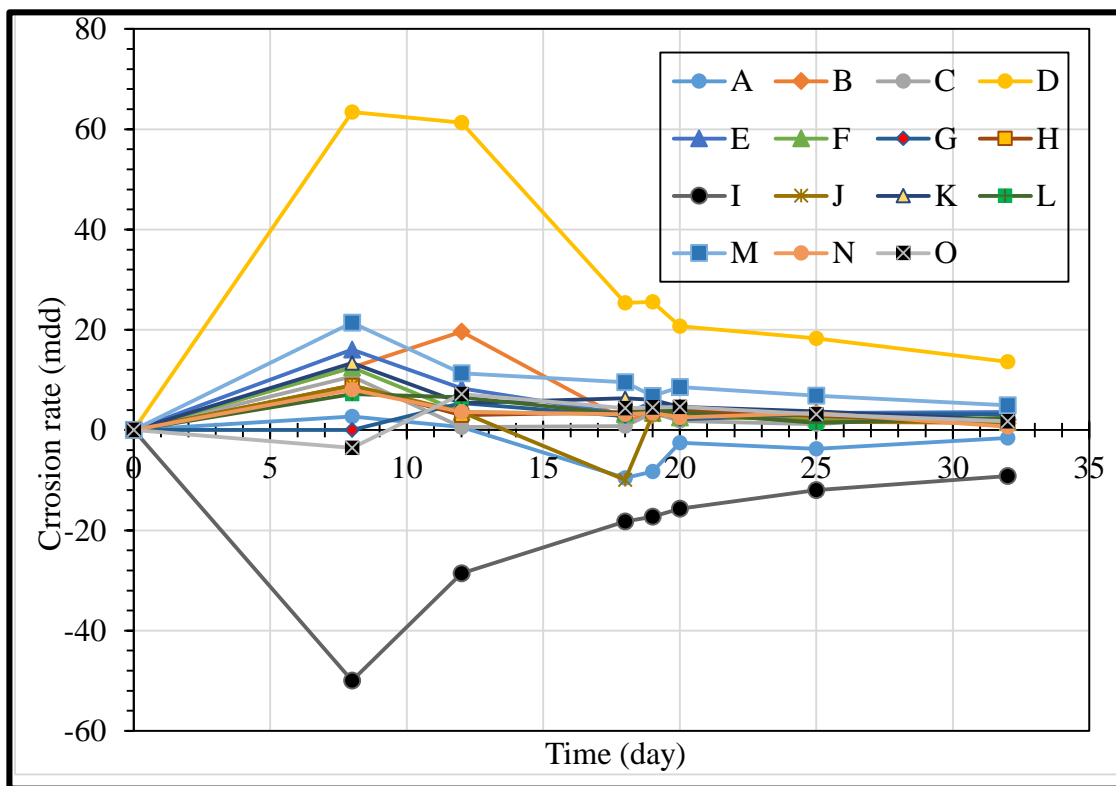


Figure (4.27) The relationship between corrosion rate and time

From Figure (4.27) it can be noticed that the specimen (I- HA45Ag1) is preferable where it has the lowest corrosion rate and specimen (D-HA60) is high corrosion rate because porous layer of HA which illustrated in FESEM image. This means that a high HA/nAg protection layer on the titanium substrate is obtained because of the uniform, dense and compact layer structure of this specimen. These results indicated that titanium has less toxicity and consequently the implant life is expected to be higher. These enhancements in the anticorrosion properties of the substrates were not possible if the MAO coatings did not have excellent adhesion to the substrates so not all of the coatings that contain nanoparticles (composite coatings) exhibit higher corrosion resistance (lower corrosion rate) than the coating without nanoparticles [109].

#### **4.8. Contact Angle**

Table (4.6) and Figure below shows the contact angle that formed between Ti specimen and electrolytes (HA, HA/Ag 0.5, HA/Ag 1, HA/Ag 1.5, HA/Ag2).

Table (4.6) Contact angle between (CP-Ti) specimen and electrolytes.

Electrolyte	Contact angle
HA	37.034°
HA/Ag 0.5	48.286°
HA/Ag 1	38.827°
HA/Ag 1.5	30.105°
HA/Ag2	45.896°

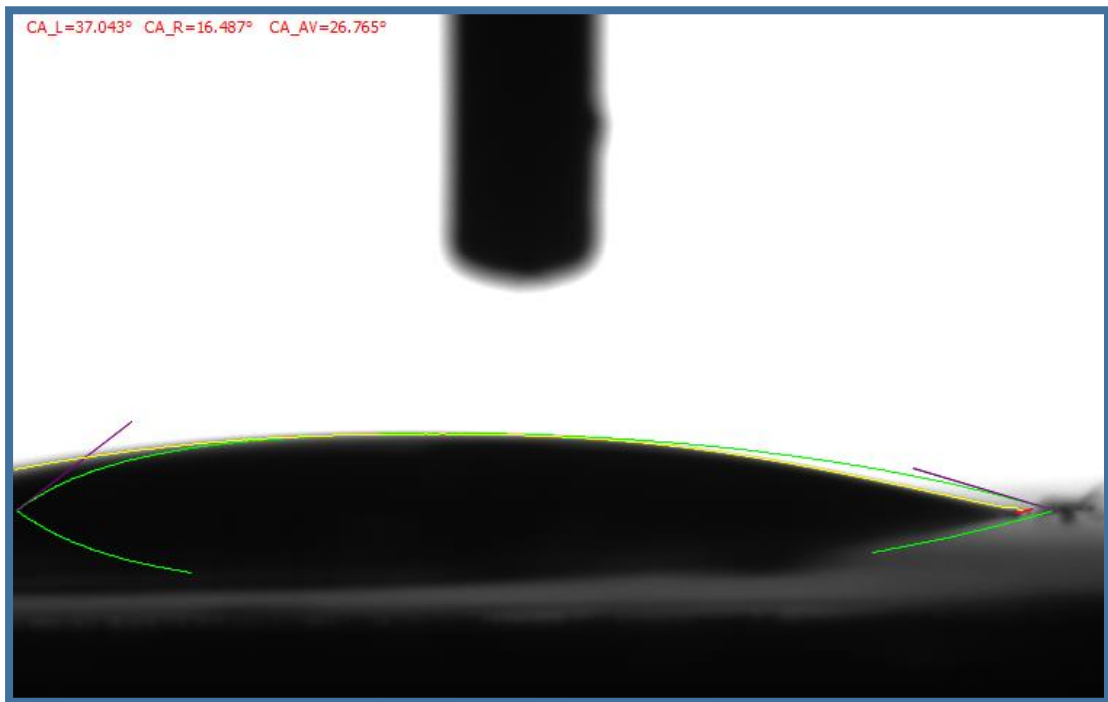


Figure (4.28) Contact angle between CT-Ti specimen and HA electrolyte

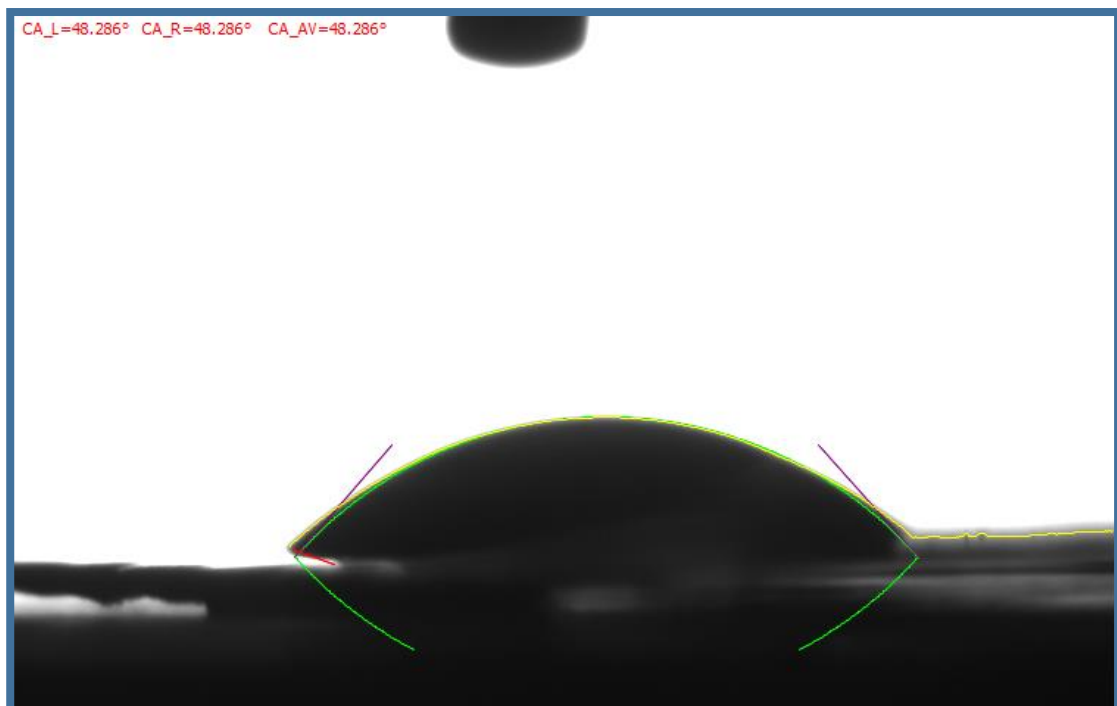


Figure (4.29) Contact angle between CT-Ti specimen and HA/Ag0.5 electrolyte

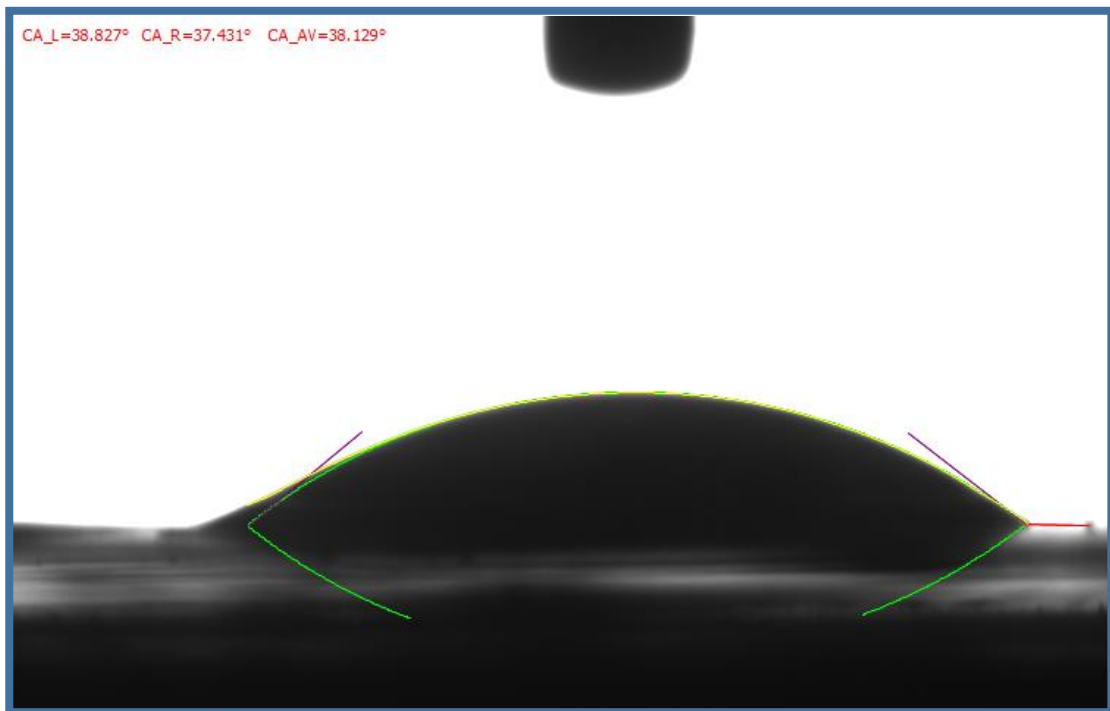


Figure (4.30) Contact angle between CT-Ti specimen and HA/Ag1 electrolyte

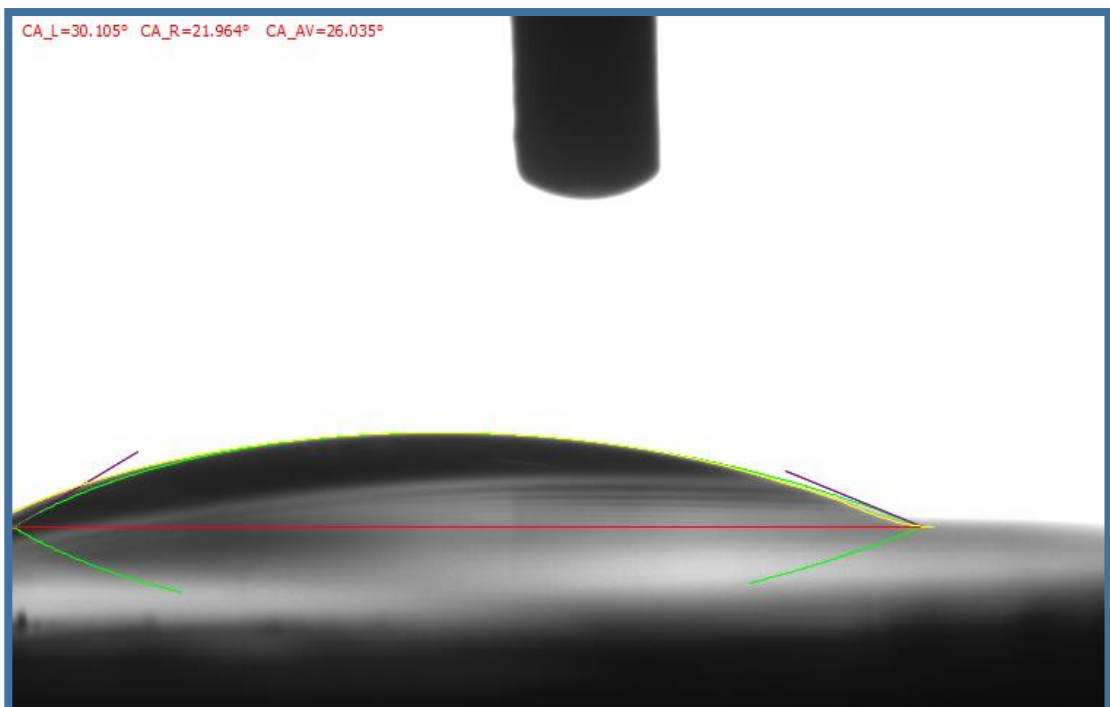


Figure (4.31) Contact angle between CT-Ti specimen and HA/Ag1.5 electrolyte

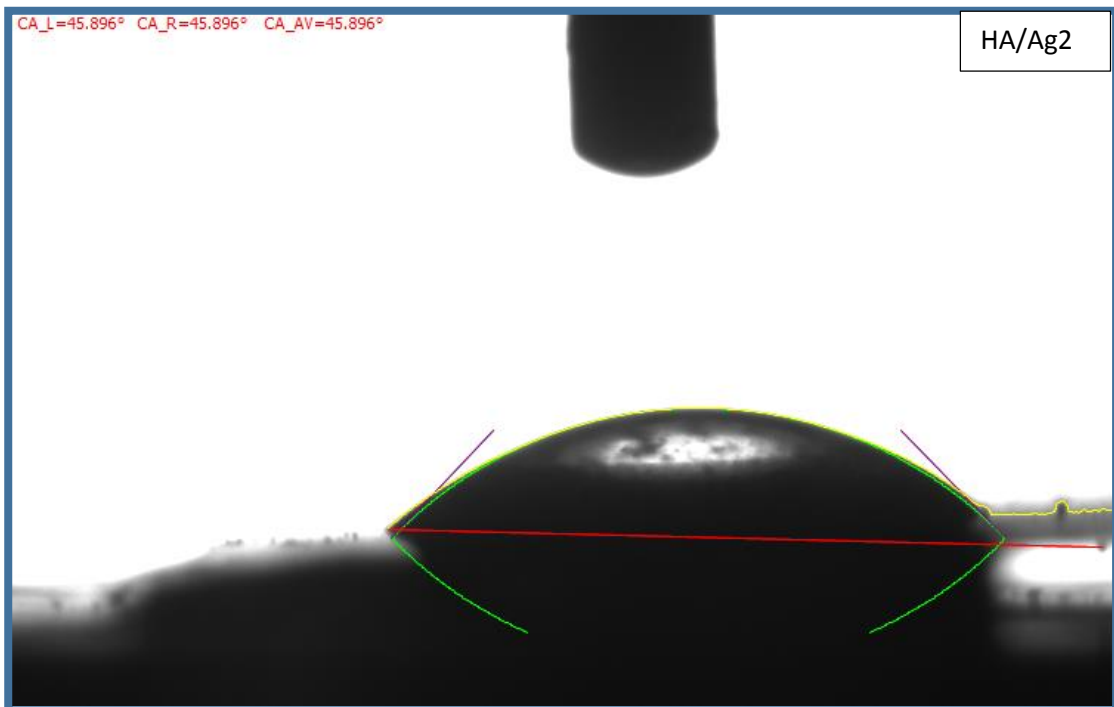


Figure (4.32) Contact angle between CT-Ti specimen and HA/Ag2 electrolyte

Obviously, the angle of contact differed with the increase in the percentage of nano silver in the hydroxyapatite (HA) electrolyte and the best wettability was achieved when using (HA/Ag 1.5) electrolyte and in this case, contact angle and surface tension were small compared to other angles. The decrease in the surface tension of the electrolyte indicates the lack of cohesion of its molecules, and therefore this electrolyte leads to the formation of a non-bonding coating and contains cracks, and this was proven by antibacterial testing, where bacteria grew on the specimen (HA45Ag1.5)

#### **4.9. Histological results**

The current study's histological results from the Hematoxylin and Eosin stain (H&E) under a light microscope revealed the creation of new bone trabeculae in all of the groups tested (control and experimental ) as show in figures below. The main histological change in the bone, at 40 day characterized by Figure (4.33)

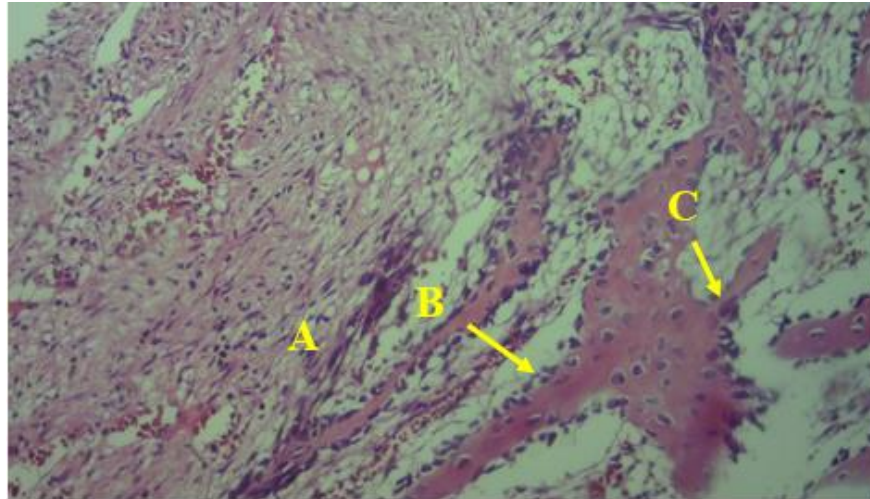


Figure (4.33) A section in the bone treated with (CP-Ti) group at 40 day show A- collagen fibers in the woven bone B- Metabolically active osteoblasts line woven bone C- Osteoclast (H & E stain 40X).

(CP-Ti) group histological slice revealed new bone trabeculae bordered by osteoblasts and filled by osteocytes.

The main histological change in the bone, at 40 day of coating (HA60) group characterized by Figure (4.34 a, b, c)

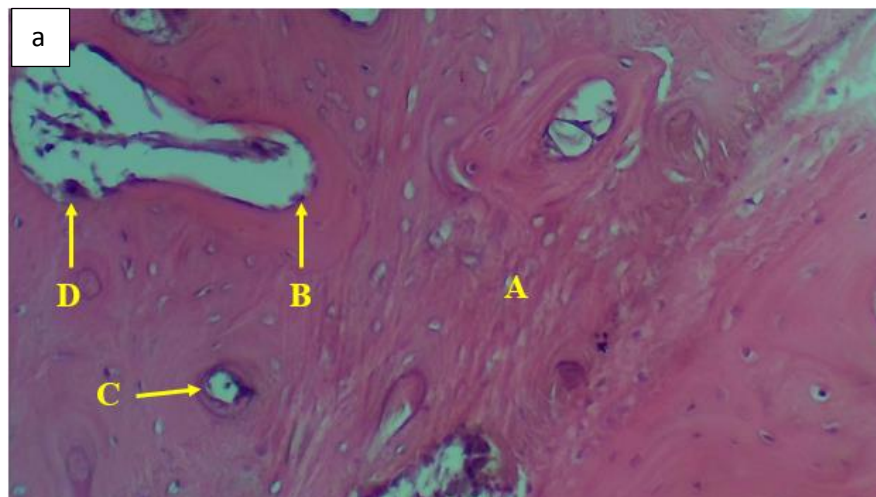


Figure (4.34 a) A section in the bone treated with coating (HA60) group at 40 days show A- The Woven bone that characterized by haphazard organisation of collagen fibers B- osteoblasts C- Haversian canals, D- Osteoclast. (H & E stain 40X).

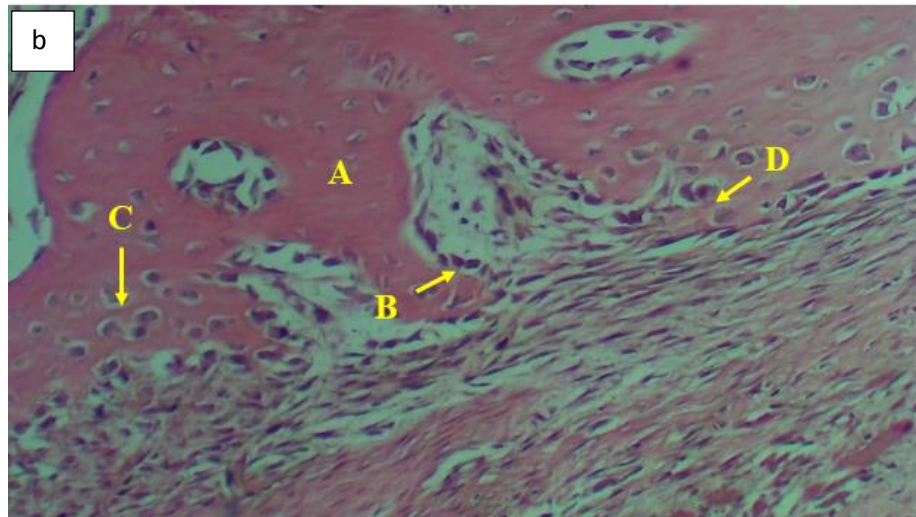


Figure (4.34 b) A section in the bone treated with coating (HA60) group at 40 day show A- The Woven bone that characterized by organisation of collagen fibers with increases the activity of B- osteoblasts C- osteocytes and D- osteoclasts (H & E stain 40X).

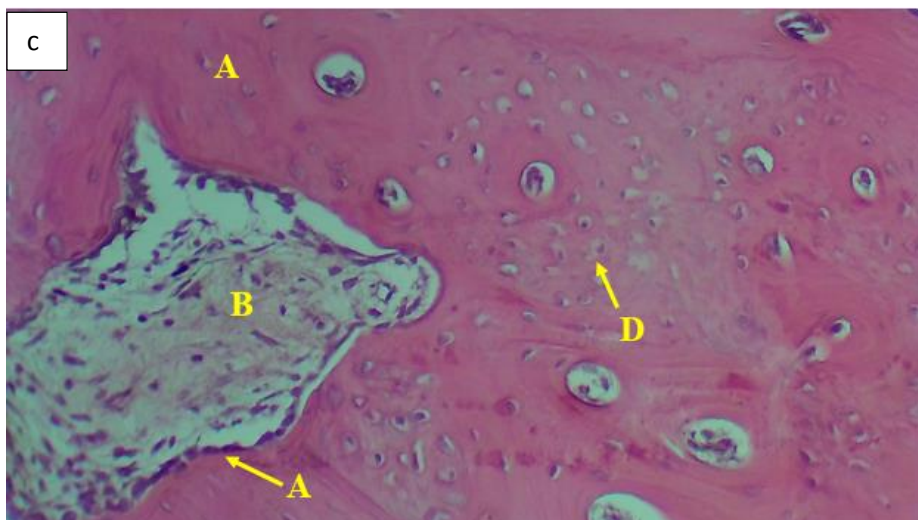


Figure (4.34 c) A section in the bone treated with coating (HA60) group at 40 day show A- lamellar bone organization with B- Area of bone remodeling and activity of C-osteoblasts and D- osteocytes (H & E stain 40X).

The main histological change in the bone, at 40 day of composite coating (HA60 Ag 0.5) group characterized by Figure (3.35)

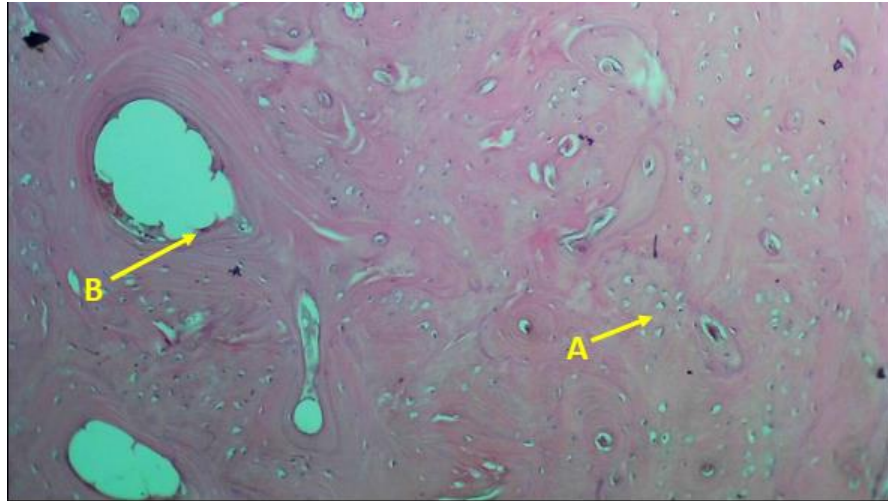


Figure (4.35) A section in the bone treated with composite coating HA60 Ag 0.5) group at 40 day show the compact bone is composed of calcified extracellular material, the bone matrix and 2 major cell types which are A- Osteoblast B- Osteocytes which are found in cavities (lacunae) between bone matrix layers (H & E stain 40X).

The main histological change in the bone, at 40 day of composite coating (HA60Ag1) group characterized by Figure (4.36)

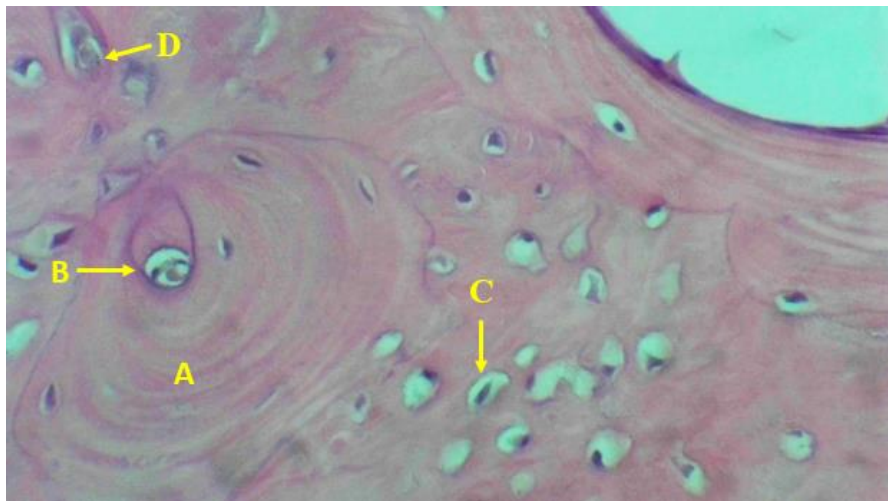


Figure (4.36) A section in the bone treated with composite coating (HA60Ag1) group at 40 day show A- The compact bone is composed of calcified extracellular material, the bone matrix B- (HC), Haversian canals C- lacuna and lamellar bone D- Osteoclast. (H & E stain 40X).

The main histological change in the bone, at 3 day of composite coating (HA60Ag 1.5) group characterized by Figure (4.37 a, b)

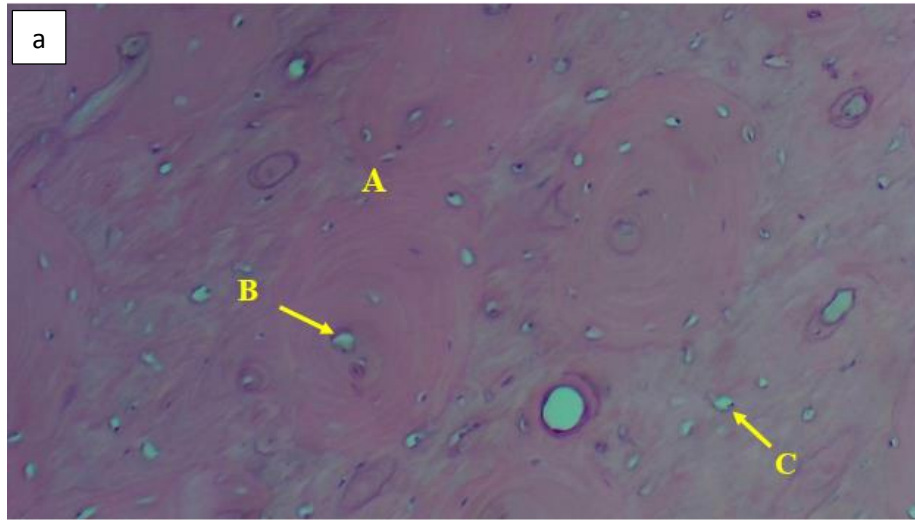


Figure (4.37 a) A section in the bone treated with composite coating (HA60Ag 1.5) group at 3 days show A- the compact bone is composed of calcified extracellular material, B- Haversian canals, C- Osteocyte within lacuna.

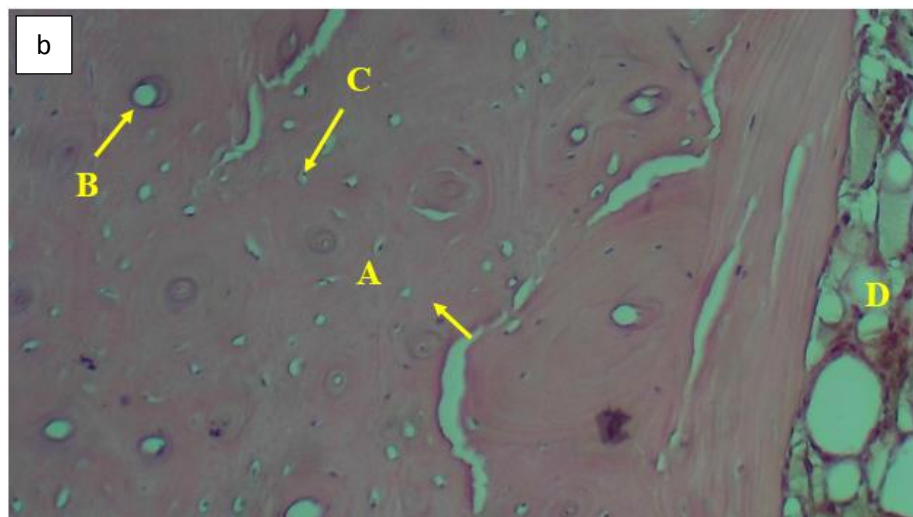


Figure (4.37 b) A section in the bone treated with composite coating (HA60Ag 1.5) group at 3 days show A the compact bone B- Haversian canals, C- Osteocyte within lacuna and D- marrow (H & E stain 40X).

The main histological change in the bone, at 3 day of coating (HA60Ag 2) group characterized by Figure (4.38)

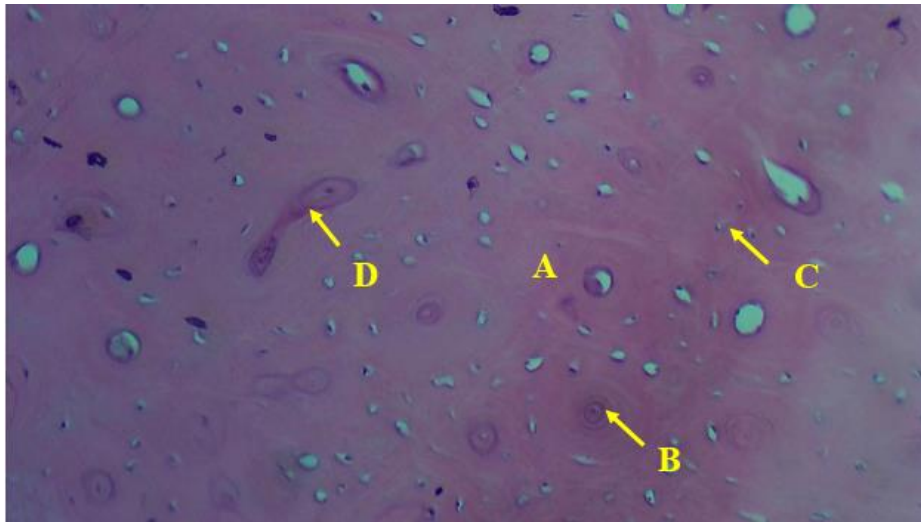


Figure (4.38) A section in the bone treated with composite (HA60Ag 2) group at 3 days show A- The matrix of the central portion of the wall are arranged concentrically around B- Haversian canals C- Osteocyte within lacuna D- Volkmann's canal (H & E stain 40X).

Even if nAg possess tremendous advantages that recommend them for novel and challenging biomedical applications[86] but the increasing medical and food applications of nAg raise concerns about their safety, including potential health consequences of human exposure. Bulk silver has been used in hygienic and medicinal applications for thousands of years nAg, however, possess distinct physicochemical properties compared to its bulk counterparts that result in a dramatic increase in toxicity because of their unique cell-contactable surface areas from their high surface-to-volume ratio [110]. The toxic effect of nAg was evident when used composite coating {(HA60Ag 1.5) on (CP-Ti) & ((HA60Ag 1.5))} groups, which the high percentage of nAg caused the death of the rabbit after 3 days of implantation process.

## *Chapter Five*

### *Conclusions and Recommendations*

#### **5.1 Conclusions**

Based on the obtained results, the following conclusions are reached at:

- 1- Increase in the thickness of the coating with the increase in the coating time.
- 2- Increase the proportion of nano silver in the electrolyte leads to a decrease of roughness.
- 3- The effect composite coating (HA & HA/nAg) on CP-Ti substrate is clearly effective against bacteria where this type of coating kills bacteria compared to the base specimen.
- 4- Specimen (HA45Ag1) is preferable because it has the lowest corrosion rate in (Ringer's solution)
- 5- The angle of contact differs with the increase in the percentage of nano silver in the hydroxyapatite (HA) electrolyte and the best wettability is achieved when using HA/Ag1.5 electrolyte.
- 6- If the percentage of silver is more than 1 g/L, the solution becomes toxic and does not apply in the human body.

**5.2 Recommendations**

For future work, the following are suggested:

- 1- Checking the adhesion to the (HA & HA/nAg) coating layer on titanium substrate.
- 2- Study the hardness with nano scale to the (HA & HA/nAg) coating layer on titanium substrate.
- 3- Diagnosing the type of bacteria through antibacterial test.
- 4- Corrosion rate calculation in other physiological solution stimulated the human body fluid such as Hank solution and Synthetic blood plasma.
- 5- Study wear properties to the (HA & HA/nAg) coating layer and comparison with Ti substrate.
6. Coating without hydroxyapatite.

## **References**

- [1] Emanuel Horowitz and John L. Torgesen . "Biomaterials". (1975).
- [2] Dahman, Yaser. (2019). "Biomaterials Science and Technology: Fundamentals and Developments". 10.1201/9780429465345
- [3] Mahajan, A. & Sidhu, Sarabjeet. (2017). "Surface modification of metallic biomaterials for enhanced functionality: a review". *Materials Technology*. 1-13. 10.1080/10667857.2017.1377971.
- [4] Patel NR, Gohil PP. "A review on biomaterials: scope, applications & human anatomy significance". *Int J Emerg Technol Adv Eng*. 2012;2:91–101.
- [5] Hussein, M. A., Mohammed, A. S., & Al-Aqeeli, N. (2015). "Wear characteristics of metallic biomaterials: a review". *Materials*, 8(5), 2749-2768.
- Miranda, M., Fernández, A., Díaz, M., Esteban-Tejeda, L., López-Esteban, S., Malpartida, F., ... & Moya, J. S. (2010). Silver-hydroxyapatite nanocomposites as bactericidal and fungicidal materials. *International journal of materials research*, 101(1), 122-127.
- [6] Raghavendra, G M & Varaprasad, Kokkarachedu & Jayaramudu, Tippabattini. (2015). "Biomaterials: Design, Development and Biomedical Applications". 10.1016/B978-0-323-32889-0.00002.
- [7] Singh, R., & Dahotre, N. B. (2007). "Corrosion degradation and prevention by surface modification of biometallic materials". *Journal of Materials Science: Materials in Medicine*, 18(5), 725-751.
- [8] Baddar, B. I., Shah, A., Ayu, H. M., Daud, R., & Dambatta, M. S. "Hydroxyapatite and Thermal Oxidation as Intermediate Layer on Metallic Biomaterial for Medical Implant: A Review". (2019).

- [9] Nasab, M. B., Hassan, M. R., & Sahari, B. B. "Metallic biomaterials of knee and hip-a review". (2010). *Trends Biomater. Artif. Organs*, 24(1), 69-82.
- [10] Kaur, M., & Singh, K. "Review on titanium and titanium based alloys as biomaterials for orthopaedic applications". (2019). *Materials Science and Engineering: C*, 102, 844-862.
- [11] Oldani, Carlos & Dominguez, Alejandro. "Titanium as a Biomaterial for Implants". (2012). 10.5772/27413.
- [12] Kuroda, K., & Okido, M. "Hydroxyapatite coating of titanium implants using hydroprocessing and evaluation of their osteoconductivity". (2012). *Bioinorganic chemistry and applications*, 2012.
- [13] Li, L. H., Kim, H. W., Lee, S. H., Kong, Y. M., & Kim, H. E. "Biocompatibility of titanium implants modified by microarc oxidation and hydroxyapatite coating". (2005). *Journal of Biomedical Materials Research Part A: An Official Journal of The Society for Biomaterials, The Japanese Society for Biomaterials, and The Australian Society for Biomaterials and the Korean Society for Biomaterials*, 73(1), 48-54.
- [14] Miranda, M., Fernández, A., Díaz, M., Esteban-Tejeda, L., López-Esteban, S., Malpartida, F., ... & Moya, J. S. "Silver-hydroxyapatite nanocomposites as bactericidal and fungicidal materials". (2010). *International journal of materials research*, 101(1), 122-127.
- [15] Ionita, D., Grecu, M., Ungureanu, C., & Demetrescu, I. "Antimicrobial activity of the surface coatings on TiAlZr implant biomaterial". (2011). *Journal of bioscience and bioengineering*, 112(6), 630-634.
- [16] Marambio-Jones, C., & Hoek, E. M. "A review of the antibacterial effects of silver nanomaterials and potential implications for human health

and the environment". (2010). *Journal of Nanoparticle Research*, 12(5), 1531-1551.

[17] Ionita, Daniela & Dincă, Mirela & Titorencu, Irina & Demetrescu, Ioana. "Merit and demerit effects of silver nanoparticles in the bioperformance of an electrodeposited hydroxyapatite: Nanosilver composite coating". (2012). *Journal of Nanoparticle Research*. 14. 10.1007/s11051-012-1152-6

[18] Qiu ZY, Chen C, Wang XM, Lee IS. "Advances in the surface modification techniques of bone-related implants for last 10 years. *Regen Biomater*". 2014 Nov;1(1):67-79. doi: 10.1093/rb/rbu007. Epub 2014 Oct 20. PMID: 26816626; PMCID: PMC4668999.

[19] Pan, Y. K., Chen, C. Z., Wang, D. G., & Zhao, T. G. "Improvement of corrosion and biological properties of microarc oxidized coatings on Mg–Zn–Zr alloy by optimizing negative power density parameters". (2014). *Colloids and Surfaces B: Biointerfaces*, 113, 421-428.

[20] Wang, Y., Yu, H., Chen, C., & Zhao, Z. "Review of the biocompatibility of micro-arc oxidation coated titanium alloys". (2015). *Materials & design*, 85, 640-652.

[21] Niinomi, M. (Ed.). "Metals for biomedical devices". (2019). Woodhead publishing.

[22] Chen, Q., & Thouas, G. A. "Metallic implant biomaterials". (2015). *Materials Science and Engineering: R: Reports*, 87, 1-57.

[23] JOON B. PARK JOSEPH D. BRONZINO. "Biomaterials PRINCIPLES and APPLICATIONS". (2002).

[24] Chakraborty, R., Seesala, V. S., Sen, M., Sengupta, S., Dhara, S., Saha, P., ... & Das, S. "MWCNT reinforced bone like calcium phosphate—

Hydroxyapatite composite coating developed through pulsed electrodeposition with varying amount of apatite phase and crystallinity to promote superior osteoconduction, cytocompatibility and corrosion protection performance compared to bare metallic implant surface". (2017). *Surface and Coatings Technology*, 325, 496-514.

[25] Hussein, M. A., Mohammed, A. S., & Al-Aqeeli, N. "Wear characteristics of metallic biomaterials: a review". (2015). *Materials*, 8(5), 2749-2768.

[26] Saini, M., Singh, Y., Arora, P., Arora, V., & Jain, K. "Implant biomaterials: A comprehensive review". (2015). *World Journal of Clinical Cases: WJCC*, 3(1), 52.

[27] Niinomi, Mitsuo. "Metallic biomaterials. *Journal of artificial organs: the official journal of the Japanese Society for Artificial Organs*". (2008). 11. 105-10. 10.1007/s10047-008-0422-7.

[28] Balamurugan, A & Rajeswari, Sivasankari & Balossier, Gérard & Rebelo, Avito & Ferreira, José. "Corrosion aspects of metallic implants — An overview". (2008). *Materials and Corrosion*. 59. 855 - 869. 10.1002/maco.200804173.

[29] Liu, X., Chu, P. K., & Ding, C. "Surface modification of titanium, titanium alloys, and related materials for biomedical applications". (2004). *Materials Science and Engineering: R: Reports*, 47(3-4), 49-121.

[30] Cunha, Alexandre. "Multiscale Femtosecond Laser Surface Texturing of Titanium and Titanium Alloys for Dental and Orthopaedic Implants". (2015).

- [31] Das, K., Bose, S., & Bandyopadhyay, A. "Surface modifications and cell-materials interactions with anodized Ti". (2007). *Acta biomaterialia*, 3(4), 573-585.
- [32] Hanawa, T. "Titanium-tissue interface reaction and its control with surface treatment". (2019). *Frontiers in bioengineering and biotechnology*, 7, 170.
- [33] Banerjee, D., & Williams, J. C. "Perspectives on titanium science and technology". (2013). *Acta Materialia*, 61(3), 844-879.
- [34] Brunette, D. M., Tengvall, P., Textor, M., & Thomsen, P. (Eds.). "Titanium in medicine: material science, surface science, engineering, biological responses and medical applications". (2012). Springer Science & Business Media.
- [35] Song, W. H., Jun, Y. K., Han, Y., & Hong, S. H. "Biomimetic apatite coatings on micro-arc oxidized titania". (2004). *Biomaterials*, 25(17), 3341-3349.
- [36] Eliaz, N. "Corrosion of metallic biomaterials: A review". (2019). *Materials*, 12(3), 407.
- [37] Li, Y., Yang, C., Zhao, H., Qu, S., Li, X., & Li, Y. "New developments of Ti-based alloys for biomedical applications". (2014). *Materials*, 7(3), 1709-1800.
- [38] Azevedo, C. R. F., & Hippert Jr, E. D. U. A. R. D. O. "Failure analysis of surgical implants in Brazil". (2002). *Engineering Failure Analysis*, 9(6), 621-633.
- [39] Nasab, M. B., Hassan, M. R., & Sahari, B. B. "Metallic biomaterials of knee and hip-a review". (2010). *Trends Biomater. Artif. Organs*, 24(1), 69-82.

- [40] Nuss, K. M., & von Rechenberg, B. "Biocompatibility issues with modern implants in bone-a review for clinical orthopedics". (2008). *The open orthopaedics journal*, 2, 66.
- [41] Priyadarshini, B., Rama, M., Chetan, & Vijayalakshmi, U. "Bioactive coating as a surface modification technique for biocompatible metallic implants: a review".(2019). *Journal of Asian Ceramic Societies*, 7(4), 397-406.
- [42] Chew, Kean & Hussein, Sharif & Zein, Sharif & Ahmad, Abdul Latif. "The corrosion scenario in human body: Stainless steel 316L orthopaedic implants". (2012). *Natural Science*. 04. 10.4236/ns.2012.43027.
- [43] Qiu, Z. Y., Chen, C., Wang, X. M., & Lee, I. S. "Advances in the surface modification techniques of bone-related implants for last 10 years". (2014). *Regenerative biomaterials*, 1(1), 67-79.
- [44] Hanawa, T. "In vivo metallic biomaterials and surface modification". (1999). *Materials Science and Engineering: A*, 267(2), 260-266.
- [45] Al-Amin, M., Abdul Rani, A. M., Abdu Aliyu, A. A., Bryant, M. G., Danish, M., & Ahmad, A. "Bio-ceramic coatings adhesion and roughness of biomaterials through PM-EDM: a comprehensive review".(2020). *Materials and Manufacturing Processes*, 35(11), 1157-1180
- [46] Breme, J., Biehl, V., & Hoffmann, A. "Tailor-Made Composites Based on Titanium for Medical Devices". (2000). *Advanced Engineering Materials*, 2(5), 270-275.
- [47] Duan, K., & Wang, R. "Surface modifications of bone implants through wet chemistry". (2006). *Journal of Materials Chemistry*, 16(24), 2309-2321.

- [48] Nouri, Alireza. "Introduction to surface coating and modification for metallic biomaterials". (2015).
- [49] Reis, E. C. C., Borges, A. P., Araújo, M. V., Mendes, V. C., Guan, L., & Davies, J. E. "Periodontal regeneration using a bilayered PLGA/calcium phosphate construct". (2011). *Biomaterials*, 32(35), 9244-9253.
- [50] Tian, P., & Liu, X. "Surface modification of biodegradable magnesium and its alloys for biomedical applications". (2015). *Regenerative biomaterials*, 2(2), 135-151.
- [51] Poovathikkal, Suvaneeth & Nair, Narayanan. "BIOMATERIALS AND BIOCOMPATIBILITY". (2018). 161. 10.20959/wjpr201810-12253.
- [52] L. L. Hench and J. Wilson . "An introduction to bioceramics". 1993, Singapore, World Scientific Publishing Co Pte Ltd.
- [53] Cattini, A. "Coatings of bioactive glasses and hydroxyapatite and their properties". (2013). (Doctoral dissertation, Limoges).
- [54] Iezzi, G., Scarano, A., Petrone, G., & Piattelli, A. "Two human hydroxyapatite-coated dental implants retrieved after a 14-year loading period: A histologic and histomorphometric case report". (2007). *Journal of periodontology*, 78(5), 940-947.
- [55] Fernandez-Pradas, J. M., Serra, P., Morenza, J. L., & De Aza, P. N. "Pulsed laser deposition of pseudowollastonite coatings". (2002). *Biomaterials*, 23(9), 2057-2061.
- [56] Vitale-Brovarone, C., Baino, F., Tallia, F., Gervasio, C., & Verné, E. "Bioactive glass-derived trabecular coating: a smart solution for enhancing osteointegration of prosthetic elements". (2012). *Journal of Materials Science: Materials in Medicine*, 23(10), 2369-2380.

- [57] Rouahi, M., Champion, E., Hardouin, P., & Anselme, K. "Quantitative kinetic analysis of gene expression during human osteoblastic adhesion on orthopaedic materials". (2006). *Biomaterials*, 27(14), 2829-2844.
- [58] Deligianni, D. D., Katsala, N. D., Koutsoukos, P. G., & Missirlis, Y. F. "Effect of surface roughness of hydroxyapatite on human bone marrow cell adhesion, proliferation, differentiation and detachment strength". (2000). *Biomaterials*, 22(1), 87-96.
- [59] Donglu Shi. "Introduction to Biomaterials". 2006. page 29
- [60] Levingstone, T. J., Ardhaoui, M., Benyounis, K., Looney, L., & Stokes, J. T. "Plasma sprayed hydroxyapatite coatings: Understanding process relationships using design of experiment analysis". (2015). *Surface and Coatings Technology*, 283, 29-36.
- [61] Dobrádi, A., Enisz-Bódogh, M., & Kovács, K. "Plasma spraying of bioactive glass-ceramics containing bovine bone". (2017). *Processing and Application of Ceramics*, 11(2), 113-119.
- [62] Duta, L., & Popescu, A. C. "Current status on pulsed laser deposition of coatings from animal-origin calcium phosphate sources". (2019). *Coatings*, 9(5), 335
- [63] Vahabzadeh, S., Roy, M., Bandyopadhyay, A., & Bose, S. "Phase stability and biological property evaluation of plasma sprayed hydroxyapatite coatings for orthopedic and dental applications". (2015). *Acta biomaterialia*, 17, 47-55.
- [64] Rodriguez-Lorenzo, L. M., Vallet-Regí, M., Ferreira, J. M. F., Ginebra, M. P., Aparicio, C., & Planell, J. A. "Hydroxyapatite ceramic bodies with tailored mechanical properties for different applications". (2002). *Journal of biomedical materials research*, 60(1), 159-166.

- [65] Gshalaev, V. S., & Demirchan, A. C. (Eds.). "Hydroxyapatite: Synthesis, properties, and applications". (2012). Nova Biomedical
- [66] Akram, M., Ahmed, R., Shakir, I., Ibrahim, W. A. W., & Hussain, R. "Extracting hydroxyapatite and its precursors from natural resources". (2014). *Journal of Materials Science*, 49(4), 1461-1475.
- [67] Sadat-Shojai, M., Khorasani, M. T., Dinpanah-Khoshdargi, E., & Jamshidi, A. "Synthesis methods for nanosized hydroxyapatite with diverse structures". (2013). *Acta biomaterialia*, 9(8), 7591-7621.
- [68] Pu'ad, N. M., Koshy, P., Abdullah, H. Z., Idris, M. I., & Lee, T. C. "Syntheses of hydroxyapatite from natural sources". (2019). *Heliyon*, 5(5), e01588.
- [69] Elliott, J. C., Wilson, R. M., & Dowker, S. E. P. "Apatite structures". (2002). *Advances in X-ray Analysis*, 45, 172-181.
- [70] Rujitanapanich, S., Kumpapan, P., & Wanjanoi, P. "Synthesis of hydroxyapatite from oyster shell via precipitation". (2014). *Energy Procedia*, 56, 112-117.
- [71] Uddin, Mohammad & Matsumoto, Takuya & Okazaki, Masayuki & Nakahira, Atsushi & Sohmura, Taiji. "Biomimetic Fabrication of Apatite Related Biomaterials". (2010). 10.5772/8777.
- [72] Yoshikawa, H., & Myoui, A. "Bone tissue engineering with porous hydroxyapatite ceramics". (2005). *Journal of Artificial Organs*, 8(3), 131-136.
- [73] Chetty, A., Wepener, I., Marei, M. K., Kamary, Y. E., & Moussa, R. M. "Synthesis, properties, and applications of hydroxyapatite". (2012). Nova Science Publishers.

- [74] Lu, J., Yu, H., & Chen, C. "Biological properties of calcium phosphate biomaterials for bone repair: a review". (2018). RSC advances, 8(4), 2015-2033.
- [75] Golubkov, P. E., Pecherskaya, E. A., Karpanin, O. V., Shepeleva, Y. V., Zinchenko, T. O., & Artamonov, D. V. "Automation of the micro-arc oxidation process". (2017, November). In J. of Phys.: Conf. Ser. (Vol. 917, p. 092021).
- [76] Sridhar, Shreyas & Alagan, Viswanathan & Venkateswarlu, bullet & Rameshbabu, N. & Parthasarathi, N.. "Enhanced visible light photocatalytic activity of P-block elements (C, N and F) doped porous TiO<sub>2</sub> coatings on Cp-Ti by micro-arc oxidation". (2015). Journal of Porous Materials. 22. 545–557.
- [77] Sarbishei, S., Sani, M. A. F., & Mohammadi, M. R. "Study plasma electrolytic oxidation process and characterization of coatings formed in an alumina nanoparticle suspension". (2014). Vacuum, 108, 12-19.
- [78] Jiang, B. L., & Ge, Y. F. "Micro-arc oxidation (MAO) to improve the corrosion resistance of magnesium (Mg) alloys". (2013). In Corrosion Prevention of Magnesium Alloys (pp. 163-196). Woodhead Publishing.
- [79] Narayanan, T. S., Park, I. S., & Lee, M. H. "Strategies to improve the corrosion resistance of microarc oxidation (MAO) coated magnesium alloys for degradable implants: Prospects and challenges". (2014). Progress in Materials Science, 60, 1-71.
- [80] Aravind, S., Prabhu, M. G., Kaushik, D., & Kumar, K. S. "Review on Nanocoating for Bio-Implants". (2017).

- [81] Kantharia, N., Naik, S., Apte, S., Kheur, M., Kheur, S., & Kale, B. "Nano-hydroxyapatite and its contemporary applications". (2014). *Bone*, 34(15.2), 1-71.
- [82] Sadat-Shojai, M., Khorasani, M. T., Dinpanah-Khoshdargi, E., & Jamshidi, A. "Synthesis methods for nanosized hydroxyapatite with diverse structures". (2013). *Acta biomaterialia*, 9(8), 7591-7621.
- [83] Corrêa, Juliana & Mori, Matsuyoshi & Sanches, Heloísa & Cruz, Adriana & Poiate Jr, Edgard & Poiate, Isis. "Silver Nanoparticles in Dental Biomaterials. *International journal of biomaterials*". (2015). 2015. 485275. 10.1155/2015/485275.
- [84] Saini, M., Singh, Y., Arora, P., Arora, V., & Jain, K. "Implant biomaterials: A comprehensive review". (2015). *World Journal of Clinical Cases: WJCC*, 3(1), 52.
- [85] Hemati, S., Asnaashari, O., Sarvizadeh, M., Motlagh, B. N., Akbari, M., Tajvidi, M., & Gookizadeh, A. "Topical silver sulfadiazine for the prevention of acute dermatitis during irradiation for breast cancer". (2012). *Supportive Care in Cancer*, 20(8), 1613-1618.
- [86] Burduşel, A. C., Gherasim, O., Grumezescu, A. M., Mogoantă, L., Fica, A., & Andronescu, E. "Biomedical applications of silver nanoparticles: An up-to-date overview". (2018). *Nanomaterials*, 8(9), 681.
- [87] Furqan, W.A. "Electrophoretic Deposition of Hydroxyapatite-Nano Silver Powder Particles on Duplex Stainless Steel for Biomedical Applications". (2021). University of Kufa, Faculty of Engineering, Materials Engineering Department.
- [88] Chen, W., Liu, Y., Courtney, H. S., Bettenga, M., Agrawal, C. M., Bumgardner, J. D., & Ong, J. L. "In vitro anti-bacterial and biological

properties of magnetron co-sputtered silver-containing hydroxyapatite coating". (2006). *Biomaterials*, 27(32), 5512-5517.

[<sup>89</sup>] Lee, J. S., & Murphy, W. L. "Functionalizing calcium phosphate biomaterials with antibacterial silver particles". (2013). *Advanced Materials*, 25(8), 1173-1179.

[<sup>90</sup>] Chourifa, H., Bouloussa, H., Migonney, V., & Falentin-Daudré, C. "Review of titanium surface modification techniques and coatings for antibacterial applications". (2019). *Acta biomaterialia*, 83, 37-54.

[91] Chen, W., Oh, S., Ong, A. P., Oh, N., Liu, Y., Courtney, H. S., ... & Ong, J. L. "Antibacterial and osteogenic properties of silver- containing hydroxyapatite coatings produced using a sol gel process". (2007). *Journal of Biomedical Materials Research Part A: An Official Journal of The Society for Biomaterials, The Japanese Society for Biomaterials, and The Australian Society for Biomaterials and the Korean Society for Biomaterials*, 82(4), 899-906.

[92] Zhang, B. G., Myers, D. E., Wallace, G. G., Brandt, M., & Choong, P. F. "Bioactive coatings for orthopaedic implants—recent trends in development of implant coatings". . (2014). *International Journal of Molecular Sciences*, 15(7), 11878-11921.

[93] Bapat, R. A., Chaubal, T. V., Joshi, C. P., Bapat, P. R., Choudhury, H., Pandey, M., ... & Kesharwani, P. "An overview of application of silver nanoparticles for biomaterials in dentistry". (2018). *Materials Science and Engineering: C*, 91, 881-898.

[<sup>94</sup>] Saravanan, S., Nethala, S., Pattnaik, S., Tripathi, A., Moorthi, A., & Selvamurugan, N. "Preparation, characterization and antimicrobial activity of a bio-composite scaffold containing chitosan/nano-hydroxyapatite/nano-

silver for bone tissue engineering". (2011). International journal of biological macromolecules, 49(2), 188-193.

[95] Kondepudi, K. K., Srivastava, R., Bishnoic, M., Kaur, B., & Satpati, B. "Biom mineralization of hydroxyapatite in silver ion-exchanged nanocrystalline ZSM-5 zeolite using simulated body fluid. (2016).

[96] Yang, Z., Gu, H., Sha, G., Lu, W., Yu, W., Zhang, W., ... & Wang, L. "TC4/Ag metal matrix nanocomposites modified by friction stir processing: surface characterization, antibacterial property, and cytotoxicity in vitro". (2018). ACS applied materials & interfaces, 10(48), 41155-41166

[97] Batebi, K., Khazaei, B. A., & Afshar, A. "Characterization of sol-gel derived silver/fluor-hydroxyapatite composite coatings on titanium substrate". (2018). Surface and Coatings Technology, 352, 522-528.

[98] Guo, C., Xue, J., & Dong, Y. "Fabrication and characterization of hydroxyapatite nanomaterial dual deposited with nano silver and zinc oxide". (2018). Materials Letters, 219, 182-185.

[99] Dalavi, P. A., Prabhu, A., Shastry, R. P., & Venkatesan, J. "Microspheres containing biosynthesized silver nanoparticles with alginate-nano hydroxyapatite for biomedical applications". (2020). Journal of Biomaterials Science, Polymer Edition, 31(16), 2025-2043.

[100] Dicu, M. M., Abrudeanu, M., Moga, S., Negrea, D., Andrei, V., & Ducu, C. "Preparation of ceramic coatings on titanium formed by micro-arc oxidation method for biomedical application". (2012). Journal of Optoelectronics and Advanced Materials, 14(January-February 2012), 125-130

[101] Aktug, S. L., Kutbay, I., & Usta, M. "Characterization and formation of bioactive hydroxyapatite coating on commercially pure zirconium by

micro arc oxidation". (2017). *Journal of Alloys and Compounds*, 695, 998-1004.

[102] Wang, P., Wu, T., Xiao, Y. T., Zhang, L., Pu, J., Cao, W. J., & Zhong, X. M. "Characterization of micro-arc oxidation coatings on aluminum drillpipes at different current density". (2017). *Vacuum*, 142, 21-28

[103] Teker Aydogan, D., Muhaffel, F., Menekse Kilic, M., Karabiyik Acar, O., Cempura, G., Baydogan, M., ... & Cimenoglu, H. "Optimisation of micro-arc oxidation electrolyte for fabrication of antibacterial coating on titanium". (2018). *Materials technology*, 33(2), 119-126.

[104] Du, Q., Wei, D., Wang, Y., Cheng, S., Liu, S., Zhou, Y., & Jia, D. "The effect of applied voltages on the structure, apatite-inducing ability and antibacterial ability of micro arc oxidation coating formed on titanium surface". (2018). *Bioactive materials*, 3(4), 426-433

[105] Huang, Q., Li, X., Elkhoory, T. A., Liu, X., Zhang, R., Wu, H., ... & Liu, Y. "The Cu-containing TiO<sub>2</sub> coatings with modulatory effects on macrophage polarization and bactericidal capacity prepared by micro-arc oxidation on titanium substrates". (2018). *Colloids and Surfaces B: Biointerfaces*, 170, 242-250.

[106] Abdul Wahed Kadhim Rajeh." *Engineering metallurgy,advanced materials, foundation, properties, handling and application*". 2016.

[107] Luna, L. G. "Manual of histological staining methods of the armed forced institute of pathology". (1968). (3rd Ed ed.). New York Toroto London Sydney: Graw-Hill Book. Company.

[108] Suvarna , S. K., Layton, C., & Bancroft, J. D. "Bancroft's Theory and Practice of Histological Techniques". (2013). Nottingham, UK: Elsevier.

[109] Shokouhfar, M., & Allahkaram, S. R. "Effect of incorporation of nanoparticles with different composition on wear and corrosion behavior of ceramic coatings developed on pure titanium by micro arc oxidation". (2017). *Surface and Coatings Technology*, 309, 767-778.

[110] Guo, X., Li, Y., Yan, J., Ingle, T., Jones, M. Y., Mei, N., ... & Chen, T. "Size-and coating-dependent cytotoxicity and genotoxicity of silver nanoparticles evaluated using in vitro standard assays". (2016). *Nanotoxicology*, 10(9), 1373-1384.

## ملخص البحث

تقنيات الطلاء هي طرق بسيطة وبدائية للحصول على سطح معدل. تعد أكسدة القوس الصغير (MAO) واحدة من أكثر الطرق القابلة للتطبيق لترسيب طبقة من السيراميك الحيوي المسامية على التيتانيوم النقي التجاري (CP-Ti) وسبائكه. تبحث الدراسة الحالية في تأثير متغيرات أكسدة القوس الصغير (الوقت ، مكونات الإلكتروليت) على خواص الطبقة المترسبة لتحديد أفضل قيم لمتغيرات أكسدة القوس الصغير. الطبقات المطلية هي الهيدروكسي اباتايت أو الهيدروكسي اباتايت المدمج مع الفضة النانوية بمقدار (٠,٥ ، ١ ، ١,٥ ، ٢) غم / لتر إلى محلول الهيدروكسي اباتايت.

كانت نتائج سمك الطلاء هي زيادة سمك الطلاء مع زيادة وقت الطلاء. أظهر فحص FESEM أن الزيادة في الوقت أدت إلى زيادة ترسب الفضة النانوية. أظهر فحص AFM أن خشونة السطح تزداد مع تقليل وقت الترسيب. كان تأثير الطلاء المركب (HA & HA / Ag) على ركيظة CP-Ti فعالاً بشكل واضح ضد البكتيريا وتفضل العينة (HA45Ag1) حيث تحتوي على أقل معدل تآكل ، اختلفت زاوية التلامس مع زيادة نسبة الفضة النانوية في محلول الهيدروكسي اباتايت وأفضل قابلية للبلل تم تحقيقها عند استخدام المحلول ذو النسبة HA / Ag1.5. إذا كانت النسبة المئوية للفضة أكثر من ١ غم/مل يصبح المحلول ساماً ولا يطبق في جسم الإنسان هذا ما تم استنتاجه من العملية الجراحية والزرع في الجسم الحي.



جمهورية العراق

وزارة التعليم العالي والبحث العلمي

جامعة بابل

كلية هندسة المواد

قسم هندسة المعادن

تحضير وفحص طلاء مركب على اساس من التيتانيوم  
ذي النقاوة التجارية بواسطة الأكسدة بالقوس الكهربائي  
الميكروي

رسالة مقدمه الى

كلية هندسة المواد/ جامعة بابل

وهي جزء من متطلبات نيل درجة الماجستير في هندسة المواد/ المعادن

من قبل

سجى عادل حمزة جاسم

بأشراف

أ.م.د. نبأ ستار راضي

٢٠٢١ م

1443 هـ